MENDEL UNIVERSITY IN BRNO
FACULTY OF AGRONOMY

Ph.D. thesis

Brno 2015 **Ing. Maja Stanisavljević**

Mendel University in Brno
Faculty of Agronomy
Department of chemistry and biochemistry

Quantum dots and their interaction with biomolecules

Ph.D. thesis

Studijní obor: 4106V017 Zemědělská chemie

Thesis supervisors:

Doc. RNDr.Vojtěch Adam, Ph.D.

Mgr. Markéta Vaculovičová, Ph.D.

Candidate:

Ing. Maja Stanisavljević

Brno 2015

PROHLÁŠENÍ

Prohlašuji, že disertační práce na téma „Kvantové tečky a jejich interakce s biomolekulami“ je samostatným autorským dílem podle Autorského zákona. Nositelem majetkového autorského práva je pracoviště a univerzita.

Výsledky práce shrnuté v této závěrečné práci byly financovány z veřejných prostředků z Evropských fondů a státního rozpočtu České republiky.

Disertační práce a výsledky v ní prezentované jsou dílem vypracovaným v Laboratoři metalomiky a nanotechnologií působící na půdě Agronomické fakulty Mendelovy univerzity v Brně a mohou být použity k dalšímu prezentování případně ke komerčním účelům jen se souhlasem vedoucího disertační práce a děkana. V opačném případě se jedná o porušení zákona.

dne …….

podpis…….

Tato práce vznikla v rámci CEITEC - Středoevropského technologického institutu s pomocí výzkumné infrastruktury financované projektem CZ.1.05/1.1.00/02.0068 z Evropského fondu regionálního rozvoje.

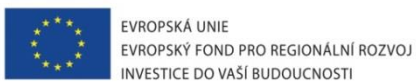

Acknowledgements

I would like to express my gratitude to all the people who have supported and helped me through my Ph.D. work:

I would like to thank to Professor René Kizek and Vojtěch Adam for accepting me into their group and giving me the opportunity for gaining more knowledge and professional experience.

My special gratitude goes to Markéta Vaculovičová for all her patience, guidance and advice through past years.

I thank to all my colleagues (past and present members of the group) from Laboratory of Metallomics and Nanotechnologies for their cooperation and professionalism.

I want to thank to my friends for all their support, love, tolerance, all sad and happy moments that we have shared all these years. I am grateful to my parents for being there for me with their endless and unconditional love allowing me to become who I am.

Finally, I especially thank to my sister and nephews for all life-changing moments they have brought into my life.

Abstrakt

V této práci byly syntetizovány kvantové tečky pomocí mikrovlnné syntézy a povrchově modifikovány různými způsoby pro umožnění interakce s vybranými biomolekulami. Mezi použité konjugační způsoby patří nespecifická interakce, streptavidin-biotin konjugace a vazba pomocí syntetického peptidu. Kvantové tečky pokryté glutathionem o velikosti 2 nm umožnily interakci s velkým žlábkem DNA, zatímco kvantové tečky pokryté streptavidinem specificky interagovaly s biotinylovaným oligonukleotidem. Nakonec, streptavidin-biotin interakce bylo využito i pro vazbu apoferitinu s magnetickými částicemi.

Klíčová slova: Kvantové tečky, biokonjugace, DNA oligonukleotidy, kapilární elektroforéza

Abstract

In this study CdTe QDs were synthetized via microwave irradiation method. Further they have been modified for purposes of their interaction with biomolecules using different conjugation approaches. Applied conjugation chemistries were non-specific interaction, streptavidin-biotin affinity. Glutathione modified CdTe QDs of 2 nm size were capable of non-specific interaction with major groove of DNA, while streptavidin modified CdTe QDs served as specific linker for biotinylated oligonucleotides. Further, streptavidin-biotin interaction was used for coupling of apoferritin and magnetic nanoparticles.

Key words: quantum dots, bioconjugation, DNA, oligonucleotides, capillary electrophoresis

Contents

1 Introduction

Reading any historical overview about nanotechnology the year 1959 and the name of Richard Feynman will show up. Physicist Richard Feynman gave a brilliant speech in 1959 which is usually pointed out as turning–point in the development of nanotechnology. In his speech he predicted that scientists will manipulate individual atoms making anything possible, back than words of this physicist sounded rather like science fiction than reality of the science. Shortly after, William McLellan has constructed a working electric motor that fits inside a cube, 5 cm on each side and won first challenge set up at Feynman's speech. 25 years later second challenge was fulfilled by Tom Newman who wrote the first page of "A tale of two cities" by Charles Dickens on the head of a pin with a beam of electrons, showing that Feynman prophecy was not science fiction. Beside designing materials in nanoscale this event triggered a development of the instruments for measurements at the required level such as atomic force microscope.

Today nanotechnology is involved in development of many technologies, science and industry. There already exist a variety of everyday products relied on nanomaterials such as sunscreens, cosmetics, sports goods, faster-recharging batteries, tires, cell phones, digital cameras and many others. Further, in computer science nanomaterials are employed in constructing transistors that are fast, powerful and small so one day entire memory will be placed on a single tiny chip followed by decreasing overall size of the computers and perhaps introduce us into new era in this field.

Growing concern for the environment and struggle for sustainable development of the society has brought into the light question of exploitation renewable sources of energy such as sunlight or wind. Nanomaterials, precisely speaking colloid quantum dots are involved in the construction of the solar panels which are more efficient and promise inexpensive solar power.

Nanomaterials with their specific characterization have found their way also to medicine. These materials in medical application are valuable for disease diagnostic pathways and therapeutics where nanopaticles can facilitate specific targeting and be used as platform for targeted drug delivery minimizing the risk of normal tissue damage. They are important part of biosensors construction for recognition of any

genetic and molecular changes. Regenerative medicine uses nanomaterials for cell and tissue growing stimulation in or outside of the body as well as the application is moving toward development of the nanorobots and precise nanosurgery.

It is clear that Feynman's prediction was true and manipulating individual atoms has brought numerous advantages and pushed known borders further promising bright future for nanomaterals.

2 Aims

- Summarization of the literature information on QDs characteristics, surface modification and conjugation with biomolecules and their investigation by capillary electrophoresis method.
- Literature analysis devoted to application of QDs for analytical and bioanalytical applications such as sensor and labeling applications, fluorescence resonance energy transfer purposes and imaging applications.
- Investigation of bioconjugation possibilities of QDs with nucleic acids
- Investigation of coupling options between QDs and proteins

3 Literary overview

3.1 Quantum dots

Nanotechnology is relatively young scientific field which deals with matters at the very small scale - nanoscale. Though it development has started earlier, visionary speech of Richard P. Feynman in 1959 (Feynman 1960)is considered as turning – point followed by fast progress of the nanotechnology. It is still evolving field which brings a lot of novelty and improvements into the science. Nanotechnology engineers materials with characteristics between atoms and bulk materials and today under that name a variety of different materials are considered. Nanoparticles are one of them and they have a few properties which make them appealing for commercialization. Quantum dots (QDs) belong to the family of nanoparticles and they are successfully applied in biosensing, drug delivery, i*n vitro* and *in vivo* imaging. Due to their specific optical and electronic properties, relatively simple synthesis and possibility of versatile surface modification they have allured a lot of attraction.

The first description of semiconductor nanocrystals which have been found in the literature was given by Efros and Ekimov, Russian scientists (Ekimov and Onushchenko 1981; Efros 1982). Quantum dots are semiconductor nanocrystals within 1 to 100 nm size, usually spherically shaped. Inorganic core is composed from the elements of the II-VI groups (most common CdSe or CdTe) and/or III-V groups (InP) of periodic system.

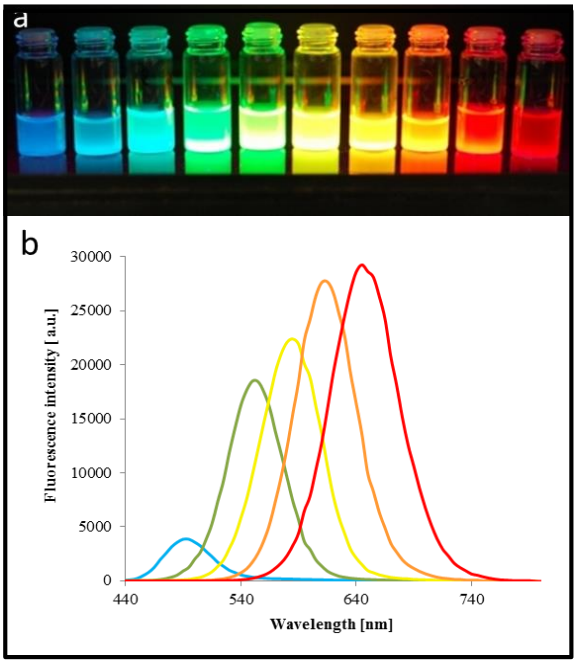

Figure 1. Quantum dots. (a) Size-tunable photoluminescence properties of CdTe QDs visualized under the UV light. (b) Emission spectra of different CdTe QDs.

Quantum dots consisted only of their core have rather poor optical properties due to narrow band gaps (Murray, Norris et al. 1993) and therefore usually outer epitaxially-grown layer of another semiconductor material with wider band gap is added. The most commonly used shell material is ZnS which plays several roles such as enhancement of the band gap width follow QDs photoluminescence (PL), electronically insulate the core, protects the QDs from oxidation and prevents leaching of the core material into the surrounding solution (Guyot-Sionnest 2008).

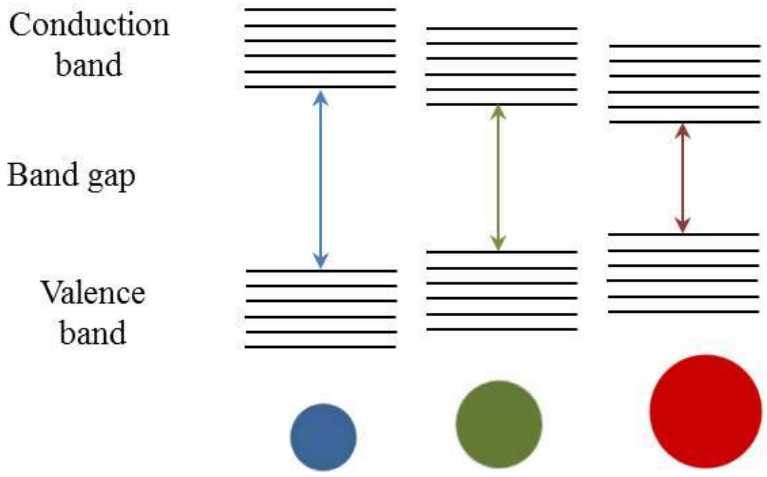

Figure 2. Schematic illustration of quantum confinement effect. Quantum confinement can shift the band gap of the semiconductor providing tunability dependent of the QDs. Similar to the 'particle in a box' model, excitons in smaller nanocrystals experience stronger quantum confinement, resulting in larger photoluminescence energy or emission in shorter wavelengths (blue range).

Further unique characteristics such as symmetric and narrow emission, continuous absorption spectra and high emission quantum yields originate from quantum confinement as well as their name quantum dots. In these small particles conductive and valence bands have been formed due to interaction of the highest occupied atomic levels of the atomic species and lowest unoccupied levels. Upon excitation an electron is promoted from the valence band to the conductive creating electrostatically bound electron-hole pair called exciton. In bulk materials electron and holes can move around but still remain together due to Coulomb electrostatic attraction, but in the crystal the exciton has a finite sized terminated by Bohr exciton diameter. If the particles size get smaller than Bohr radius the exciton is spatially confined which results in increasing their energy causing energy level shifting to the higher levels. So smaller quantum dots will absorb and emit in blue range and bigger in red range of the spectra and it can be concluded that emission wavelength is dependent on the size (Smith and Nie 2010; Rosenthal, Chang et al. 2011). Aforementioned superior characteristics of the absorption and emission spectra, together with good photostability, longer fluorescent lifetime and higher molar extinction coefficient have imposed QDs as adequate replacement of the organic fluorophores (Walling, Novak et al. 2009).

In spite of many advantages QDs have some shortcomings which had to be taken into consideration before application such as blinking, biocompatibility and their bigger size than conventional fluorophores. However, all this shortcomings are overcome to the some extant or are the object of studying and improvement (Smith and Nie 2010).

3.2 Synthesis of quantum dots

3.2.1 Organometallic synthesis

It is still the most popular method of QDs synthesis introduced by Murray et al. in 1993 (Murray, Norris et al. 1993). Organometallic synthesis involves very high temperature needed for nucleation and growth of nanocrystals, toxic precursors, organic solvents and surfactants, but obtained QDs are highly monodisperse, size-tunable and surface coated. Usually in the procedure as precursor dimethyl cadmium ($CdMe_2$) and trioctylphosphine telluride (TOPTe) are used as Cd and Te precursor, respectively and loaded into the flask with organic solvents trioctylphosphine (TOP) and its oxide (TOPO). The reaction is performed under an inert atmosphere and 300°C for dissolving precursor and nucleation followed by 230-260°C for nanocrystals growth. Final products of this procedure are hydrophobic QDs which have to be modified for water-solubility and biocompatibility and highly toxic and possible pyrophoric reactants. Today a variety of less toxic and dangerous precursors and stabilizers have been proposed and applied (Qu, Peng et al. 2001; Cao and Wang 2004; Asokan, Krueger et al. 2005). Nevertheless problems of the reproducibility, lack of the control and the overall costs of the procedure are its major disadvantages.

3.2.2 Aqueous synthesis of quantum dots

The second most often used synthesis method for direct producing of water-soluble QDs with good stability and biocompatibility is aqueous synthesis. This procedure follows a similar rout as organometallic method. Reactions are carried out in three-necked flask with reflux condenser.

Heavy metal precursors are metal salts, such as $Cd(ClO_4)_2$ easily dissolved in water, while chalcogens precursors can be bought as commercial solid powder (eg. $Na_2Te_2O_3$) or prepared in reaction procedures before usage in QDs synthesis (eg. H_2Te, NaHTe). Commercial powder of $Na_2Te_2O_3$ is air-stabile chemical which enables synthesis under ambient conditions, while H_2Te and NaHTe are unstable under these conditions and

require inert environment. The step of the metal salts dissolving in the water occur in the presence of the thiols as stabilizing agents, such as 2-mercaptoethanol, 2-thioglycerol, thioglycolic acid (TGA). The thiols enable control over the QDs synthesis kinetics, passivate surface, provide stability, solubility and surface functionality of the QDs and additional surface modification are not needed (Farkhani and Valizadeh 2014). Aqueous method is considered more environment-friendly and less expensive than organometallic, easy with high reproducibility, but comparing to the organometallic procedure QDs have lower degree of the crystallinity, wider particle size distribution and lower quantum yields (Gaponik, Talapin et al. 2002).

3.2.3 Microwave irradiation

Aforementioned shortcomings of the aqueous synthesis including a long reaction time in range of hours and/or days have been overcome by employing microwave irradiation. Microwave synthesis has gained a lot of attention due to producing high-quality QDs with enhanced quantum yield in shorter time (Huang and Han 2010). The benefits of microwave irradiation could be explained by dielectric heating. It is absorbed more strongly by polar materials and based on polar difference between solvents and precursors QDs can rapidly grow. Further, dielectric heating provide uniform heating of the entire sample volume comparing to the convective, which reduce thermal gradient effects enabling good control over the size distribution of QDs (Schumacher, Nagy et al. 2009). Commonly by microwave irradiation CdTe, CdSe, CdS, $Zn_{1-x}Cd_xS$ and ZnSe quantum dots are synthesized. Further functionalization of QDs with thiol ligands is possible as well as thiol ligands could be used as sulfur precursor for microwave synthesis (Qian, Li et al. 2005).

3.2.4 The other ways of synthesis

The organometallic and water-based synthesis methods are very successful in production of highly fluorescent QDs but usage of highly toxic chemicals strongly limits their application in clinical field. Following growing concern for environmental pollution more eco-friendly paths of QDs synthesis has been searched based on fundamental principles of ‘green chemistry’. This involves usage of biocompatible and non-toxic solvents, precursors, reducing agents and stabilizers such as bovine serum albumin like reducing and stabilizing agent (Ahmed, Guleria et al. 2014).

Ayele et al. have successfully used oleic acid as capping ligand in combination with microwave irradiation procedure (Ayele, Chen et al. 2011). More recently, even bigger

attention was given to the biosynthesis of QDs. Biosynthesis is new and unexplored area of synthesis method and involves biological organisms and their metabolic pathways in preparation of QDs of certain composition, size, shape and functionality (Dahl, Maddux et al. 2007). In the literature can be found publication which have used different microorganism such as *Escherichia coli(Mi, Wang et al. 2011),* yeast *Saccharomyces cerevisiae* (Bao, Hao et al. 2010)for synthesis of QDs with high photoluminescence. Synthesis in earthworm metabolic pathways has been demonstrated as well (Stuerzenbaum, Hoeckner et al. 2013).

Microbial synthesis is done either intracellular or extracellular and each of these QDs has their specific characteristics and is naturally capped with the proteins from the system with good stability and compatibility for any biological application. However, there are some challenges that microbial synthesis still has to overcome like improving size and shape control, obtaining larger amount of QDs during synthesis as well as explanation of the synthesis mechanisms which are at this point mostly unknown (Narayanan and Sakthivel 2010).

3.3 Surface modification of quantum dots

QDs are generally synthesized by the organometallic method using hydrophobic surfactants creating final product also hydrophobic and non-soluble in aqueous environment which are not properties acceptable for biological application. QDs water-solubility was gained through their surface modification and used ligands have to fulfill some requirements such as maintenance of stability in biological buffers and high resistance to photobleaching in aqueous media, the presence of functional groups available for conjugation with targeted biomolecule and minimization of hydrodynamic size. Methods for surface modification can be grouped into three approaches: ligand exchange, encapsulation and silica coating (Zhang and Clapp 2011).

Under the ligand exchange the replacement of the original hydrophobic ligand with a hydrophilic one is understood. The most frequently used anchors are thiol groups due to their strong affinity to Cd and Zn which are present on the surface of the QDs. Nie's group has introduced first protocol for QDs ligand exchange procedure with an monothiol, mercaptoacetic acid (Chan and Nie 1998). Later, the other monothiol ligands have been introduced such as mercaptopropionic acid (MPA), mercaptoundecanoic (MUA), cystamine, and cysteine. Shortcoming of monothiol ligands is their instability

under acid conditions due to thiols deprotonation and displacement from surface enabling QDs precipitation as well as dynamic interaction between thiols and ZnS resulting in short life time of the particles. Mattousi et al. have introduced dihydrolipoic acid (DHLA), a dithiol ligand instead of monothiols once (Mattoussi, Mauro et al. 2000). DHLA ligand greatly improved life time of the particles; however they were stable only under basic condition which induced further modification of the DHLA with polymers such as polyethyleneglycol (PEG). DHLA-PEG coated QDs have stability over the whole range of pH values, from acidic to basic; PEG successfully protects QDs from hydrolysis and biochemical reaction and enables introduction of functional group (eg. carboxyl, amine, hydroxyl and biotin). However these modifications cannot maintain high photoluminescence of native QDs.

Encapsulation is process in which native QDs hydrophobic ligands intercalates with hydrophobic section of amphiphilic ligands, while hydrophilic section offers water-solubility of the QDs. Usually used amphiphilic ligand are phospholipids and polymers containing alkyl chains. Due to significantly large size and weak hydrophobic interaction these QDs are not applicable in biological environment.

Silica coating is very similar process to encapsulation with difference, that during silica coating, silane derivatives displace hydrophobic ligands from the QDs surface, creating the silica network around the QDs. Usual crosslinking between silane molecules raises the stability. Further silica shell can be modified to have different functional groups, while their main drawback is complicated synthesis procedure comparing to the ligand exchange.

3.4 QDs bioconjugation with biomolecules

QDs application in biology considers their linking to the biomolecules of the interest. Ideally, bioconjugation chemistry should fulfill several conditions such as control over the number (ratiometric conjugation) biomolecules attached per one QD; control over the orientation of the attached biomolecule; provide desirable distance between QDs and biomolecules; not altering function of biomolecules nor QDs. Generally speaking the bioconjugation chemistries could be divided on covalent and non-covalent conjugation (Algar, Prasuhn et al. 2011). Most of the currently used conjugation methods are borrowed from conventional protein labeling chemistry and use carboxyl, amine and thiol groups for coupling via crosslinkers.

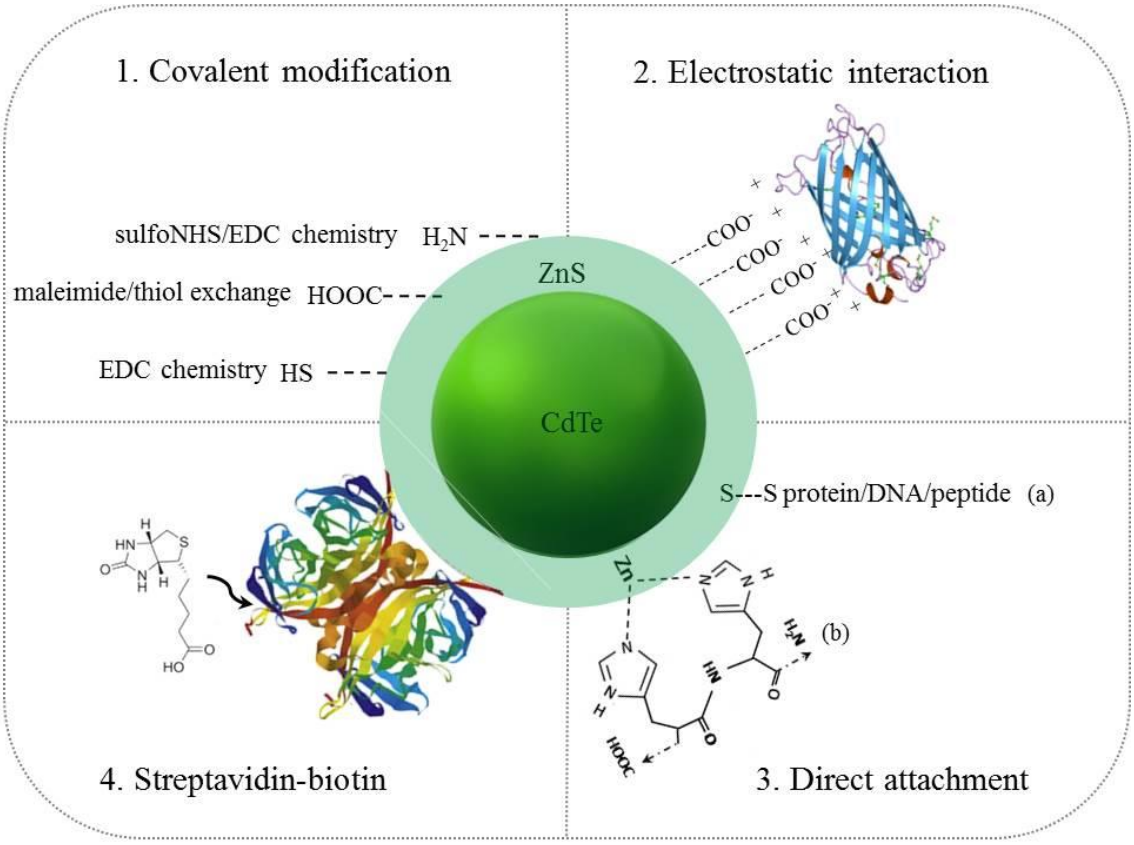

Figure 3. Methods of conjugation biomolecules to QDs. Schematic diagram with most common bioconjugation method. Method 1 shows covalent modification via crosslinking chemistry regarding the functional groups present on the QDs surface. Method 2 uses electrostatic interaction between opposite charged QDs and biomolecules, in the scheme protein. Method 3 shows direct attachment of biomolecules to the metal atoms on the QDs surface via dative thiol bond (a) or metal affinity coordination (b). Method 4 uses non covalent streptavidin-biotin interaction. Adapted from (Sapsford, Pons et al. 2006).

Carbodiimide chemistry or EDC (N-(3-dimethylaminopropyl)-N'-ethylcarbodiimide) mediated condensation of the carboxyls and amines to an amide bond is the most popular method of the bioconjugation. In practice bonding is performed in the presence of N-hydroxysulfosuccinimide (sulfo-NHS) for improving the solubility of reagents and increasing the coupling efficiency. EDC crosslinking is most efficient under the acidic condition and requires a large excess of the EDC to prevent competing hydrolysis.

Though it is very easy to obtain and cheap, EDC coupling usually require a lot of empirical optimization, purification steps followed by common lack of the orientation

control, possible crosslinking between proteins or QDs and proteins. Further sulfosuccinimidyl 4-(N-maleimidomethyl)cyclohexane-1-carboxylate sulfo-SMCC as heterobifunctional crosslinker was used. It has an amine-reactive sulfo-NHS-ester group and sulfhydryl reactive maleimide group and it can be used for two-step conjugation under near-physiological conditions (Sapsford, Algar et al. 2013).

Streptavidin-biotin linking is very common conjugation chemistry. Streptavidin is a tetramer isolated from *Streptomyces avidinii* with very strong affinity towards biotin Streptavidin-biotin interaction one of the strongest non-covalent interaction known in nature. Complex is formed very fast; four biotins could be bound with one streptavidin and complex exhibits strong stability at extreme pH, temperature and even to denaturing agents. Due to small size of biotin any molecule can be biotinylated which is why this conjugation is widely applied. Streptavidin modified QDs as well as biotinylated QDs have been used in practice. Streptavidin-biotin complex is followed by shortcomings such as unwanted crosslinking and lack of possibility to control orientation of the molecules on the QDs surface (Blanco-Canosa, Wu et al. 2014).

Very good alternative to covalent or streptavidin-biotin interaction is polyhistidine-metal-affinity conjugation. Conjugation is based on the ability of the histidine's imidazole side chain to chelate transitional metals such as zinc(II), one of the dominant elements on the QDs surface. However it remains unclear whether polyhistidine (His_n) tags bind directly to the QDs surface due to possible defects in the surface coverage or His_n tags displace ligands. Further histidine metal affinity coordination in combination with chemoselective ligation reaction provide an excellent control over the QDs bioconjugation regarding the ratio of attached biomolecules, orientations and distance between QDs and conjugates (Prasuhn, Blanco-Canosa et al. 2010). A great advantage and challenge hidden in this method is ability of engineering desired proteins/peptides with appended polyhistidine sequence for assembly onto the QDs surface through metal affinity coordination. Also no reactive chemistry involved so purification steps have been avoided simplifying the procedure.

Pioneers of the non-covalent interaction between QDs and biomolecules are Mattoussi et al. They have used engineered maltose binding protein (MBP) consisting a positively charged domain which electrostatically interact with negative charged QD. However this approach has limited application in biological environment since electrostatic interaction is not specific or stable enough (Mattoussi, Mauro et al. 2000; Rosenthal, Chang et al. 2011).

A variety of conjugation methods have been proposed and investigated in order to facilitate biolabeling and improve QDs application. The choice of the proper bioconjugation method is strongly dependent on the biomolecule of interest. What should be kept on mind is that alongside bioconjugations improvement, surface modification advancement is very important aspect as well, almost inseparable. Non-covalent coupling refers to electrostatic interaction and direct adsorption between QDs and targeted biomolecule.

3.5 Application of the QDs

All aforementioned QDs properties, modification and altering have been done in purposes of different life science applications. Their good brightness and photostability led to application in labeling experiments, while surface modification and bioconjugation possibilities promote QDs as fluorescent probes for *in vivo* imaging as well as in biosensing and sensor designing (Walling, Novak et al. 2009).

3.5.1 Fluorescent probes based on direct interaction with QDs

PL of QDs is based on the recombination of excitons which can be influenced with any surface modification causing PL quenching or enhancement. This was used for designing sensors for metal ions which can be directly adsorbed on the QDs causing PL change or attached due to adequate surface ligand (Wu, Zhao et al. 2014). The pioneers of this area are Chen and Rosenzweig which have detected Cu(II) ions in the presence of Zn(II) ions in aqueous solution by thioglycerol-capped CdS QDs (Chen and Rosenzweig 2002).

Metal ion detection via direct adsorption is very complicated process and there are several mechanisms that lead either to fluorescence quenching or enhancement in the metal presence. For example, detection of Hg(II), Cu(II), Ag(I) and Pb(II) ions can be based in their competing with thiol ligand present on the QD surface. Ligand detaching will leave surface traps open for electron capturing from the conductive band leading to the quenching and other consequence of detaching which leads to quenching fluorescence signal is aggregation of the QDs (Ali, Zheng et al. 2007; Ke, Li et al. 2012). Similarly fluorescence enhancement detected in the presence of Zn(II) and Cd(II) ions can be explained by passivation of the surface defect of S or Se and Te vacancies in their presence. Zn(II) eliminates surface defect and take a part in exciton confinement which led to PL increase (Chen, Zhang et al. 2004).

On the other hand QDs can be conjugated to the special receptors able to ligand or chelate metal ions. This work was pioneered by Gatt´as-Asfura and Leblanc. They used a pentapeptide Gly-His-Leu-Leu-Cys which use Cys for QDs conjugation and Gly-His site binds the Cu(II) and Ag(I) metal ions (Gattas-Asfura and Leblanc 2003). Further choices of the receptors are Schiff-bases, azamacrocycle and suparamolecular receptors with macrocyclic or caged moiety (Wu, Zhao et al. 2014).

The majority of QDs application in the sensor is actually relied on fluorescence resonance energy transfer (FRET), especially for biological application. Several metal ions based on FRET have been designed which will be explained in following text.

3.5.2 QDs-FRET based nanosensors

FRET is a process of non-radiative energy transfer from energy donor to acceptor (FRET pair) via dipole-dipole interaction and does not include a photon emission. FRET occurs if spectral overlap of FRET pair is bigger than 30%; this distance provides favorable dipole orientation of the donor and acceptor. Also FRET is limited with the distance of pair which should be within 1 to 10 nm (Lakowicz 1999).Commonly as FRET pairs organic dyes were used but they suffer from very short fluorescence lifetime, inadequate spectral overlapping, chemical and photochemical degradation, self-aggregation and interaction with environment. QDs overcome all this specified shortcomings and emerge themselves as a new class of sensors.

Sensors are usually designed to target a specific or wanted class of biomolecules. Biomolecules are organic compounds produced by living organism in specific shapes and dimensions. They have incorporated functional groups which determinate their chemical properties and large molecule called macromolecules are usually built out of simpler block molecules. Biomolecules are important as they control almost every aspect of organisms and any disorders in their synthetic or metabolic pathways can cause serious illnesses and some of them are genetically inherited. From this is clear that these molecules could be used as markers for detection and diagnosis.

Regarding the interaction with QDs following biomolecules could be of interest: peptides, proteins and antibodies, enzymes and ribozymes, oligonucleotides and aptamers, carbohydrates, lipids, drugs and other biologically active small molecules (Algar, Prasuhn et al. 2011). The most challenging part of designing QDs-FRET based system lies in the designing interaction between QDs usually used as energy donor to

and energy acceptor or to the biomolecule itself carrying the acceptor. Therefore, the latest trends in QDs and biomolecules interaction could be easily followed.

The majority of work is oriented toward detection of nucleic acids and proteolytic activities of enzymes as potential fast diagnostic tools. In here, some of the sensors will be presented. More detail analysis of the literature on this topic is presented in a review manuscript, which is a part of this thesis.

The first sensor for detection of nucleic acid used streptavidin-biotin affinity to bring biotinylated sandwich hybridized target DNA to streptavidin-modified QDs (Zhang, Yeh et al. 2005). Further QDs have been modified with 11-mercaptoundecyl tri(ethylene glycol) alcohol **(**EG_3OH**)**/11-mercaptoundecyl tri(ethylene glycol) acetic acid (EG_3COOH**)** where EG_3 group enhance the stability and solubility. Modified QDs were conjugated via carboxyl-to-amine crosslinker to capturing DNA and used as energy donor (Zhou, Ying et al. 2008). Positively charged PEG-DHLA-derived ligand modified QDs were used for simple electrostatic interaction with negatively charged single-stranded DNA (ssDNA) as sensor set up (Lee, Choi et al. 2009), also usage of cationic polymers as electrostatic linkers between QDs and single stranded DNA (ssDNA) have been reported (Peng, Zhang et al. 2007). Thiol modified oligonucleotide probes directly attached to the immobilized QDs on fused-silica optical fiber and via hybridization process target DNA was detected endorsing immobilization as new platform (Algar and Krull 2009; Algar and Krull 2009). Latest novelty related to the immobilization importance is the detection of nucleic acid is paper-based assay. Assay uses direct attachment of the oligonucleotide probe to the gluthatione (GSH) capped QDs immobilized via imidazol ligands to the paper (Noor, Shahmuradyan et al. 2013).

Designing a sensor for detection of enzymatic activity required synthesis of the peptide with specific sequence as cleavage site for specific enzyme (Shi, Rosenzweig et al. 2007), but most of the sensors are based on polyhistidine tagged peptides for attachment via metal-affinity coordination on the QDs surface, frequently DHLA modified. Usually, N-terminus contained hexahisitidine sequence, helix-linker spacer region, enzyme-specific cleavage site and on its C-terminal cysteine for attachment of the dye. Sensor have been designed for different enzymes such as metalloproteinases (Li, Xue et al. 2013), collagenase, thrombin and chymotrypsin (Medintz, Clapp et al. 2006), caspase-3 (Boeneman, Mei et al. 2009) and HIV-1 protease for *in vi*vo imaging (Biswas, Cella et al. 2011; Cella, Biswas et al. 2014). Analogy to nucleic acid detection, paper-based assay for enzymatic activity detection were designed, based on

the same polyhistidine metal-affinity coordination toward QDs and imidazole modification of paper for QDs immobilization (Petryayeva and Algar 2013).

Immunoassays have not stayed unaffected by new labeling materials. For designing assay for TNT detection an anti-TNT antibody was bound to DHLA-capped QDs via metal-affinity coordination and a TNT analogue was placed on antigen binding site. Detection was carried out by displacement of the analogue in the presence of TNT (Goldman, Medintz et al. 2005).

Immunoassays in combination with QDs as fluorescent label were also included in design of the sensor estrogen (Wei, Lee et al. 2006), maltose (Medintz, Clapp et al. 2003) and detection of phatogens such as *Aspergilus amstelodami* in which PEGylated QDs were crosslinked with SMCC to the anti-*Aspergilus* antibody (Kattke, Gao et al. 2011) or viruses (Zekavati, Safi et al. 2013). Also detection of microorganisms toxins such as aflatoxins B1 were reported using carbodiimide chemistry between antibody and QDs (Zekavati, Safi et al. 2013). Noteworthy is that hybridization-based probes are equally used for detection of bacteria and viruses such as *Helicobacter pylori* (Shanehsaz, Mohsenifar et al. 2013) and avian influenza virus H5N1 (Chou and Huang 2012), respectively.

Monitoring pH value of the environment is highly employed parameter in almost every field not just in the science but in industry and agriculture as well. QDs-FRET based nanosensors for pH monitoring were reported. System contains pH indicator dye like squaraine or fluorescent protein mOrange while QDs are used as reference dye (Snee, Somers et al. 2006; Dennis, Rhee et al. 2012). Other interesting application of these nanosensors can be observed in detection of environment pollutant. Among the most common ones are heavy metals such as cadmium, mercury, lead and others. Sensor designs are based on the QDs surface modification toward targeted heavy metal. N-acetyl-L-cysteine functionalized QDs were designed for Hg(II) ion detection (Hu, Hu et al. 2013), dithizone capped QDs for Pb(II) (Zhao, Rong et al. 2013) and zincon modified QDs for Zn(II) and Mn(II) sensing (Ruedas-Rama and Hall 2009) are some of the examples. Similarly, as for lead detection, dithiozone capped QDs were used for organophosphorus pesticides (Zhang, Mei et al. 2010).

3.5.3 Cellular labeling and imaging with QDs

In 1998 the first labeling experiments were reported for labeling F-actin filaments and HeLa cells. For labeling HeLa cells QDs were attached to transferrin (Chan and Nie 1998) which enabled endocytotic uptake as well. In F-actin filaments labeling streptavidin-bitoin interaction with QDs was used and QDs modified with trimethoxysilylpropyl urea and acetate groups were used for nucleus labeling (Bruchez, Moronne et al. 1998). Further mortalin and p-glycoprotein tumor cells important molecules were labeled with QDs (Kaul, Yaguchi et al. 2003; Sukhanova, Devy et al. 2004). The convenience of multiplexing with QDs was used by Hoshino et al. for intracellular labeling of nucleus and mitochondria. Green QDs with carboxyl group and red QDs with amine group were conjugated with targeted peptides for mitochondria and nucleus labeling, respectively via different crosslinkers (Hoshino, Fujioka et al. 2004). Yezhelyev et al. used different colors QDs conjugated with different specific antibodies against biomarkers for labeling five different breast cancer biomarkers. All biomarkers have been found in different cell parts and successfully labeled (Yezhelyev, Al-Hajj et al. 2007). Interesting work done by Hahn et al. has shown how labeling can improve detection. In peculiar case bacteria *Escherichia coli* O157:H7 labeled with green QDs was detected form a bacterial cell mixture by flow cytometry. QDs labeled *E. Coli* comparing to organic dye-labeled have shown a full order of magnitude increase in the detection limit (Hahn, Keng et al. 2008).

QDs application in cellular labeling and imaging meets a crucial problem of the cell entering. Several pathways are known: direct microinjection, electroporation (process which uses charge to physically deliver QDs through the membrane), passive uptake (endocytosis) and peptide induced transport (Wang and Wang 2014) and several are not fully understood. Passive uptake is a natural cells transport, but molecule up taken on that way can be stored in granular compartment around nucleus never penetrating the nucleus. Microinjection method is time consuming approach and a number or labeled cell is limited, while electroporation cause QDs aggregation in the cytoplasm and cell death. However, it should not have been neglected that specific QDs functionalization have significant influence on the cell uptake and different ones have been reported (Chen, He et al. 2014).

3.5.4 *In vivo* application

In vivo, a Latin expression can be translated as in the living body of the plant, animal or human which means that experiments are conducted inside intact organism. QDs have growing contribution to *in vivo* experiments and they enable acquisition of images over a long period time due to photostability and resistance to photobleaching. Their large surface area permits the assembly of peptides, antibodies, the others biomolecules and contrast agents. QDs modification must enable them stability under the biochemical processes which will encounter in the living body (Jin, Hu et al. 2011). *In vivo* imaging is followed by absorbance and scatter by tissues and their autofluorescence upon excitation which is solved by engineering QDs with near-infrared (NIR) emission (700-1000 nm) because absorbance and scattering are significantly lower at that range. Autofluorescence is dependent on the emission wavelength and as QDs have broad absorption spectra appropriate wavelength can be picked in purposes of autofluorescence elimination. Penetration of the light into the tissues is low and though NIR QDs have been designed for deeper penetration limits stands to about 3 cm (So, Xu et al. 2006). Injection of the QDs into the live animal is usually done intravenously or subcutaneously and delivered to the bloodstream.

Jiang et al. have used transferring conjugated QDs with NIR emission for *in vivo* monitoring on mouse heart and femur. Also Zimmer et al. have used DHLA modified QDs in NIR emission range and used it for monitoring of the tissue fluids and visualizing of the sequential lymph nodes (Zimmer, Kim et al. 2006).

Particular interest is shown for QDs application into lymph node mapping in cancer. Kobayashi et al. have used five different reporter QDs for multicolor imaging. Carboxyl conjugated QDs were injected into five different region for visualization of the lymphatic flow and to study drainage patterns toward primary lymph node (Kobayashi, Hama et al. 2007; Kosaka, Ogawa et al. 2009). Ballou et al. have used carboxyl-PEG and metoxyl-PEG quantum dots for mapping sentinel lymph nodes. Carboxyl-PEG quantum dots were monitor in large numbers of lymph nodes while metoxyl-PEG have been seen only in the nodes near the tumor (Ballou, Ernst et al. 2007). Phospholipid encapsulated QDs with NIR emission were injected subcutaneously in the paw of the mouse was used by Pic et al. to demonstrate accumulation of the QDs in regional sentinel lymph node within 5 minutes after injection and highest concentration was reaches at 4 hours and gradually fell over during 10 days as well as showing low uptake in other organs (Pic, Pons et al. 2010).

Growing tumor needs nutrition supply normally carried by bloodstream. Tumor cells through angiogenesis form new blood vessels net for their blood supply and it is fundamental step into transition of tumors from benign to malignant state. Receptors, such as integrin are highly expressed in tumor cells while angiogenesis occurs and can be used for diagnostics. Cai et al. injected tri-peptide quantum dots conjugate which specifically binds to integrin and nonspecific control into the tail vain of the mouse. The results have shown that is possible to differentiate cancer based on the integrin expression levels(Cai, Shin et al. 2006).

However limiting factor for *in vivo* application of the QDs is their inorganic core and capping agents as potential toxic materials. Toxicity studies of the QDs are conflicting and this remains open question. Further size of the QDs prevents renal clearance from the organism and with the time they will be accumulated in the liver, organ sensitive to cadmium toxicity (Byers and Hitchman 2011)

3.6 Review I

STANISAVLJEVIC, M.; VACULOVICOVA, M.; KIZEK, R.; ADAM, V. Capillary electrophoresis of quantum dots: Minireview. Electrophoresis 35(14): 1929-1937

ISSN: 0173-0835

DOI: 10.1002/elps.201400033

Participation in the work of the author Stanisavljevic M.: literature research 90% and manuscript preparation 60%.

Capillary electrophoresis is analytical technique used for separation according to the charge and size of molecules. CE in combination with laser induced fluorescence detection was eshablished as powerful technique for characterization, analysis and/or separation of QDs and latest available data were summarized in following review:

Maja Stanisavljevic[1]
Marketa Vaculovicova[1,2]
Rene Kizek[1,2]
Vojtech Adam[1,2]

[1]Department of Chemistry and Biochemistry, Faculty of Agronomy, Mendel University in Brno, Brno, Czech Republic
[2]Central European Institute of Technology, Brno University of Technology, Brno, Czech Republic

Received January 18, 2014
Revised February 17, 2014
Accepted March 13, 2014

Review

Capillary electrophoresis of quantum dots: Minireview

It has been already three decades, since the fluorescent nanocrystals called quantum dots (QDs) appeared and attracted attention of a broad scientific community. Their excellent not only optical but also electronic properties predetermined QDs for utilization in a variety of areas. Besides lasers, solar cells, and/or computers, QDs have established themselves in the field of (bio)chemical labeling as well as medical imaging. However, due to the numerous application possibilities of QDs, there are high demands on their properties that need to be precisely controlled and characterized. CE with its versatile modes and possibilities of detection was found to be an effective tool not only for characterization of QDs size and/or surface properties but also for monitoring of their interactions with other molecules of interest. In this minireview, we are giving short insight in analysis of QDs by CE, and summarizing the advantages of this method for QDs characterization.

Keywords:
Capillary electrophoresis / Conjugation / Quantum dots / Separation
DOI 10.1002/elps.201400033

1 Introduction

Nanotechnology is widely spread technology applied in almost every field of science today [1–6]. Its backbone is hidden in principle of creating or engineering materials in the atomic or molecular scale. The year 1959 in history of nanotechnology can be marked as turning point because of brilliant speech of Richard P. Feynman who gave the vision that science and technology can be based on nanoscale [7]. However, the beginning of nanotechnology or closely speaking of nanomaterials was given much earlier by Michael Faraday in 1857 by observing characteristics of gold nanoparticles produced in aqueous solution [8]. Nanotechnology roots are tightly connected with development of colloids and physical chemistry, thus the great names such as Albert Einstein with his Brownian motion theory and Nobel prized Jean-Baptiste Perrin should not be neglected [9].

The biggest member of the family of nanomaterials is a group of nanoparticles that covers metal nanoparticles, metal oxide nanoparticles, polymer nanoparticles, and/or silica nanoparticles. The most interesting is group of gold nanoparticles with their well-known optical characteristics as absorption, luminescence, and stability. Iron nanoparticles also play important role due to their magnetic properties [10–12]. Beside nanoparticles, carbon-based nanomaterials such as nanotubes, fullerenes, graphene which exhibit very good optical, electrochemical, and adsorptive properties are subject of constant investigation [13]. Other nanomaterials which cannot be neglected nor considered less important are liposomes [14, 15] and dendrimers [16, 17].

In this review, we focused on finding of articles containing phrases quantum dot (QD) and electrophoresis. We were interested mainly in the field of characterization of these unique materials using electrophoresis and further in biomolecules binding.

1.1. Quantum dots

QDs belong to the family of nanoparticles and they are defined as semiconductor nanocrystals with size from 1 to 10 nm usually spherical shape, but they can also be cubic, rod-like, or tetrapod-like [18]. QDs are mostly made of elements of II–VI groups as CdSe, CdTe (Fig. 1A), CdS, and ZnSe or III–V groups as InP and InAs [19, 20] and their optical and electronic properties can be placed between those of bulk materials and isolated molecules or atoms [21]. Size-depending properties and quantum confinement give them unique characteristics such as symmetric and narrow emission (Fig. 1B and C), continuous absorption spectra, and high emission quantum yields. For biological and medical usage, their photostability and resistance to chemical degradations are

Correspondence: Dr. Vojtech Adam, Department of Chemistry and Biochemistry, Mendel University in Brno, Zemedelska 1, CZ-613 00 Brno, Czech Republic
E-mail: vojtech.adam@mendelu.cz
Fax: +420-5-4521-2044

Abbreviations: **EDC**, 1-ethyl-3-(3-dimethylaminopropyl) carbodiimide hydrochloride; **FRET**, fluorescence resonance energy transfer; **HRP**, horseradish peroxidase; **PAA**, polyacrylamide; **QD**, quantum dot; **SMCC**, succinimidyl 4-[*N*-maleimidomethyl]-cyclohexane-1-carboxy; **TOPO**, trioctylphosphine oxide

Colour Online: See the article online to view Figs. 1–3 in colour.

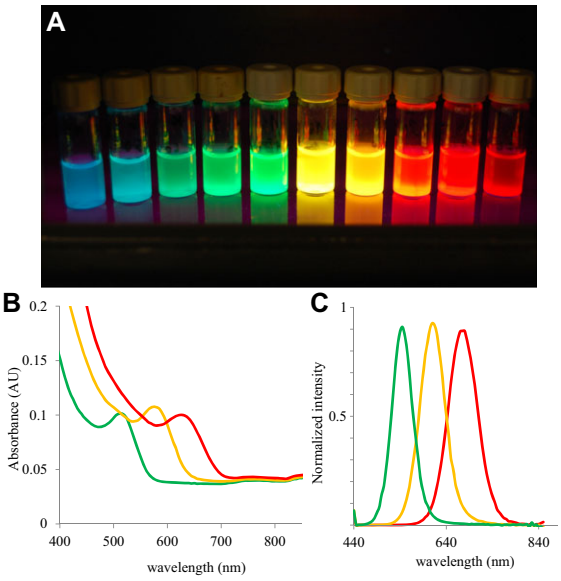

Figure 1. (A) Photography of quantum dots made from CdTe under various conditions. For more experimental details, see [84]. (B) Absorption spectra of three types of CdTe QDs. (C) Normalized emission spectra of three types of CdTe QDs (excitation wavelength: 400 nm).

valuable [22, 23]. However, the core of QDs created with inorganic elements is toxic for living systems and cells. Moreover, QDs are usually hydrophobic and this makes them unsuitable for working in aqueous environment or for any application in biological system. Therefore, synthesis methods of water-soluble QDs have been developed [24–26] and different surface modifications provide easy conjugations with biomolecules trough covalent or noncovalent attachment [27, 28]. Nowadays, when concern for environment is emphasized, more environment-friendly technologies are explored and used for QDs synthesis [29–31]. The newest discovery in this field is the synthesis of QDs in earthworms using earthworm's metal detoxification pathway for it [32].

QDs exhibit one specific phenomenon called "blinking" defined as fluctuations in luminescence. Besides blinking on QDs luminescence effect environment, some molecules or reagents can cause increasing or decreasing of fluorescent signal of QDs. The blinking and the environment influence can cause limitation and issues in QDs application or analysis and are considered as drawbacks. The mechanism and explanations of drawbacks remain unknown and unclear [33]. Nevertheless, the topic which still occupies and worries science is the toxicity of QDs. On the other hand, one may mention that even large-scale production of these materials cannot cope with the well-known sources of metals, which are much greater. Even modified QDs bring doubts because nobody can tell with certainty what will happen to the materials used for modification in biological environment [34]. Other opened question is the environment itself and disposal of QDs in it [35]. Development and improving of QDs are equally followed with research about their toxicity [36–38] and even methods for evaluation of their toxicity have been developed [39]. Based on these facts, there still remain unanswered questions concerning these materials and their well characterization is one of the keys to answer them.

1.2 Capillary electrophoresis

In the area of nanomaterials, CE is powerful tool not only for analysis of nanomaterial properties and validation of the synthesis process, but also for monitoring of nanomaterials interactions with other molecules. CE-LIF method was found as excellent method for not only characterization of QDs based on their fluorescent properties but also for analysis of biomolecules employing QDs as an efficient fluorescent label [22, 40]. Moreover, in the 90s, chip-based electrophoresis experienced a big breakthrough representing miniaturization of CE [41, 42]. Microchip electrophoresis provides very good separation with low sample and reagent consumption. Due to separation channels with even lower amount of injected analyte, extremely sensitive detection technique is required more than over before and therefore highly fluorescent labels are essential [43].

2 Characterization of QDs with CE

Progress in technology of CE is still going further. Basic CE method was modified and developed according to different separation mechanisms and conditions. Based on these advances, CE methods have been used for characterization and separation of QDs CZE, MEKC, and CGE, as we discussed on the following paragraphs.

Characterization of QDs was done by Song et al. with CGE employing LIF detector for the first time [44]. This group used linear polyacrylamid (PAA) as sieving media as successful choice for characterization and separation of different size QDs, also providing valuable information of QDs behavior in wide pH range. Very important is a study of peak broadening in sieving media as well as percentage of used sieving media. A challenge to perform characterization of QDs with CZE was fulfilled by Pereira et al. [45]. Measurements included characterization of commercially available QDs with ultraviolet (UV) detection, LIF detection, and sodium phosphate as BGE. Two CE instruments were constructed solely for the study of QDs and ADS620 and T2-Evitag QDs were analyzed. The degree of net negative charge present on the QD surface can be assessed based on the migration times.

Very interesting insight in QDs separation was given by Pyell and co-workers on CdSe/ZnS/SiO_2 core/shell/shell nanocrystals [46]. Pyell's group was using, previously given by Ohshima group [47], formula of electrophoretical mobility μ independence of zeta potential ζ, particle radius r, and ionic strength I. The theory matched with practice and it proofed that mobility and size of nanoparticles are in nonlinear function. A comparison of calculated with experimentally determined distributions of the electrophoretic mobility

clearly showed that the observed broad bands in CE studies of colloidal nanoparticles are mainly due to electrophoretic heterogeneity resulting from the particle size distribution. The calculated data were in a good agreement by transmission electron microscopy method. Therefore, this procedure is well suited for the routine production control of charged nanoparticles with a ζ potential of 50–100 mV.

In addition, CZE was used for monitoring synthesis conditions which determine size of QDs with CdTe in core and with thioglycolic acid as capping agent by Clarot et al. [48]. In following work, Li et al. used CE method with added polymer additives as sieving medium to BGE for size determination of CdSe/ZnS QDs and observing the influence of different concentration of polymer to separation resolution, concentration of BGE, and pH. Novelty of this work was mathematical formula for size calculation, which relied on correlation between electrophoretic mobility and QD size. Confirmation of formula accuracy was done by transmission electron microscopy method [49].

Interesting work was done by Oswaldowski group [50], where they have used MEKC and CZE to separate mixture of CdSe QDs coated with cationic, anionic, and nonionic surfactants. The method is relied on the formation of bilayer between hydrophobic trioctylphosphineoxide (TOPO) and ionic and nonionic surfactants and gives a possibility of monitoring interactions between these layers. Oswaldowski group have also done research using preconcentration and micellar plug as a new method for analysis of QDs surface modified with amphiphilic, bidentate ligands, and biologically active molecules, which give QDs neutral or charged surface [51–53]. Besides, the role of ligands on growth rate and size distribution of CdTe QDs was monitored by micellar electrokinetic CE with LIF detector and it was confirmed that proper ligands give QDs bigger size, but narrower size distribution [54].

An interesting analysis of BSA-coated QDs was done by Bucking et al. [55]. A preparation method for BSA-coated CdSe/ZnS, ZnS:Mn^{2+}/ZnS and InP/ZnS core/shell QDs was described and their electrophoretic properties were compared. Characterization was done in combination of agarose gel electrophoresis, dynamic light scattering, laser Doppler electrophoresis, and isotachophoresis methods. It was assumed that a negative charge observed in CdSe/ZnS and ZnS:Mn^{2+}/ZnS QDs originated from the crystals due to defects in the crystal's lattice. This behavior was not observed in InP/ZnS QDs, probably due to a more covalently assembled lattice with fewer defects. Finally, InP/ZnS QDs showed almost the same behavior as the CdSe/ZnS QDs, both particles could be water-soluble without affecting their colloidal stability, confirming the successful conjugation to BSA, which attracted attention as possible coating because of solubility in concentrated salt solutions, low cost, and variety of functional groups capable of interaction.

However, the best resolution for QDs separation, whose surface was modified with trioctylphosphine oxide/trioctylphosphine (TOPO/TOP) and SDS, was done by Carrillo-Carrion et al. using MEKC. Authors separated QDs with 0.5 nm difference in diameter and 19 nm difference in luminescence emission maximum [56]. The summary of CE conditions employed for QD analysis is given in Table 1.

3 CE of bioconjugated QDs

As it was aforementioned, after preparation of quantum dots, their surface has to be capped, functionalized, and/or bioconjugated. Applying surface modification and bioconjugation on QDs certainly affects their characteristics important for CE analysis, such as size, charge, and therefore electrophoretic mobility. Selected bioconjugation strategies are schematically demonstrated in Fig. 2.

Pioneers in this work were Huang et al., who observed QDs capped with mercaptoprotionic acid as ligand and coupled with BSA and horseradish peroxidase (HRP). The authors efficiently separated bioconjugated QDs and free QDs adjusting buffer's pH foreseeing that CE-LIF will be used in further investigations of bioconjugated QDs [57]. QDs were coupled to BSA via electrostatic attraction and to HRP via covalent conjugation using EDC reagent. The E% of QD–BSA conjugation was about 54.9% and the splitting peak profiles for BSA–CdTe QDs were caused by BSA isoforms. In the case of HRP-QD conjugates, it was observed that with increased buffer pH, the negative charges of the QD bioconjugate increased. With the decrease in buffer pH, the negative charges of the QD bioconjugate were reduced, and the QD bioconjugates migrated slower than free QDs. The E% was calculated to be 91.7%, and this result illustrated that HRP was successfully labeled with QDs using EDC.

Application of QDs as fluorescent label in immunoassay was reported for the first time by Feng et al. [58]. QDs were conjugated with antibody and subsequently tested by electrophoretic separation of free antibody and antibody–antigen complex. Satisfactory separation of complex from free antibody could be achieved with 20 mM sodium tetraborate as separation buffer, at pH 9.8. On three differently bioconjugated QDs — with streptavidin, biotin, and IgG — Vicente and Colon showed using CE-LIF that electrophoretical mobility is dependent on biomolecule attached on QDs, and using polymeric additives can improve the resolution of bioconjugates. The group was also observing separation of bioconjugated QDs with different emission maxima using one excitation source. Besides, this was first reported separation of three differently bioconjugated QDs, because, only separation of QDs and bioconjugated QDs has been performed since than [59].

After this successful bioconjugation QDs with antibodies, more research have followed from other authors showing that QDs have a bright future as fluorescent label in immunoassay probes. Wang et al. reported how QDs enhanced immunoassay for the detection of antibenzo(a)pyrene diol epoxide-DNA adducts in lung cancer. Authors prepared QD-antibody-DNA complex and using CE-LIF method they showed how the formed complex can be not only successfully separated but also focused by the method [60]. Liskova

Table 1. Summary of CE methods and separation parameters applied for analysis of QDs and their bioconjugates

QDs type	CE method	BGE	Capillary parameters l_{eff}/l_{tot};ID	Capillary coating	Detection	References
CdTe-MPA	CGE	2xTB (178 mM Tris and 178 mM boric acid (pH 8.8), 5% PAA)	30/40 cm; 75 μm	Linear polyacrylamide (PAA)	PDA; LIF	[44]
CdTe/CdS-MPS (ADS620), CdSe/ZnS carboxylic acid (T2-Evitag)	CZE	Sodium phosphate (5–25 mM, pH 7.5–11)	42/49.5 cm; 51 μm	Uncoated fused-silica	UV; LIF	[45]
CdSe/ZnS/SiO2	CZE	17.5, 8.74, 4.37 mM Britton Robinson buffer pH 9.0	20/27 cm; 18.7/25.7 cm; 17.8/24.4 cm; 75 μm	Uncoated fused-silica	UV	[46]
CdTe/ZnS with thiogycolic acid	CZE	25 mM borate pH 8.5	30/37 cm; 75 μm	Uncoated fused-silica	UV, PDA	[48]
CdSe/ZnS	CGE	25 mM tetraborate (pH 9.2) water-soluble polymeric additive (PEG, PVP, PVA)	35/60 cm; 75 μm	Uncoated fused-silica	LIF	[49]
CdSe/TBP/TOPO//SDS, CdSe/TBP/TOPO//N101, CdSe/TBP/TOPO//CTAB	MEKC/CZE	20–100 mM SDS or CTAB, 10 mM sodium tetraborate/ 20 mM sodium tetraborate buffer (pH 9.2)	60/70 cm; 75 μm	Uncoated fused-silica	PDA	[50]
CdSe NCs with dihydrolipoic acid, 1,10-phenathroline derivative, DNA oligomer	MEKC/CZE	50 mM SDS with 10 mM sodium tetraborate/10 mM sodium tetraborate pH 9.4; 5 or 10 mM sodium tetraborate, pH 9.4 by adding methanol or ACN in the range up to 40% v/v	60/70 cm; 75 μm	Uncoated fused-silica	PDA	[51, 53]
CdSe/ZnS with dihydrolipoic acid and/or α-diimine derivatives	MEKC/CZE	50 mM SDS with 10 mM sodium tetraborate;75 mM SDS with 10 mM sodium phosphate/20 mM potassium chloride pH 6.0	60/70 cm; 75 μm	Uncoated fused-silica	PDA	[52]
CdTe/ZnS with mercaptoacetic acid, l-cysteine (Cys) and reduced glutathione	MEKC	25 mM borate with 50 mM SDS pH 8.5	50/57 cm, 75 μm	Uncoated fused-silica	LIF	[54]
CdSe/ZnS/BSA, InP/ZnS/ BSA	Agarose GE/ITP	Tris–glycine buffer, gel (running buffer and sample buffer ((5 stock solution, 50% glycerine in Tris–glycine buffer))/leading electrolyte: 60 mM Tris pH 9.1; terminating electrolyte: 25 mM glycine	N/A	N/A	Conductivity and UV	[55]

l_{eff}: effective length of the capillary; l_{tot}: total length of the capillary; MPA: mercaptopropionic acid; MPS: sodium mercaptoproprionate; PDA: photodiode array detectors; TB: Tris-boric acid buffer; TBP: tributylphosphine.

et al. pointed out the importance of the binding way of QDs and proteins, emphasizing antibodies, in the immunoluminescence probes. In this paper, the authors observed and optimized conjugation of QDs and antibodies via two different zero-length cross-linkers, long-chain linkers, and highly specific linkers, concluding that the best choice are highly specific linkers, which do not compromise effective usage of antibodies what can happen with nonselective linkers [61]. The same group of authors prepared QDs–ovalbumin complex and observed creating antigen–antibody complex and its separation from free conjugates of QDs in the following paper [62]. The obtained CE-LIF electropherograms clearly showed the successful QDs and antiovalbumin interactions (Fig. 3A).

Biomolecules with QDs are usually bonded through strong covalent bonds, but Shi et al. gave a new way of bonding them by simple adsorption of antibodies on the QD's surface. Characterization was done by CE-LIF, fluorescence spectrometry, and fluorescence correlation spectroscopy and these QDs had high luminescence, small radii, and good stability in aqueous environment [63].

The simple adsorption of antibodies on the QDs surface as well as commonly used bioconjugation via organic linkers such as 1-ethyl-3-(3-dimethylaminopropyl)carbodiimide

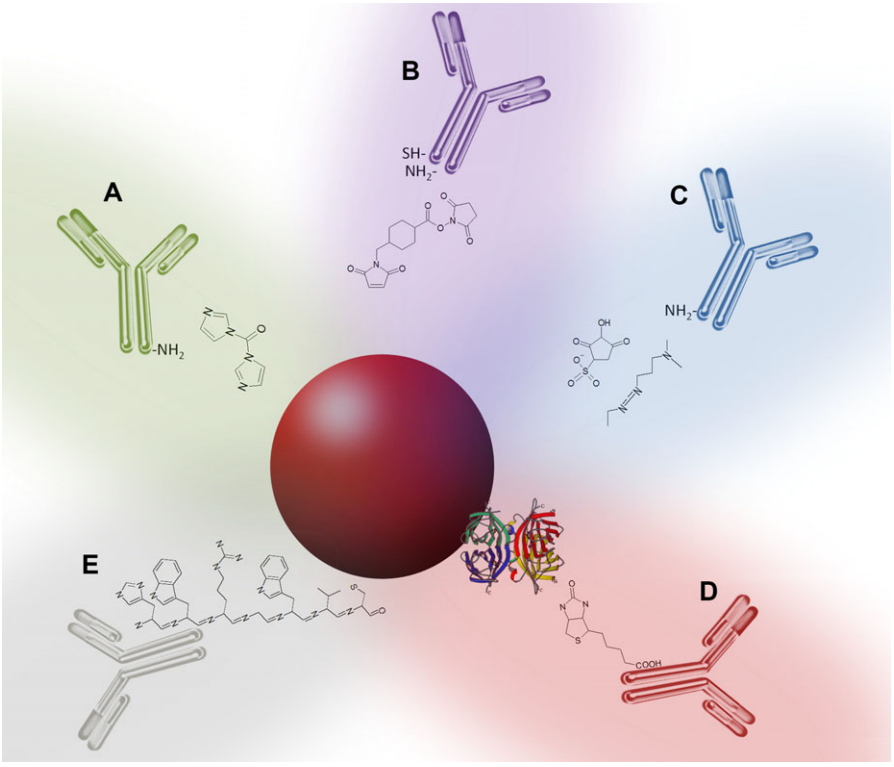

Figure 2. Summary of QD–antibody conjugation strategies. The conjugation serves as surface modification of dots to further bind antibodies. The following substances are used for this purpose: (A) carbonyldiimidazole, (B) succinimidyl 4-[*N*-maleimidomethyl]-cyclohexane-1-carboxy, (C) EDC/sulfo-NHS, (D) biotin-streptavidin, and (E) heptapeptide HWRGWVC. All of these strategies are based on the affinity of antibodies with the mentioned compounds. Sulfo-NHS: *N*-hydroxysulfosuccinimide.

(EDC) or two-step procedure combining EDC with *N*-hydroxysulfosuccinimide may lead to the inactivation of the antibody due to the sterically inappropriate binding. This was addressed in the work of Janu et al. [64], where an artificial peptide was used as a linker with specificity to the Fc fragment of the antibody and therefore active site remained active (Fig. 3B). Moreover, the important aspect investigated by Wang et al. was the influence of p*I* of biomolecule as well as pH of the used buffer and it was showed that efficiency of biomolecule–QDs conjugation is highly dependent of this values and CE-LIF and fluorescence correlation spectroscopy as suitable methods for observation [65]. Later, the bioconjugation of QDs with a short oligonucleotide sequence via streptavidin–biotin linkage was demonstrated by Stanisavljevic et al. employing the CE-LIF and CE-UV for the evaluation of the interaction process [66]. Bioconjugation possibilities are summarized in Table 2.

4 Detection modification using QDs

QDs with their great fluorescent properties can enhance CE detection of the samples in many different scientific fields, what will be subject of the following chapter. Relaying on successful application of QDs in immunoassay, possible usage of QDs in fluorescence resonance energy transfer (FRET) analysis was next challenge. In the literature in FRET as energy-transfer processes, QDs are playing role of energy donors. Li's group reported FRET analysis based on QDs as donor–acceptor system. Two different QDs were attached to antibody and antigen whose strong affinity brings QDs close enough to make FRET. CE-LIF was successfully applied in this work [67]. A combination of in-cuvette fluorescent analysis and CE with fluorescent detection (CE-FL), Wang and Xia observed binding process between Cy5-labeled polyhistidine peptide denderimer and glutathione-capped CdSe QDs and proofed CE-FL as a powerful analytical method [68]. In the following paper, the same authors observed amide bond cleavage by a specific protease based on FRET and monitored it by CE-FL [69]. Inspired with variety of biomolecules conjugated with QDs, Wang et al. brought a new idea of detecting residues of glucose. The authors conjugated QDs with concanavalin (con A), lectinprotein, which react with specific sugar residues. CE-LIF was used for validation of "one-step" and "two-step" conjugation procedure between con A and QDs mediated by glutaraldehyde [70].

Li et al. work combine QD and CE in DNA mutations analysis improving conventional molecular beacon methods. QD molecular beacon probes measured by CE are more sensitive, accurate, have low sample consumption, and provide simultaneous multiplex detection [71]. Metal-enhanced fluorescent effect is very promising, particularly Ag and Au nanoparticles enhancing strength of the electromagnetic field increase the fluorescence of nearby fluorophores. This phenomenon was used by the same authors enhancing QDs fluorescent with Au nanoparticles. Needed distance was provided by modifying particles with the wanted base numbers of two complementary DNA oligonucleotides. This method was successfully monitored by CE-LIF [72]. Zhao et al. used characteristics of QDs to enhance CE-chemiluminescence

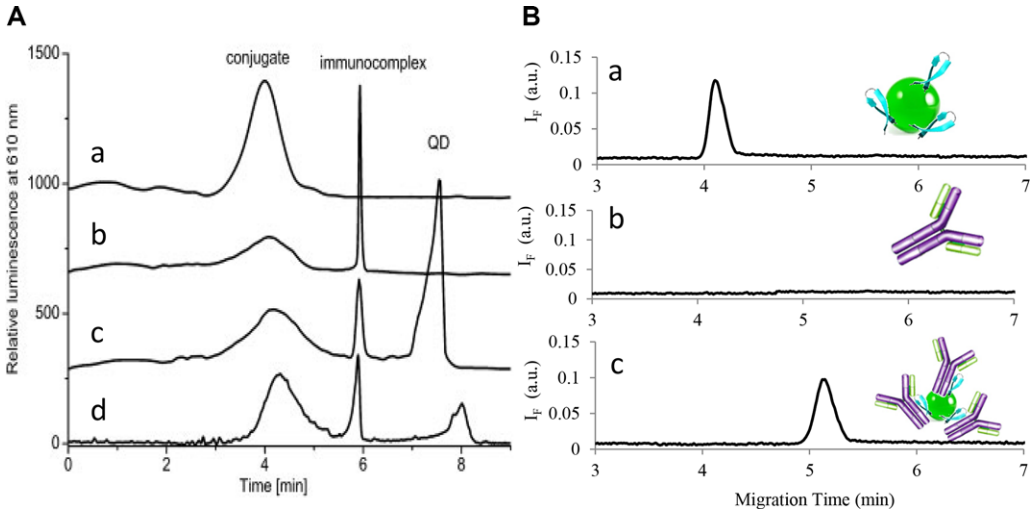

Figure 3. (A) CE-LIF of (a) HWRGWVC-QDs, (b) human immunoglobulins, and (c) their bioconjugate. Experimental conditions—excitation: 488 nm, emission: 520 nm, capillary: 75 μm id, 47.5 cm/40 cm, BGE: 20 mM sodium borate, pH 9.2, voltage: +20 kV, injection: 3.4 kPa, 20 s. (B) CE-LIF electropherograms of crude reaction mixture after conjugation between QDs and antiovalbumin, the same mixture after the addition of ovalbumin and free QDs. (a) Conjugate of 3.5 nm CdTe QDs (emission maximum 610 nm) with antiovalbumin. (b) Formation of immunocomplex with equimolar amount of ovalbumin. (c) Standard addition of free QDs at concentration 1.2×10^{-5} M. (d) Conjugate of QDs with ovalbumin. Formation of immunocomplex with equimolar amount of antiovalbumin (conditions are the same as in b and c) and addition of free QDs. Separation conditions: BGE 0.1 M Tris/TAPS at pH 8.3. Bare silica-fused capillary: id 75 mm, effective/total length 15/25 cm. Excitation at 488 nm (Ar-ion laser), detection at 610 nm. Separation and injection voltage: 6 kV. Reprinted with permission from [62].

Table 2. Summary of biomolecules conjugated to QDs and interactions used for bioconjugation

Molecule	Bonding via	CE mode	References
BSE	Electrostatic attraction	CE-LIF	[57]
Horseradish peroxidase	1-Ethyl-3-(3-dimethylaminopropyl) carbodiimide hydrochloride, EDC	CE-LIF	[57]
Human IgM	Succinimidyl 4-[*N*-maleimidomethyl]-cyclohexane-1-carboxylate (SMCC) and DTT	CE-LIF	[58]
Streptavidin	An active ester coupling reaction	CE-LIF	[59]
Biotin	Carbodiimide-mediated coupling reaction	CE-LIF	[59]
IgG	SMCC and DTT	CE-LIF	[59]
Goat F(ab′)2 anti-mouse IgG secondary antibody	EDC/sulfo-NHS	CE-LIF	[60]
Antiovalbumin	EDC/sulfo-NHS	CE-LIF	[61, 62]
Antiovalbumin	Carbonyldiimidazole	CE-LIF	[61]
Antiovalbumin	Sulfo-SMCC	CE-LIF	[61]
Antiovalbumin	Oxidized antibody glycans	CE-LIF	[61]
Epidermal growth factor receptor antibody	Adsorption affinity	CE-LIF	[63]
Human IgG	Short artificial peptide—HWRGWVC	CE-LIF, CE-UV	[64]
Proteins (AFP1A6, AFP2A5, streptavidin, Erbitux, and peroxidase)	EDC/sulfo-NHS	CE-LIF	[65]
Cancer sequence BCL-2	Streptavidin-biotin linkage	CE-LIF, CE-UV	[66]
Viral hepatitis B virus	Streptavidin-biotin linkage	CE-LIF, CE-UV	[66]

AFP1A6: mouse anti-human alpha-fetoprotein antibody; AFP2A5: mouse anti-human alpha-fetoprotein antibody; BCL-2: B-cell lymphoma 2; Erbitux: commercial name of the epidermal growth factor receptor (EGFR) antibody; Sulfo-NHS: *N*-hydroxysulfosuccinimide.

detection of neurotransmitters such as dopamine and epinephrine.

Obtained results indicate that chemiluminescence detection signal increased with the increasing of QDs size. This improved and simplify detection of these neurotransmitters is important as indicators of mental diseases such as multiple sclerosis, and/or Parkinson's disease [73].

Today, one of the wide-spread concerns of human population is usage of chemical treatments in agriculture and food industry. This is why rapid and efficient way of their

detection is asked. QDs and CE-LIF with their characteristics are promising methods for analysis of these substances. Chen and Fung used CE and QDs for detection of organophosphorus pesticides in tomato. Procedure involve immobilization of QDs onto the capillary wall and making mercaptopropyltrimethoxysilane network, this method is called MEKC-QD/LIF method. The method gave very good results by detecting ten times lower concentration than maximum residue levels allowed by Codex Alimentarius Commission [74]. The principle of this method is taking the advantage of the enhancement of the QD fluorescence by interaction with organophosphorus pesticides and when they are passing through the detection window. Moreover, the resolution of the separation was increased by using SDS as a buffer additive and therefore MEKC principle was introduced.

Recently, it has been proven that QDs may be utilized also as a fluorescent agent in the indirect LIF detection [75]. By this method, nicotinyl pesticide residues in vegetables were determined in carrot, cucumber, and tomato. Also in this case, the SDS was utilized as a buffer modifier.

Another food industry application is for detection of acrylamide or 2-propenamide contaminants occurring in products prepared by high temperature, in this case potato crisps. The issue of detection of contaminants was its weak UV absorption. QDs as fluorescent labeling material in combination with LIF as detector solved the lack of UV absorption. QD–acrylamide complex was analyzed by MEKC-QD/LIF method as in the previous case [76].

Beside pesticides and contaminants, propylpareben, sodium dehydroacetate, sorbic acid, benzoic acid, and sodium propionate as food preservatives were determined by CE and QDs as background substance [77] as well as analysis plant peptide hormone from tomato called systemin [78].

In aforementioned description of QD's characteristics, one of the concerning facts is their influence on environment. Celiz et al. described how CE-LIF can be powerful method for studying of the interaction between QDs and humic substances (humic and fluvic acids) in waters. To follow quantitative information of free zinc or cadmium ICP-MS in combination with CE-LIF was used. Data obtained from research showed that there is no degradation of QDs in the environment, but they do not exclude influence of sunlight and other environment parameters which have not been considered here [79].

5 Conclusion

QDs have already found wide applications in different scientific fields. Following rapid growth of technology they are one of the most promising nanoparticles. Taking into consideration the great size-dependent characteristics and high luminescence of QDs, CE as analytical method is very suitable for their analysis, especially in combination with LIF detector. High separation efficiency of CE and its relative methods is enabling detail investigations on the interaction mechanisms between QDs and biomolecules and it is also beneficial for characterization of the nanoparticles during their routine production.

Moreover, the employment of semiconductors light sources such as high-power LEDs and/or laser diodes covering nearly the whole range of wavelengths is advancing significantly the miniaturization process. Chip-based CE with LED (laser diodes)-induced florescence detection is pushing the progress toward portable instruments and therefore the application of fluorescent tags is inevitable. Such miniaturization may decrease the size of analytical instruments to the hand-held appliances which enables the realization of the point-of-care concept in practice. Furthermore, the broad excitation band of QDs is extremely beneficial for multicolor labeling because only single-wavelength excitation source is needed. The fact that the excitation wavelength of the most QDs is close to 400 nm is moreover beneficial due to the fact that the emission wavelengths of currently commercially available high-power LEDs are currently approaching 400 nm.

Improvements in QDs synthesis and its application are followed with research about their toxicity and deleterious effect on living systems. Cadmium accumulates in the liver, bones, and kidneys. Exposure of QDs cadmium core to UV light or air will cause surface oxidation and release free cadmium ions that have harmful effect. Nevertheless, in the existing research it is also proven that ZnS layer and coating can provide safe longtime measurements in vitro [80]. When we are talking about harmful effect of QDs, cadmium every day consumption data should be taken into consideration. Cadmium is a common pollutant in environment caused by nature (volcano activity, erosions, etc.) and mainly human (smoking, mining, fossil fuel combustion, phosphate fertilizers, electronic and municipal waste, etc.) activity. In 2010, World Health Organization and Food and Agriculture Organization established a provisional tolerable monthly intake for cadmium of 25 μg/kg body weight. Concentration of cadmium in a cigarette smoke is not negligible and it is within the range from 1000 to 3000 μg/kg [81, 82]. From one pack of cigarettes, which contains 20 cigarettes, 2–4 μg of Cd deposits into the smokers lungs and some of it is released into the air [83]. A moral dilemma in science is: could we use QDs knowing risks for human health? Hitherto research with QDs benefits has advantage over their toxicity. Neither possibility of releasing free cadmium ions should be overlooked nor QDs numerous advantages.

The financial support of the following project IGA TP1/2013 is highly acknowledged. M.V. wishes to express her thanks to project CZ.1.07/2.3.00/30.0039 for financial support.

The authors have declared no conflict of interest.

6 References

[1] Hanus, M. J., Harris, A. T., *Prog. Mater. Sci.* 2013, *58*, 1056–1102.

[2] Duran, N., Marcato, P. D., *Int. J. Food Sci. Technol.* 2013, *48*, 1127–1134.

[3] Banyal, S., Malik, P., Tuli, H. S., Mukherjee, T. K., *Curr. Opin. Pulm. Med.* 2013, *19*, 289–297.

[4] Qu, X. L., Brame, J., Li, Q. L., Alvarez, P. J. J., *Accounts Chem. Res.* 2013, *46*, 834–843.

[5] Fouda, M. M. G., Abdel-Halim, E. S., Al-Deyab, S. S., *Carbohydr. Polym.* 2013, *92*, 943–954.

[6] Rhee, J. W., Wu, J. C., *Trends Cardiovasc. Med.* 2013, *23*, 39–45.

[7] Feynman, R. P., *Eng. Sci.* 1960, *23*, 22–36.

[8] Riehemann, K., Schneider, S. W., Luger, T. A., Godin, B., Ferrari, M., Fuchs, H., *Angew. Chem.-Int. Edit.* 2009, *48*, 872–897.

[9] Rao, C. N. R., Kulkarni, G. U., Thomas, P. J., Edwards, P. P., *Chem.-Eur. J.* 2002, *8*, 29–35.

[10] De, M., Ghosh, P. S., Rotello, V. M., *Adv. Mater.* 2008, *20*, 4225–4241.

[11] Sykora, D., Kasicka, V., Miksik, I., Rezanka, P., Zaruba, K., Matejka, P., Kral, V., *J. Sep. Sci.* 2010, *33*, 372–387.

[12] Lu, A. H., Salabas, E. L., Schuth, F., *Angew. Chem.-Int. Edit.* 2007, *46*, 1222–1244.

[13] Scida, K., Stege, P. W., Haby, G., Messina, G. A., Garcia, C. D., *Anal. Chim. Acta* 2011, *691*, 6–17.

[14] Cserhati, T., Szogyi, M., *Biomed. Chromatogr.* 2010, *24*, 1265–1272.

[15] Wiedmer, S. K., Jussila, M. S., Riekkola, M. L., *Trac-Trends Anal. Chem.* 2004, *23*, 562–582.

[16] Biricova, V., Laznickova, A., *Bioorganic Chem.* 2009, *37*, 185–192.

[17] Castagnola, M., Zuppi, C., Rossetti, D. V., Vincenzoni, F., Lupi, A., Vitali, A., Meucci, E., Messana, I., *Electrophoresis* 2002, *23*, 1769–1778.

[18] Mattoussi, H., Palui, G., Na, H. B., *Adv. Drug Deliv. Rev.* 2012, *64*, 138–166.

[19] Hines, M. A., Guyot-Sionnest, P., *J. Phys. Chem.* 1996, *100*, 468–471.

[20] Kuang, H., Zhao, Y., Ma, W., Xu, L. G., Wang, L. B., Xu, C. L., *Trac-Trends Anal. Chem.* 2011, *30*, 1620–1636.

[21] Tomczak, N., Janczewski, D., Han, M. Y., Vancso, G. J., *Prog. Polym. Sci.* 2009, *34*, 393–430.

[22] Byers, R. J., Hitchman, E. R., *Prog. Histochem. Cytochem.* 2011, *45*, 201–237.

[23] Sobrova, P., Blazkova, I., Chomoucka, J., Drbohlavova, J., Vaculovicova, M., Kopel, P., Hubalek, J., Kizek, R., Adam, V., *Prion* 2013, *7*, 349–358.

[24] Duan, J. L., Song, L. X., Zhan, J. H., *Nano Res.* 2009, *2*, 61–68.

[25] Ramanery, F. P., Mansur, A. A. P., Mansur, H. S., *Nanoscale Res. Lett.* 2013, *8*, 1–13.

[26] Shi, J. J., Wang, S., He, T. T., Abdel-Halim, E. S., Zhu, J. J., *Ultrason. Sonochem.* 2014, *21*, 493–498.

[27] Green, M., *J. Mater. Chem.* 2010, *20*, 5797–5809.

[28] Sperling, R. A., Parak, W. J., *Philos. Trans. R. Soc. A-Math. Phys. Eng. Sci.* 2010, *368*, 1333–1383.

[29] Wang, C., Jiang, Y., Zhang, Z. P., Liu, X. M., Li, S. Y., Chen, Y., Li, G. H., *J. Nanosci. Nanotechnol.* 2010, *10*, 5036–5041.

[30] Beri, R. K., Khanna, P. K., *J. Nanosci. Nanotechnol.* 2011, *11*, 5137–5142.

[31] Bera, S., Singh, S. B., Ray, S. K., *J. Solid State Chem.* 2012, *189*, 75–79.

[32] Sturzenbaum, S. R., Hockner, M., Panneerselvam, A., Levitt, J., Bouillard, J. S., Taniguchi, S., Dailey, L. A., Khanbeigi, R. A., Rosca, E. V., Thanou, M., Suhling, K., Zayats, A. V., Green, M., *Nat. Nanotechnol.* 2013, *8*, 57–60.

[33] Smith, A. M., Nie, S. M., *Accounts Chem. Res.* 2010, *43*, 190–200.

[34] Hoshino, A., Hanada, S., Yamamoto, K., *Arch. Toxicol.* 2011, *85*, 707–720.

[35] Morelli, E., Cioni, P., Posarelli, M., Gabellieri, E., *Aquat. Toxicol.* 2012, *122*, 153–162.

[36] Hauck, T. S., Anderson, R. E., Fischer, H. C., Newbigging, S., Chan, W. C. W., *Small* 2010, *6*, 138–144.

[37] Holgate, S. T., *J. Biomed. Nanotechnol.* 2010, *6*, 1–19.

[38] Han, X. L., Lai, L., Tian, F. F., Jiang, F. L., Xiao, Q., Li, Y., Yu, Q. Y., Li, D. W., Wang, J., Zhang, Q. M., Zhu, B. F., Li, R., Liu, Y., *Small* 2012, *8*, 2680–2689.

[39] Wang, L. L., Zheng, H. Z., Long, Y. J., Gao, M., Hao, J. Y., Du, J., Mao, X. J., Zhou, D. B., *J. Hazard. Mater.* 2010, *177*, 1134–1137.

[40] Ryvolova, M., Smerkova, K., Chomoucka, J., Hubalek, J., Adam, V., Kizek, R., *Electrophoresis* 2013, *34*, 801–808.

[41] Manz, A., Graber, N., Widmer, H. M., *Sens. Actuator B-Chem.* 1990, *1*, 244–248.

[42] Harrison, D. J., Manz, A., Fan, Z. H., Ludi, H., Widmer, H. M., *Anal. Chem.* 1992, *64*, 1926–1932.

[43] Saito, R. M., Coltro, W. K. T., de Jesus, D. P., *Electrophoresis* 2012, *33*, 2614–2623.

[44] Song, X. T., Li, L., Chan, H. F., Fang, N. H., Ren, J. C., *Electrophoresis* 2006, *27*, 1341–1346.

[45] Pereira, M., Lai, E. P. C., Hollebone, B., *Electrophoresis* 2007, *28*, 2874–2881.

[46] Pyell, U., *Electrophoresis* 2008, *29*, 576–589.

[47] Ohshima, H., *J. Colloid Interface Sci.* 2001, *239*, 587–590.

[48] Clarot, I., Wolpert, C., Morosini, V., Schneider, R., Balan, L., Diez, L., Leroy, P., *Curr. Nanosci.* 2009, *5*, 154–159.

[49] Li, Y. Q., Wang, H. Q., Wang, J. H., Guan, L. Y., Liu, B. F., Zhao, Y. D., Chen, H., *Anal. Chim. Acta* 2009, *647*, 219–225.

[50] Oszwaldowski, S., Zawistowska, K., Grigsby, L. K., Roberts, K. P., *Cent. Eur. J. Chem.* 2010, *8*, 806–819.

[51] Oszwaldowski, S., Zawistowska-Gibula, K., Roberts, K. P., *Anal. Bioanal. Chem.* 2011, *399*, 2831–2842.

[52] Oszwaldowski, S., Zawistowska-Gibula, K., Roberts, K. P., *Cent. Eur. J. Chem.* 2011, *9*, 572–584.

[53] Oszwaldowski, S., Zawistowska-Gibula, K., Roberts, K. P., *Microchim. Acta* 2012, *176*, 345–358.

[54] Zhang, Y. H., Zhang, H. S., Ma, M., Guo, X. F., Wang, H., *Appl. Surf. Sci.* 2009, *255*, 4747–4753.

[55] Bucking, W., Massadeh, S., Merkulov, A., Xu, S., Nann, T., *Anal. Bioanal. Chem.* 2010, *396*, 1087–1094.

[56] Carrillo-Carrion, C., Moliner-Martinez, Y., Simonet, B. M., Valcarcel, M., *Anal. Chem.* 2011, *83*, 2807–2813.

[57] Huang, X. Y., Weng, J. F., Sang, F. M., Song, X. T., Cao, C. X., Ren, J. C., *J. Chromatogr. A* 2006, *1113*, 251–254.

[58] Feng, H. T., Law, W. S., Yu, L., Li, S. F. Y., *J. Chromatogr. A* 2007, *1156*, 75–79.

[59] Vicente, G., Colon, L. A., *Anal. Chem.* 2008, *80*, 1988–1994.

[60] Wang, Z. X., Lu, M. L., Wang, X. L., Yin, R. C., Song, Y. L., Le, X. C., Wang, H. L., *Anal. Chem.* 2009, *81*, 10285–10289.

[61] Liskova, M., Voracova, I., Kleparnik, K., Hezinova, V., Prikryl, J., Foret, F., *Anal. Bioanal. Chem.* 2011, *400*, 369–379.

[62] Kleparnik, K., Voracova, I., Liskova, M., Prikryl, J., Hezinova, V., Foret, F., *Electrophoresis* 2011, *32*, 1217–1223.

[63] Shi, C., Huang, X. Y., Dong, C. Q., Chen, H. J., Ren, J. C., *Chin. Chem. Lett.* 2009, *20*, 1119–1122.

[64] Janu, L., Stanisavljevic, M., Krizkova, S., Sobrova, P., Vaculovicova, M., Kizek, R., Adam, V., *Electrophoresis* 2013, *34*, 2725–2732.

[65] Wang, J. J., Huang, X. Y., Zan, F., Guo, C. G., Cao, C. X., Ren, J. C., *Electrophoresis* 2012, *33*, 1987–1995.

[66] Stanisavljevic, M., Janu, L., Smerkova, K., Krizkova, S., Pizurova, N., Ryvolova, M., Adam, V., Hubalek, J., Kizek, R., *Chromatographia* 2013, *76*, 335–343.

[67] Li, Y. Q., Wang, J. H., Zhang, H. L., Yang, J., Guan, L. Y., Chen, H., Luo, Q. M., Zhao, Y. D., *Biosens. Bioelectron.* 2010, *25*, 1283–1289.

[68] Wang, J. H., Xia, J., *Anal. Chem.* 2011, *83*, 6323–6329.

[69] Wang, J. H., Xia, J., *Anal. Chim. Acta* 2012, *709*, 120–127.

[70] Wang, J. H., Li, Y. Q., Zhang, H. L., Wang, H. Q., Lin, S., Chen, J., Zhao, Y. D., Luo, Q. M., *Colloid Surf. A-Physicochem. Eng. Asp.* 2010, *364*, 82–86.

[71] Li, Y. Q., Guan, L. Y., Wang, J. H., Zhang, H. L., Chen, J., Lin, S., Chen, W., Zhao, Y. D., *Biosens. Bioelectron.* 2011, *26*, 2317–2322.

[72] Li, Y. Q., Guan, L. Y., Zhang, H. L., Chen, J., Lin, S., Ma, Z. Y., Zhao, Y. D., *Anal. Chem.* 2011, *83*, 4103–4109.

[73] Zhao, Y. S., Zhao, S. L., Huang, J. M., Ye, F. G., *Talanta* 2011, *85*, 2650–2654.

[74] Chen, Q. D., Fung, Y. S., *Electrophoresis* 2010, *31*, 3107–3114.

[75] Chen, G. H., Sun, J., Dai, Y. J., Dong, M., *Electrophoresis* 2012, *33*, 2192–2196.

[76] Chen, Q. D., Zhao, W. F., Fung, Y. S., *Electrophoresis* 2011, *32*, 1252–1257.

[77] Guo, D. S., Chen, G. H., Tong, M. Z., Wu, C. Q., Fang, R., Yi, L. X., *Chin. J. Anal. Chem.* 2012, *40*, 1379–1384.

[78] Bai, Y., Du, F. Y., Yang, Y. Y., Liu, H. W., *J. Sep. Sci.* 2011, *34*, 2893–2900.

[79] Celiz, M. D., Colon, L. A., Watson, D. F., Aga, D. S., *Environ. Sci. Technol.* 2011, *45*, 2917–2924.

[80] Derfus, A. M., Chan, W. C. W., Bhatia, S. N., *Nano Lett.* 2004, *4*, 11–18.

[81] Watanabe, T., Kasahara, M., Nakatsuka, H., Ikeda, M., *Sci. Total Environ.* 1987, *66*, 29–37.

[82] Viana, G. F. D., Garcia, K. S., Menezes, J. A., *Environ. Monit. Assess.* 2011, *181*, 255–265.

[83] Ashraf, M. W., *Sci. World J.* 2012, *2012*, 1–5.

[84] Krejcova, L., Nejdl, L., Merlos Rodrigo, M. A., Zurek, M., Matousek, M., Hynek, D., Zitka, O., Kopel, P., Adam, V., Kizek, R., *Biosens. Bioelectron.* 2014, *54*, 421–427.

3.7 Review II

STANISAVLJEVIC, M.; VACULOVICOVA, M.; KIZEK, R.; ADAM, V. Quantum dots-fluorescence resonance energy transfer based nanosensors and their application

Participation in the work of the author Stanisavljevic M.: literature research 90% and manuscript preparation 70%.

Quantum dots have very importatnt role in the FRET based sensor designing usually as energy donors. Sensors designing to target specific biomolecules request appropriate interaction between QDs and biomolecules which further request suitable modification of the QDs as well as finding the best solution for its bioconjugation. In the review summarization of the latest novelty in sensors desingning follow latest achievements in the bioconjugation techniques as well as novelty in QDs surface modification are presented:

Quantum dots-fluorescence resonance energy transfer based nanosensors and their application

Maja Stanisavljevic[1], Marketa Vaculovicova[1,2], Rene Kizek[1,2], Vojtech Adam[1,2*]

[1]*Department of Chemistry and Biochemistry, Faculty of Agronomy, Mendel University in Brno, Zemedelska 1, CZ-613 00 Brno, Czech Republic, European Union*
[2]*Central European Institute of Technology, Brno University of Technology, Technicka 3058/10, CZ-616 00 Brno, Czech Republic, European Union*

***Corresponding author**
Vojtech Adam, Department of Chemistry and Biochemistry, Mendel University in Brno, Zemedelska 1, CZ-613 00 Brno, Czech Republic; E-mail: vojtech.adam@mendelu.cz; phone: +420-5-4513-3350; fax: +420-5-4521-2044

Content

1 Introduction

Nanotechnology is based on nanoscale materials and it is one of the most prominent technologies today whose growth brought numerous improvements and hopes into the science world. Novel nanomaterials have found their place in improvement of biosensors, also well-known and widespread technologies, and their sensitivity and performance. Biosensors classification is done according to multiple criteria like transduction mechanism and/or biorecognition principles [1]. In our focus will be biosensor with optical transduction mechanism or precisely speaking, based on fluorescence.

Fluorescence is a physical phenomena described for the first time by Sir David Brewster on the chlorophyll [2] and quinine by Sir John Herschel [3]. Today, a variety of very important analytical techniques based on fluorescence have been developed and used. Among them fluorescent spectroscopy and fluorescent microscopy stand out as the most precious techniques for biological application. Further fluorescence-based technique which rises great interest is fluorescence resonance energy transfer (FRET) as a specific mechanism of energy transfer between two molecules, called fluorophores, which can be easily excited with a photon. Understanding of biological processes at molecular level would be inconceivable without fluorophores, fluorescence and FRET technique. FRET has found wide application in chemistry [4-6], biology [7-10] and/or medicine [11-14].

FRET characteristics and a fact that it can be applied on molecular level measurements lined it up as the technique on which biosensors can be developed and by now it has been confirmed as suitable technique for biosensing. FRET-based sensors have not stayed unaffected by nanotechnology development. Nanoscale materials with their uniqueness have become a new challenge for biosensor designing. In this review we will give insight into development of FRET-based nanosensors after new nanomaterials have been implemented into sensor designing process.

2 FRET basics

FRET is acronym for Förster resonance energy transfer named according to its discoverer, German scientist Theodor Förster [15], the other commonly used synonym is fluorescence resonance energy transfer as it is aforementioned. In the presence of two fluorophores, the energy donor and acceptor, FRET will occur after fulfilling certain

conditions and the most important will be presented here. Detailed explanation of the fluorescence and FRET has been published in the past [16-18].

FRET involves non-radiative transfer of energy between donor and acceptor fluorophores, also called FRET pairs. Energy transfer between FRET pair is the result of long range dipole–dipole interaction between them and does not include a photon emission. FRET is strongly dependent of several parameters, such as:

- spectral overlap between the emission spectrum of the donor and absorption spectrum of the acceptor
- distance between the donor and acceptor molecules
- quantum yield and fluorescence lifetime of the fluorophores
- relative orientation of the donor-acceptor dipoles

FRET will occur when overlap of the emission spectrum of the donor and absorption spectrum of the acceptor is bigger than 30% and the distance is less than 10nm. Fulfilling this conditions the mutual dipole orientation will be satisfied as well [19]. The distance between FRET pair is not only defining will FRET occur or not but the efficiency of energy transfer have the same dependence of the distance and mathematically is expressed with the following equation:

$$E = R_o^6 / (R_o^6 + r^6)$$

where E is efficiency of energy transfer, R_o is Förster distance (the distance at which energy efficiency is 50%) and r is the donor-acceptor distance.

The others, but not less important properties are quantum yield and fluorescence lifetime of the fluorophores. Larger quantum yield means approaching to the unity and displaying the brighter emission and represents number of emitted photons relative to the number of absorbed. The more photons are emitted from the donor the better energy transfer will occur. Fluorescence lifetime, on the other hand, determined how long will fluorophore interact with the environment and provide emission information, or in other words it is average time that molecule spends in the excited state before relaxation [17].

Both of these properties are dependent on rates of radiative and non-radiative decay because they are tightly connected to depopulation of excited state which determinate fluorescent characteristic of the fluorophores [17, 20].

FRET can be detected by monitoring the acceptor fluorescence and/or the acceptor quenching. In FRET system quenching will be observed when the acceptor belongs to

the family of molecules called quenchers which after excitation are returned to their ground state via non-radiative decay pathways [21].

Due to aforementioned conditions that fluorophores have to achieve it is obvious that designing FRET encounter a lot of limitations and shortcomings as well as fluorophores as an inevitable part. Fluorophores shortcomings commonly observed are donor/acceptor spectral overlap, chemical and photochemical degradation, their tendency to react with environment and self-aggregation, short fluorescence lifetime, in general about 10 ns [20, 22]. Regarding improvement of their characteristics encapsulation in different materials was offered [23-24], but beside improvement of existing fluorophores, new nanomaterials have been explored and used for the sensing.

3 Quantum dots as new fluorophores. Quantum dots versus conventional organic fluorophores.

Regarding FRET one of the most interesting nanomaterials are nanoparticles, especially quantum dots (QDs). QDs are semiconductors made out of the elements from groups II and VI or groups III and V in PSE. They are known for their small size (1-10nm) and size-dependent optical and electronic properties caused by quantum confinement [25]. By now QDs have been confirmed as suitable alternative for fluorophores used in FRET based biosensors and other fluorescence techniques. They offer several advantages over organic dyes; some of them will be discussed according to FRET desirable characteristics and are presented in the table 1.

QDs as new generation of fluorophores have several advantages over conventional ones. Also, QDs have one characteristic unique to them and incomparable with organic fluorophores, it is the ability of tuning emission range as a result of core size regulation during synthesis follows quantum confinement. QDs broad excitation spectra and narrow defined emission peak allows multicolor QDs to be excited from one source without emission signal overlap [26-27], also 10-100 times lager molar extinction coefficient than fluorophores has as a result brighter spectra comparing the conventional fluorophores [28-29]. This induce large Stokes shift (difference between peak absorption and peak emission wavelengths) of QDs in a range of 300-400nm [30]. These advantages enable imaging and/or tracking multiple molecular targets at the same time as well as elimination of background autofluorescence. Background autofluorescence can emerge in biological samples causing detection of mixed signals

from autofluorescence and fluorophores fluorescence making a fluorescence lifetime of the fluorophore very important. QDs (20-50 ns lifetime) have superiority over fluorphores with their few nanoseconds fluorescence lifetime [31]. Synergy of these advantages will diminish autofluorescence in biological samples due to facts that large Stokes shift will make signal mixing unfeasible and QDs fluorescence lifetime will ensure that QDs emission last longer than background autofluorescence. Further notable advantage is high quantum yield from 40% to 90% and due to their inorganic core they are highly resistant to the photobleaching and/or chemical degradation [32-33].

QDs are not flawless, they suffer of luminescence intermittency known as blinking which can cause problems in applications and usually have been overcome by shell engineering and/or decreasing the excitation intensity [34-35], and then their inorganic nature and insolubility has been successfully diminished by different coating and capping agents. Since they are an order of magnitude bigger that organic dyes QDs sometimes are not so applicable if the probe size is important [31]. The major drawbacks are synthesis costs and high toxicity of the used precursors. Also, their overall toxicity remains a common subject of discussions and possible solution have been found in so called “green synthesis” [36-38] or biosynthesis [39-41] of QDs.

4 QD-FRET based sensor

4.1 QD-FRET sensors for nucleic acid

A very first QD-FRET based sensor for the detection of DNA was designed by Zhang et al. FRET system consisted streptavidin modified CdSe/ZnS QD with photoluminescence (PL) emission at 605nm (QD605) as energy donor and organic fluorophore Cy5 as energy acceptor. The sandwich hybrid was formed by binding complementary Cy5-labeled reporter probe and biotinylated capture probe with target DNA and hybrid is driven toward QDs surface via strong streptavidin-biotin affinity. Confocal fluorescence spectroscopy was used for measuring a photon burst whenever single nanosensor assembly passes through a diffraction-limited detection volume inside a microcapillary. It is established that 54 hybrids could be self-assembled on individual QD causing significant increase of the FRET efficiency and provide achievement of4.8 fM as LOD which was improvement comparing to the 0.48 pM obtained from molecular beacon. Designed sensor in combination with oligonucleotide ligation assay was successfully applied for detection of a point mutation characteristic for ovarian

tumors [42]. Further Chen et al. have successfully combined QD-FRET and single molecule detection (SMD) for detection of target DNA directly in solution and without prior separation or amplification [43]. Later, for improving detection sensitivity of previously formed QD-FRET based DNA sensor [42] Zhang et al. have conducted detection under the capillary microfluidic flow. The new conditions have shown significant improvement related to FRET efficiency, photobleaching prevention, higher sensitivity and lower sample consumption (~5 orders of magnitude less). Observed improvement of the FRET efficiency is caused by DNA deformation in the capillary [44]. Problem of the non-specific adsorption of DNA on the QDs surface is common problem in nucleic acid sensors design and Zhou et al. have offered solution in 11-mercaptoundecyl tri(ethylene glycol) alcohol **(**EG_3OH**)**/11-mercaptoundecyl tri(ethylene glycol) acetic acid (EG_3COOH**)**capped QDs, where introduced EG_3 group provided surface stabilization as well as prevention of non-specific adsorption of DNA. Target DNA was covalently attached to the (EG3OH)/(EG3COOH) capped QDs through carboxyl-to-amine crosslinker and was used as energy donor while Alexa 594 labeled complementary DNA was energy acceptor in the designed system. Further they have shown that target DNA attached to (EG3OH)/(EG3COOH) capped QDs could be used for detection of the non-labeled complementary DNA by introduction of a double-stranded DNA intercalating dye, such as ethidium bromide (EB). During the hybridization process EB was intercalated into double-strand hybrid and upon QDs excitation FRET occurred between QDs and EB. Authors have successfully designed system suitable for the detection of labeled as well as non-labeled DNA with sensitivity of 1nM measured on a conventional fluorimeter [45]. Further Algar et al. likewise [45] have designed system with two different color QDs as donors and EB as energy acceptor showing that EB can be used even for multiple detections of DNA, while usual QDs-FRET based sensors for simultaneous detection of two different targeted DNA consisted green MAA-capped CdSe/ZnS QDs and target sequences of spinal muscular atrophy labeled Cy3 and red MAA-capped CdSe/ZnS QDs with Alexa Fluor 647-labeled target sequence for detection of *E.coli* [46]. The simplicity of electrostatic attraction was used by Peng et al. to bring the donor and acceptor into the proximity which enables FRET to occur. They have used cationic polymer, poly(diallyldimethylammonium chloride (PDADMAC) as an electrostatic linker between blue TGA capped CdTe QDs and Cy3 labeled single stranded DNA(Cy3-ssDNA) as energy donor and acceptor respectively. In the presence of the sample DNA

and after hybridization process occurred decrease of QDs/Cy3-ssDNA PL was observed, due to more rigid structure of dsDNA which increase distance between donor and acceptor [47]. Still decreased PL was observed due to aggregation of QDs caused by hybridization. Improved positively charged DHLA-2,2'-(ethylenedioxy)bis(ethylamine)–derived ligand (DEDEA) and polyethylene glycol (PEG5000) modified CdSe/ZnS QDs were used by Lee et al. for formation of an electrostatic complex with negatively charged ssDNA labeled with carboxytetramethylrhodamine-TAMRA without the QDs aggregation due to charge neutralization after hybridization as aforementioned major drawback [48].

Mostly in the QD-dye FRET systems, QDs as energy donors contribute to the increase of dye's fluorescence used for detection. In the system designed by Mao et al. QDs were used for dye fluorescence quenching and its recovery was used for detection. This characteristic behaviour was observed when CdS QDs interacted with acridine orange (AO), a DNA intercalating dye. However, in the presence of calf thymus DNA (ctDNA), ctDNA and AO created a binary ion-association of AO-ctDNA resulting in AO fluorescence recovery. Further QD-AO interaction was prevented by electrostatic repulsion between ctDNA and QDs [49]. In existing sensors chemical conjugation between target nucleic acid and labeling dye always occurs, but there are environments, such as intracellular, where chemical interaction is impossible. Vannoy et al. were focused in designing the system which will enable detection of nucleic acid in these conditions. They proposed a competitive displacement-based assay. The system consisted CdSe/ZnSQD$_{605}$conjugated to the Alexa Fluor 647 (A647) labeled double stranded DNA (dsDNA) via streptavidin-biotin linkage while dsDNA system was consisted of the ssDNA probe hybridizated with 18-mer long reporter with three base-pair mismatches and labelled with A647 quenched the PL of QDs (Figure 1.). The presence of the 98-mer ssDNA fully complementary to the ssDNA probe caused displacement of the 18-mer reporter and recovery of the QDs PL. Loading capacity of QDs to dsDNA was 1:6 in molar ratio [50].

DNA-triggered dye transfer designed by Michaelis et al. was a big step forward as a solution for spectral cross-talk between QDs and dye as well as lack of the needed distance. Sensor consisted 3′-thiolated oligonucleotide labeled with cyanine dye used as dye donor and oligonucleotide attached to the QDs surface via streptavidin-biotin affinityat it 3′-end and at 5′-end had cysteine moiety which was used as dye acceptor. In the presence of a complementary nucleic acid, after the hybridization, transfer of the

linked fluorophore from the oligonuclotide dye donor to theoligonucleotide dye acceptor occrred via a native chemical ligation-type mechanism providing bigger proximity between QDs and dye and consequently improving FRET efficiency. System was successfully applied on the DNA-analogous peptide nucleic acids (PNA) which binds complementary DNA and RNA strands with improvedaffinity [51].

The discovery of small interfering RNA (siRNA) has brought new hope in the therapy of diseases, such as cancer, genetic disorders and viral infections, which could be based on gene therapy. siRNAs also known as short intefering RNA and/or silencing RNA are a double-stranded RNA, usually 20-25 base pairs in length. They are part of RNA interference (RNAi) pathway in which they interfere with the gene expression causing messager RNA (mRNA) desintegration after transcription and disrupting translation process. Bakalova et al. have reported a QD-FRET based nanosenor for the screening of siRNAs with high accessibility and affinity to the respective mRNA target. FRET system was based on CdSe/ZnS QDs as energy donors and organic fluorophores Cy5 as energy acceptor where QDs were conjugated with single-stranded siRNA (ss/siRNA) through carbodiimide chemistry and target mRNA was amplified in the presence of Cy5-labeled oligonucleotides. FRET signal was observed after formation of the siRNA/mRNA complex by hybridization while in case of mismatched siRNA FRET signal was not detectable [52]. Further two QD-FRET based nanosensors for intracellular tracking of siRNA have been reported by Lee et al. For investigation of endocytic cellular uptake, subcellular trafficking and unpacking of Cy5-siRNA complex they have used FRET system with positively charged polyethylenimine (PEI) modified QDs and Cy5-labeled vascular endothelial growth factor siRNA (cy5-VEGF siRNA) and for observation of the ability of Cy5-siRNA complex endocytic cellular uptake without using ATP, FRET system was consisted out of protein transduction domain (Hph-1) peptide labeled with Cy5 and PEI-QDs [53]. Beside siRNA a lot of attention was given to the micro RNAs (miRNA) which are part of RNA silencing and post-transcriptional regulation of gene expression as potential part of the therapies for some serious illnesses. miRNA sensor was designed by Zhang et al. and it used two-staged isothermal exponential amplification reaction (EXPAR) in which different miRNA can be converted into the same reporter oligonucleotide. In the first stage amplification of the miRNA occurred and in the second miRNA was converted into the reporter oligonucleotide Y. The sandwich hybrids were created out of Cy5-labeled reporter probes and biotinylated capture probes and their complementary oligonucleotides of

reporter Y and conjugated on the surface of streptavidin modified QD_{605}. LOD of the probe was 0.1aM [54]. Further miRNA and DNA designed nanosensor used MPA-QDs modified with thiolated DNA via ligand-exchange method in 1:30 molar ratio and for sandwich hybridization target DNA and Black Hole quencher labeled DNA probe was used. After hybridization with targeted DNA, QDs PL quenching was observed which has not been the case in the presence of non-complementary DNA. This nanosensor was able to detect as low as 1 fM of DNA and 10 fM of miRNA [55].

Molecular beacons (MB) are standard probes used for detection of nucleic acids relied on dual labeled hairpin-shaped single-stranded oligodeoxynucleotide (ODN) sequences for detection of target DNA via FRET. Kim et al. have created the MB with QDs applied into the QDs-FRET based sensor between MAA capped CdSe/ZnS QDs conjugated with 25 based hairpin MB (5′end) and with 4-((4-(dimethylamino)phenyl)azo)benzoic acid (DABCYL) quencher conjugated on the 3′ end of the MB. Comparing this probe to the probe which uses two fluorophores DABCYL connected to 5′ and 6-Carboxyfluorescein (6-Fam) at the 3′ it was noticed that with QD/DABCYL MB has lower fluorescence increase (around six-fold) comparing to the 6-Fam/DABCYL ten folded and that QDs size negatively influenced on the FRET efficiency, but QDs MB have shown better photostability over organic fluorophores, in 10 min 6-Fam MB have showed 15% decrease of photoluminescence while QDs MB showed none [56]. Kim et al. have also designed multiplex QDs based MB, using green, yellow and orange streptavidin modified CdSe/ZnS QDs conjugated with Black Hole Quencher 2 (BHQ2) via streptavidin-biotin affinity and 80% PL recovery upon binding of the complementary target was observed [57] Cady et al. have compared linkage strategies and fluorescence quenchers in QDs MB. Carboxyl and streptavidin modified QDs were attached to hairpin ODN as energy donors together with Black Hole Quencher-2 (BHQ-2), Iowa black FQ(IaB), and 1.4 nm Au NPs as energy acceptors. Carboxyl QDs have shown 57% greater PL recovery compared to the streptavidin linked beacon. As well usage of 1.4nm AuNP and IaB showed better PL increase comparing to the DABCYL quencher. It is also noticed, likewise [56], that greater streptavidin QDs radius have negative effect on the quenching [58]. Medintz et al. have used synthetized polyhistidine sequence for facilitating association to the DHLA-modified CdSe/ZnS QDs and/or any thiolated DNA probe. It is also used to create QDs MB which was capable for the detecting target DNA. In QD/TAMRA MB it was shown that quenching efficiency is depending of the number TAMRA labeled

DNA per QD and it can be improved with larger number of dye labeled DNA per QDs, alleviating QDs size impact [59]. Wu et al. have reported molecular beacon with silica-capped CdSe/ZnS QDs and IaB as quencher which was able to detect as low as 0.1nM concentration of the target DNA within 15min [60].

Algar et al. have presented interesting work by designing several QD-FRET based sensor for nucleic acid hybridization with immobilized QDs as energy donors. MPA modified CdSe/ZnS QDs conjugated with oligonucleotide probe were immobilized on fused-silica optical fibers modified with multidentate thiol ligands. Possible non-specific adsorption of the Cy5-labeled target on the interface active sites was prevented by a layer of denatured bovine serum albumin. After introduction of the Cy5-labeled target DNA hybridization occurred providing proximity between QDs and Cy5 required for FRET. Found limit of detection was 5nM for designed system [61]. Further the same group has reported and discussed several multiplex assays for simultaneous detection of two or more target sequences. They have designed multiplex assay consisted of green MPA capped CdSe/ZnS QDs –Cy3 and red MPA capped CdSe/ZnS QDs-Alexa Fluor 647 (A647) as FRET pairs. For multiplexing two different color QDs were coimmobilized in mixed films and in this assay single nucleotide polymorphisms (SNPs) discrimination with contrast ratios as high as 31:1 was possible [62]. The same approach of two color QDs coimmobilized were used for detection of three different nucleic acids [63]. Follow the authors have shown that multiplexing is possible even using single color QDs immobilized on optical fibers as energy donor to two, Cy3 and Rhodamine Red-X, energy acceptors [64]. Consequently idea of using immobilized QD-FRET probes was applied in chips. Chen et al. have constructed solid-phase nucleic acid hybridization assay using immobilized QDs within microfluidic channels. Immobilization of QDs inside the channels is done via hybridization of the complementary oligonucleotides assembled on the QDs surface andlocated on a glass surface inside the microfluidic channels. The second oligonucleotide sequence attached to QDs is available for hybridization with targeted DNA labeled with Cy3 and driven through channels electrokinetically enabling FRET to occur [65].

Similarly Traver et al. have designed on-chip QD-FRET based assay for detection of transduction of nucleic acids. Streptavidin modified green CdSe/ZnS QDs were immobilized into microfluidic channels on the biotinylated polydimethylsiloxane (PDMS)-glass via streptavidin-biotin affinity and energy acceptor Cy3 was conjugated to target oligonucleotide sequence. Achieved LOD of the probe was in the range of

femtomole [66]. Later on, this work was expanded on designing multiplex detection of nucleic acids in microfluidic channels [67]. The most recent reported novelty in QD-FRET based detection of nucleic acid is paper-based solid-phase assay and multicolor paper-based solid-phase assay reported by Noor et al. Paper surface have been modified with imidazole ligands for immobilization of GSH capped QDs with oligonucleotide probe self-assembled on their surface as energy donors and as energy acceptors Cy3 molecules have been used [68]. For multicolor assay paper was treated on the same way but on the surface were immobilized green and red-emitting GSH capped QDs with appropriate oligonucleotide sequence for target DNA detection as energy donors and as their FRET pair Cy3 and Alexa Fluor 647 were used [69]. In both cases selectivity of nucleic acid hybridization was demonstrated by single-nucleotide polymorphism (SNP) detection, reaching LOD in range of femtomole. Similarly Petryayeva et al. have modified polystyrene microtiter plate wells with multidentate imidazole-based surface ligands for immobilization of green- and red-emitting QD donors. On QDs surface were assembled two different oligonucleotide probe sequences and via hybridization with target oligonucleotides, were paired with Cy3 and Alexa Fluor 647acceptor dyes, respectively, creating two FRET-based detection channels. Established LOD were 4 nM for both assays, with green- and red-emitting QDs [70].

4.2 QD-FRET sensors for enzymatic activites

Enzymes are very important molecules involved in the thousands of metabolic processes. One of them are proteases, enyzmes which catalyzehydrolysis of proteins into smaller peptides and/or amino acids. They are ubiquitous in all normal metabolic processes but as well as in diseases, such as cancer, viral infections like hepatitis [71] and AIDS [72]. Proteases are, as well, involved in malignant progression like tumor angiogenesis, invasion and metastasis [73] and necessity for their monitoring and/or detection arise from the fact that they are marked as an important diagnostic tool. Designing QD-FRET based sensors for monitoring proteases activity has attracted a lot of attention recently. Designing includes several very important and complicated steps such as engineering of the linking protease-specific peptide or finding appropriate energy donors and acceptors.

Engineering enzyme-specific peptide considers designing several highly specific sites such as appropriate enzyme cleavage site, modified C- and N- terminus for attachment of the energy donors and acceptors. Chang et al. have designed collagenase-degradable

peptide sequence(GGLGPAGGCG) linking N-treminus to the PEG capped CdSe/CdS QDs via carbodiimid chemistry and sulfhydryl groups of the cysteine residues at C-terminus were used for attachment to themono-maleimide functionalized gold nanoparticle (AuNP). QDs-peptide-AuNP systemhas exhibited 71% of reduction in QDs photoluminescence (PL) while QDs:AuNP ratio was 1:6. Upon peptide cleavage in presence of 0.2mg/mL collagenase, 52% rise in luminescence over 47h exposure were observed [74]. Such a low recovery of photoluminescence could be consequence of the particles size which decrease peptide accessibility for the enzyme. However, organic fluorophoreshave been successfully used as acceptors with good% of photoluminescence recovery. Shi et al. have chosen rhodamine as an energy acceptor in two constructed FRET system [75-76]. In the both cases rhodamine labeled peptide-coated CdSe/ZnS QD have been created and QDs-peptide linkage was done by ligand-exchange in which trioctylphosphine oxide (TOPO) was exchanged with RGDC peptide and linked to rhodamine through peptide cysteine residues. In the first case probe was used to monitor proteolytic activity of extracellular matrix metalloproteinases (MMP), collagenase and the second one for trypsin activity. After excitation at 445nm QDs and rhodamine emission spectra at 545nm and 590nm, respectively were observed. Upon interaction with trypsin (500μg/mL for 15 min) 60% of signal increase of the QDs PL and a corresponding decrease in the emission of the rhodamine molecules was observed due to decreasing of the FRET efficiency [76]. The same dependence was noticed with collagenase. The activity of collagenase was observed in normal and breast cancer cell lines and it was noticed significantly higher collagenase activity in breast cancer cells than in normal ones [75]. Very similar MMP sensor has been reported by Li et al. [77]. Authors have used CdTe QDs and rhodamine B as fluorescence quencher linked with MMP sensitive peptide and monitor MMP activity in normal cell, breast cancer cell with over-expressing and low expression of MMP. MMP sensitive peptide was attached to the QD surface via EDC-sulfoNHS methodology. In 60 min exposure 73% recovery of fluorescence was observed in probes with MMP over-expressing cancer cell, while in MMP low expression cells this % was insignificant.

Medintz et al. have designed a specific peptide with N-terminal hexahistidine (His_6) sequence for easier attachment with dihydrolipoic acid (DHLA) capped QDs, cysteine at its C-terminal for dye attachement, and in between in was placed an enzyme specific cleavage site and helix-linker spacer regionto provide peptide rigidity (Figure 2.). Activity of caspase-1, thrombin, collagenase and chymotrypsin was observed in systems

consisted out of DHLA-capped QD and Cy3 as FRET pair for caspase-1 and DHLA-capped QD and QXL™520 quencher as FRET pairfor the others proteases. Important properties of the designed peptide was controlable number of peptides attached per single QD and within FRET efficiency was controlled as well as lowering of used substrate concentration (200nMQD and peptide concentration of 0.2–1.0 μM). Assays provide quantitative data including enzymatic velocity, Michaelis–Menten kinetic parameters, and mechanisms of enzymatic inhibition [78]. The same authors have monitored a protein digestion by proteinase K and papin using QD-protein conjugates as a substrate [79]. Further QD-FRET based sensor for monitoring caspase 3 proteolytic activity was reported. Caspase 3 is an important downstream protease in apoptosis. For it monitoring Boeneman et al. have engineered red fluorescent protein mCherry as peptide which included terminal His_6-sequence, caspase 3 cleavage site, as well as C terminal cysteine needed for dye attachement and T7 transcript stabilizing sequence. Engineered mCherry was ratiometrically self-assembled to the surface of DHLA capped CdSe/ZnS QDs using metal-affinity coordination leading to the FRET quenching of the QD PL along with an increase in sensitized mCherry emission which has been used as the energy acceptor as well. A 50% FRET efficiency was proven when six engineered mCherry were linked per QD. QD-fluorescent protein system enable 5–10 times less substrate and three orders of magnitude less enzyme in terms of quantity to be used. Authors were able to detect enzymatic activity at concentration of 20 pM [80]. The same group of authors has reported another caspase 3 sensor together with an Ca(II) ion sensor. Capsase3 sensor use carbodiimide chemistry to covalently link Texas Red dye-labeled peptide (SGDEVDSG) to the terminal carboxyl groups of the hydrophilic ligands on the QDs surface whilefor Ca(II) ion sensor peptide was designed for bioconjugation with DHLA-PEG QDs through polyhistidine (His_n) metal-affinity coordination and for covalent linking to CalciumRuby-Cl, a new synthetic Cu(II) sensing indicator dye [81]. Designing enzymes-specific peptide have pushed investigation of enzyimes activity further so sensor for *in vivo* monitoring was reported by Biswas et al. with HIV-1 protease (HIV-1 Pr) as model enzyme. They have used genetically programmable protein consisted of several segments; terminal His_6 sequence,protease-specific cleavage site, cysteine residue for attaching of Alexa dye,an elastin-like peptide (ELP) domain for purification, and a flanking TAT peptide. *In vivo* monitoring of HIV-1 Pr activity was done in HeLa cells with the HIV proviral plasmid transfection [82]. Similar work was done by Youngenson et al. [83] while later Biswas

et al. have reported extended application of previously made detection platform for HIV-1 Pr activity to enzyme inhibitor analysis and monitoring proteases activity through*in vivo* cleavage rates of proteases and cleavage site mutations in the presence or absence of different protease inhibitors [84].

Since QD-FRET based systems have potential to be used in diagnostics and therapeutic their miniaturization is desirable because of easier manipulation, portability, lowering the analysis costs and sample volumes. Regarding that several chip-based QD-FRET sensors have been reported along with immobilization of QDs into the surface which prevents their aggregation. Streptavidin-coated QD525 (SA-QD525) have been immobilized onthe amine-reactiveglass surface and QDs PL was quenched with fluorescent dye TAMRA attached to biotinylated MMP-7 degradable peptide (RPLALWRSK). Number of the peptides attached per QD was 50. Established chip-based assay was able to detect enzyme activity at concentration approximately 100 ng/mL [85]. The Medintz group has demonstrated monitoring of trypsin activity on electroluminescent(EL)-charged-coupled device (CCD)-microchip platform using QD bioconjugated with a trypsin substrates dye-labeled peptide. The 16-well microchip was designed and used linking peptide had the His_6 segment for self-assembly on the DHLA-PEG_{600} capped QD, enzyme cleavage site and cysteine residue for Cy3 attachment as acceptor dye. System had an optimal QD:Cy3-peptide ratio of 1:2. Designed microchip assay was used for trypsin proteolytic activity and trypsin inhibition monitoring. The EL-CCD combined the spatial detection of CCD with the simple illumination by EL strips to measure fluorescence from chips and results were compared to the conventional fluorescent plate reader measurements showing that used volumes were more than an order of magnitude lower comparing to the conventional method though limit of detection of trypsin (6.2 nM) has stayed the same [86].

An microbiochip was designed using specific micro electro mechanical system (bio-MEMS) by Lee et al. Design of the chip was based on microbeads probes where microbeads together with fixed donor and acceptor on their surface were injected into michrochip and captured by micropillars in reaction chamber. Streptavidin modified QDs were used for coupling with MMP-7 degradable peptide labeled by TAMRA quenching dye as FRET pair with the ratio of 1:20 which resulted in 90% of QDs PL quenching. Microbeads-QDs linkage was based on the streptavidin-biotin affinity. The microbiochip successfully measured QDs PL recovery in the presence of the MMP-7 after 50 min of reaction at 37^{o}C and a limit of the detection was 1 μg/mL. Advantages

of this microbichip beside reducing of reagents volume are easy handling, fabrication even in mass production and simpler detection methods.

Similarly as for nucleic acid detecton the most recent reported novelty in QD-FRET based detection and monitoring of enzyme activity is paper-based assay, firstly reported by Algar group. Cellulose fibers in the paper were modified with bidentate thiol surface ligand on which CdSeS/ZnS QDs capped with DHLA or glutathione can readily immobilize. After immobilization QDs were assembled with Alexa Fluor 555-labeled peptide substrates for proteases (trypsin, chymotrypsin and enterokinase). Enzyme specific peptides were engineered with His_6, cysteine bonding segments and enzyme-characteristic cleavage site. An portable USB spectrometer with violet LED as excitation source, digital camera, webcam and an iPhonewere sufficient for analysis on the basis of a red/green color intensity ratio in enzyme concentration 1-2 nM [87]. Their work was done toward the minimization of the analysis costs, which are usually high due to sophisticated instrumentation so the same authors have shown that even smartphone camera can be used as PL detector as well as multiplexed protease sensing are possible and easly detectable with the smartphone camera (Figure 3.) [88]. Later they have reported work with immobilized QDs and different amounts of dye-labeled peptide for trypsin activity measurement which had bright luminescence under UV/violet illumination which means that photoluminescence emission from QDs was visible by eye [89].

4.3 QD-FRET based immunoassays and organic compounds detection

Immunoassays are biochemical tests based on the antibody-antigen methodology. They are widely applied in medicine and research. Quantum dots in combination with FRET were used for designing immunoassays for variety of samples and compounds. One of the first published reports which use FRET and QDs in immunoassay was given by Goldman et al. for TNT detection. Sensor consisted of an anti-TNT specific antibody fragments attached to DHLA-CdTe-ZnS QDs via metal-affinity coordination. Black Hole Quencher-10 labeled TNT analogue was coupled to the antibody binding site and it quenched PL of the QDs. In the presence of TNT, dye-labeled analogue is displaced and PL is recovered. Detection limit was 20 ng/mL of TNT [90]. Several years later another QD-FRET based sensor for TNT has been reported. A hybrid system was based on the QDs PL quenched by the gold nanorods (AuNR) with a limit of the detection of 0.1 nM [91]. Further two immunoassaya are probably the most know QD-FRET based

sensor and they are designed for maltose detection by Medintz group. Detection is based on β-cyclodextrin displacement as an maltose analogue. First sensor consisted multiple copies of Escherichia coli maltose-binding protein (MBP) bound to QDs by a C-terminal oligohistidine segment and played a role of the sugar receptors. β-cyclodextrin-QSY®9 dark quencher conjugate was bound to MBP saccharide binding site for QDs PL quenching. Displacement of the β-cyclodextrin was caused in the presence of the maltose which was detected as PL recovery of QDs strongly dependent on maltose concentration. The second sensor uses a fluorescent dye as acceptor instead of QSY®9 dark quencher. In this case MBP-QD PL was quenched in two steps, firstly energy was transferred from QDs to Cy3-labeled MBP and then to Cy3.5-labeled cyclodextrin [92]. Also displacement mechanism was used for the glucose detection by Tang et al. Authors have designed nanobiosensorin which glucose was detectedupon fluorescence recovery. System was consisted out of QDs as an energy donors conjugated to an sugar-binding lectin protein concanavalinA (Con A) and glucose analogue, thiolated P-cyclodextrins (beta-SH-CDs) assambled on the sufrace of gold nanoparticles (AuNPs) as quenching acceptor. Fluorescence recovery was observed in the presence of glucose since it displaced AuNPs-beta-CDs segment form binding sites of the ConA. Sensor has a high sensitivity with a limit of the detectionof 50nM and shows very good selectivity toward glucose in the presence of others sugars or biological species often present in the serum [93]. Another nanosensor designed for glucose detection was based upon observation of fluorescence inhibition and the authors have introduced a pre-blocking protocol as a part of the detection system . In the system as energy donor green QDs conjugated with ConA were used and red QDs-NH_2-glu as acceptor. The authors have used ConA specificity for sugars and prebound a certain amount of the glucose into the QD-ConA acceptor which blocked the resonance energy transfer to the QDs-NH_2-glu acceptor. The more glucose is bound into bindingsites of the Con A moiety of the donor the lower is conjugation with the red QDs–NH_2-glu and the inhibition of fluorescence quenching was measured [94]. Recently an FRET-based aptamer biosensor for insulin was reported. FRET system was build between near-infrared quantum-dots (NIR-QDs) and oxidized carbon nanoparticles (OCNPs) as the energy donor and acceptor [95]. For achieving good FRET efficiency distance between QDs and antibody binding side is very important as well as the number and location of the acceptor molecules. Molecules used for QDs surface modification sometimes enlarge distance between donor and acceptor molecules causing the FRET efficiency

decrease. To overcome this problem Nikiforov et al. have designed an QD-FRET based immunoassays in which QDs surface were modified with small molecules haptens such as biotin, fluorescein and cortisol. The synthesis ofhapten-QDs conjugates was very straightforward and based on the mixing of amine-labeled QDs with excesses of the N-hydroxysuccinimidyl esters of biotin and fluorescein and, in the case of cortisol, with a carbodiimide-activated carboxylic acid derivative of the hormone.The binding of hapten-QDs to Alexa Fluor-labeled streptavidin, anti-biotin, anti-fluorescein or anti-cortisol antibody formed an FRET system and achieved limits of detection for fluorescein and cortisol was 25nM and for biotin 2nM [96]. Wei et al. have introduced QDs into the open sandwich fluoroimmunoassay (OsFIA) and estrogen was used as a model sample. System consisted of CdSe-ZnS QDs attachedat the hinge area of anti-estrogen receptor β (anti-ER-β) monoclonal antibody (McAb) as a energy donor and anti-ER polyclonal antibody (PcAb) was labeled with the acceptor Alex Flour 568 or Alex Flour 633. After 30 min of incubation with estrogen receptor β (ER-β) antigenFRET could be measured with the limit of the detection of 0.05 nM. OsFIA offers a lot simplier way of detection than ELISA because it does not require steps such as binding, washing, and blocking [97]. Another hormone QD-FRET sensor was reported but this time for estradiol. It was FRET based aptasensor using quantum dot (QD) bioconjugate as a nano-bioprobe and a high-affinity, high-specificity fluorescence-labeled anti-17 beta-estradiol aptamer as a bio-recognition molecule.Limit of the detection was 0.22 nM and probe showed really high estradiol specifity and sensitivity against potentially interfering endocrine-disrupting compounds or other chemicals [98].

4.4 QD-FRET sensors for heavy metals detection

One of the biggest problem of todays society is environment pollution with heavy metals. They are widespread, in the soil, water and air, so emerge for their rapid and sensitive detection is obvious. FRET-based nanosensors enchanced with QDs as novel fluorophores had been successfully applied for heavy metals as prominent sensing tool. Hg(II) ions belong to one of the most toxic and dangerous pollutant. QD-FRET based sensor desinged by Li et al. for Hg(II) detection used TGA capped CdTe QDs and butyl-rhodamine B (BRB) dye in Tris–HCl buffer with addition of the cetyltrimethylammonium bromide (CTMAB) in order to bring the electronegative QDs and dye closer for better FRET efficiency. In the presence of Hg(II) ions PLquenching

of TGA-CdTe QDs was observed and corresponding fluorescence enhancement of the BRB. QDs PL have been quenched because of mercury affinity toward telluride which caused Cd(II) ion displacements from the QDs surface. Reached limit of the detection was 20.3 μM [99]. Since mercury has bio-accumulative nature intracellular detection might be needed and FRET ratiometric approach is good solution, especially with long lifetime material like QDs whose emission will last longer than background autofluorescence. System with polymer-encapsulated CdSe/ZnS QDs and thiosemicarbazide-functionalized rhodamine B which is capable of non-specific adsorption on the QDs surface as energy donor and acceptor was designed by Page et al. Detection was followed by an ring-opening reaction at functionalized rhodamine B and a rise of absorption peak at 550nm which overlaps with emission maxima of the QDs and FRET occurs. Measured limit of detection is 79ppb [100]. Follow Liu et al. designed QDs-FRET ratiometric fluorescence sensors for detection of Hg(II) ions which involved CdTe QDs encapsulated into silica particles and rhodamine B as FRET pair [101]. Hu et al. used N-acetyl-L-cysteine (NAC) functionalized QDs and rhodamine 6G derivative-mercury conjugate as FRET pair for ratiometric FRET sensor. NAC stabilized QDs and gave much brighter emission then typical TGA and/or MPA stabilizators, as well as it has good affinity toward mercury ions. Sensor was employed for intracellular colorimetric imaging in live Hela cells [102]. Mainly, QDs have been used as donor in FRET systems and the system in which they play a role as acceptors are rare. In such system TGA-CdTe QDs and fluorescent brightner were used in concentration ratio 10:1 and as acceptor and donor respectively. Detection of Hg(II) ions was followed by QDs PL quenching due to strong absorption of Hg(II) ions to the carboxyl group on the QD surface [103].

Among common, bio-accumulative and persistant pollutant as well belongs lead and several QD-FRET based sensor for detection are described in the literature. CdTe QDs capped with cysteamine were used as energy donors while surface of gold nanoparticles were modified with 11-mercaptoundecanoic acid (MUA-AuNP) and were used as energy acceptors in the designed FRET system. Lead ions are detected according to the QDs PL recovery with limit of detection of 30 ppb. Supposed interaction that led to PL recovery is aggregation of MUA-AuNP in presence of lead [104]. Similarly, Zhao et al. reported lead detection with the system of dithizone (Dz) functionalized CdSe/CdS QDs, where dithizone quenched QDs PL. QDs PL recovery was observed in the presence of the lead ions caused by removal of dithizone from QDs

surface due to its strong affinity to lead ions. Limit of detecton was 0.006 nM and probe has shown satisfactory results with real environmental samples [105]. Very interesting approach was published by Wu et al. by designing QD-DNAzyme nanosensor in which fluorescence recovery of QDs is consequence of DNAzyme cleavage in the presence of the heavy metals, Pb(II) and Cu(II) were used as models. The carboxyl-silanized QDs were linked to DNAzyme through well-known zero-length crosslinker, EDC and sulfo-NHS.The achieved detection limitsfor Pb(II) and Cu(II) were 0.2 and 0.5 nM. Using different colors of QDs, Pb(II) and Cu(II) ions were successfully separated from mixture without any signal interference [106]. Further different system for Cu(II) ions were designed. Ganguly et al. have used salen coupled CdSe/ZnS QDs through condensation reaction between surface amine and salicylic aldehyde. In the presence of Cu(II) ions salen will exhibit PL quenching. Model is applied for Fe(II) ions detection as well [107]. MPA-CdTe QDs were used as energy acceptor and linked to green luminescent monodisperse phenol formaldehyde resin nanoparticles (PFR NPs) surface modified with polylectrolyte (PEI/PSS/PEI) through EDC/sulfo-NHS methodology as donor. In the system QDs-PFR NPs red color of QDs is observed, but in the presenceCu(II) ions of FRET is disrupted and QDs PL is quenched and green color of PFR NPs arise and it is visible by naked eye within 1 min [108]. Besides mercury, cadmium and lead as the most common and the most dangerous pollutant others have been subject of the detection such as zinc, potassium and others. Ruedas-Rama et al. have designed interesting QD-FRET based sensor for Zn(II) and Mn(II) ions sensing with zincon midified QDs. System has shown different behavior in the presence of these two metals. In case of Zn (II), Zn(II)-zincon absorption spectra overlaps with the emission of QDs thereby PL quenching is observed. On the other hand in the presence of Mn(II) and its binding to zincon enhancement of the PL intensity is observed as a results of deactivation of the quenching interaction between zincon and QDs (Figure 4.) [109]. Chen et al. developed a crownether(15-crown-5)-functionalized dual QDs system for potassium detection. CdSe/ZnS QDs of two different sizes were used, QD545(3.2nm), as energy donor and QD635 (5.6nm), as energy acceptor. When potassium bound an aggregation of the QDs occurred due to shortening of the distance between them causing QD545 quenching and QD653 fluorescence increase [110]. An CdTe-gold nanoparticles (AuNPs) quenching system was designed for sensing of fluoride (F^-) anion. CdTe-AuNPs were bound through formation of cyclic boronate esters whose integration with fluoride ions form trifluoro borate and disassembles CdTe

from AuNPs. The linkage breaking results in the fluorescence recovery of QDs and limit of detection for fluoride ion was measured at the concentration of 50nM [111].

4.5 pH sensors

Monitoring of pH parameter is very important in medicine, biology, agriculture, food science and many other fields. QD-FRET based pH sensor has been reported when pH indicator dyes have been used as acceptor in ratiometric sensor designing. In this sensor QDs usually play a role of the reference dye. Snee et al. have used pHindicator dye squaraine conjugated to the surface of the CdSe/ZnS QDs via EDC/sulfo-NHS methodology while designing sensor. Measuring is based on increasing FRET efficiency caused by larger spectral overlapping between QDs and dye when lowering pH. QDs photoluminescence was quenched while dye emission increased[112]. Similar work have been reported by Suzuki et al. [113], Jin et al. [114] and recently by Kurabayashi et al. [115] where fluorescein and its derivates as pH indicator dye were attached to QDs surface. For sensing intracellular pH, pH sensitive fluorescent protein mOrange or its homologue mOrange M163K were attached to carboxyl-functionalized QDs. It was demonstrated that probe is stable and resistant to photobleaching as well as it is suitable for intracellular and extracellular application [116].

4.6 Sensor for detection of microorganisms and their toxins

Microorganisms as part of our everyday life usually are harmless to us, but some of them and/or their toxins can be very dangerous causing a serious diseases and heavily endanger human life and health. Due to that their rapid and sesitive detection is needed. In this section a short insight will be given in QDs-FRET based nanosensors designing for detection of different microorganism and toxins.

Kattke et al. have developed a QD-FRET based immunoassays for mold spores in the solution on *Aspergillus amstelodami* as model microorganism presented at the Figure 5. Detection system was formed of ant-*Aspergilus* antibody conjugated amine-derivatized (PEG)-coated CdSe/ZnS QDs through succinimidyl-4-[N-maleimidomethyl]cyclohexane-1-carboxylate (SMCC) crosslinker and black hole quencher (BHQ-3)-labeled mold analytes that had a lower affinity for the antibody than *A. Amstelodami*. Fluorescence recovery was observed in the presence of *A. Amstelodami* due to (BHQ-3)-labeled mold analytes displacement. The optimized displacement immunoassay detected concentrations as low as 10^3 spores/mL in five minutes or less [117]. The toxic shock syndrome toxin-1(TSST-1)-producing

Staphylococcus aureus was successfully detected by FRET system with CdSe-ZnS QD as donors and black hole quencher (BHQ) as acceptors. QD-DNA probe was prepared by conjugating the carboxyl-modified QD and the amino-modified DNA with the EDC in ratio 1:40, respectively. PL quenching was observed after DNA hybridization between matching ssDNA-modified donor and acceptor. In the presence of targeted DNA PL recovery was observed due to BHQ-DNA detachment from the probe. Recovered QD PL is linear to the concentration of target DNA and the detection limit was 0.2 μM [118]. QD-FRET based system relied on the DNA hybridization process for providing the donor-acceptor proximity between QDs and graphen oxide (GO) was applied for *Listeria monocytogenes* detection, an foodborne pathogenic bacteria. Method is consisted of multiplexlinear-after-the-exponential (LATE) polymerase chain reaction (PCR) amplification, DNA hybridization, and QDs-GO signal detection. QD525 and QD605 were conjugated to the ssDNAamplification productsof the iap and hlyA genes, respectively due to streptavidin-biotin interaction. PL recovery was observed in the presence of the targeted DNA. Genomic DNA from *L. monocytogenes* can be detected as low as 100 fg/μL [119]. Similarly, molecular beacon based on the FRET between QDs and quenchers have been developed for *Listeria monocytogenes, Bacillus thuringiensis,* and *Salmonella Typhimurium* detection designed by Burris et al. [120]. Very simple and rapid QD-FRET based nanosensor was designed for *Helicobacter pylori* detection reported by Shaneshaz et al. Two oligonucleotides probes were differently labeled, one with TGA capped CdTe QDs andt he other with fluorescent dye TAMRA. 210 bpPCR product of urease gene of bacterium *H. pylori* was used as a complementary DNA. Complementary DNA hybridized with oligonucleotides probes brought closer QDs and TAMRA an energy donor and acceptor, respectively and enabled FRET. The measured emission of the system was 580 nm, which corresponded to the TAMRA dye emission. The limit of detection (LOD) was estimated as 4.5nM [121].

Several QD-FRET based nanosensors for bacteria toxins have been reported. Botulinum neurotoxins (BoNTs) are proteins produced by the bacterium *Clostridium botulinum*. Botulinum toxins are one of the strongest and most dangerous natural toxins known to man and could cause poisonings with fatal outcomes for humans, so there is emerge for rapid and sensitive detection of the toxins. QD-FRET based nanosensors were based on observing activity of light chain protease of the BoNT serotype A (LcA). ALcA peptide substrate was designed to consist central LcA recognition/cleavage region,C-terminal

cysteine residue for labeling with a Cy3 acceptor dye and N-terminal oligohistidine for self-assembly with PEGylated or DHLA capped CdSe/Zns QDs. Created QD-LcApep-Cy3 quenched system in the presence of the BoNT serotype A light chain protease have shown a fluorescence recovery as a detection signal. Obtain LOD was 350 pM for LcA [122].

Staphylococcal enterotoxin B (SEB) is one of the toxins produced by *Staphylococcus aureus* and commonly it is associated with food poisoning. Detection system for SEB was based on FRET between two different QDs, QD_{523} and QD_{601} which were bioconjugated to anti-SEB antibody and SEB respectively according to the carbodiimide protocol. Mutual affinity of anti-SEB antibody and SEB will enable efficient FRET between QDs, in which fluorescence quenching will be observed at QD_{523} (energy donor) and fluorescence decrease at QD_{601} (energy acceptors) [123]. Aflatoxins are group of secondary metabolites produced mainly by the fungi of *Aspergillus flavus* and *Aspergillus parasiticus*. They are harmful to human, poultry and livestock health. QD-FRET-based competitive immunoassay for aflatoxin B1detection was designed by Zekavatin et al. CdTe QDs conjugation with anti-aflatoxin B1 antibody and Rho 123-labeled aflatoxin B1-albumin both done by EDC-sulfoNHS methodology, were used as energy donor and acceptor. The proximity of the QDs and the Rho 123 provided by labeled-aflatoxin B1-albumine enabled FRET and strong Rho 123 fluorescence emission was observed. Optimum immunoreaction between the Rho 123-labeled aflatoxin B1-albumin and the QDs-labeled anti-aflatoxin B1 antibody was achieved at molar ratio of 0.6:03 μM, respectively. Aflatoxin B1 is detected according the reduction of the Rho 123 fluorescence due to competitive replacement of the labeled-aflatoxin B1-albumine with aflatoxin B1. Achieved LOD was 2×10^{-11}M [124]. Aflatoxin B1 was detection in rice grain using hapten-labeled green QDs as energy donor and monoclonal antibody (mAb)-labeled red QDs as energy acceptor between with limit of the detection of 0.13 pM (0.04 ng/mL) in rice extracts [125].

4.7 **Detection of viruses via QD-FRET based sensors**

Viruses are small infectious agents which need a host organism for living and replicating. Viruses can infect almost every living organisms, humans, animals, plants as well as bacteria. Most of the viruses have either RNA or DNA as their genetic material and they undergo the genetic mutation very quickly and due to that stand as an unsolved diagnostics and therapeutics problem. Proposed detection methods for viruses

are various, from growth of viral culture, ELISA tests, nucleic acid detection and others, but many of the methods were not widely adopted in the clinical use due to complicated and expensive procedures. Rapid, inexpensive and sensitive virus detection methods are still under the investigation. For Porcine Reproductive and Respiratory Syndrome Virus (PRRSV) two different QD-FRET based sensors were proposed. An anti-PRRSV monoclonal antibody labeled with Alex Fluor 546 (AF546) fluorescent dye was attached to the commercially protein modified green QDs as first FRET system, in the second one the same dye-labeled anti-PRRSV monoclonal antibody was used and coupled with protein A modified gold nanoparticles. In the present of the antigen antibody-antigen reaction will occur causing conformational change within the antibody structure bringing closer FRET pair and increasing FRET efficiency. For quantum dots based sensor less energy will be transferred from QDs to the AF546, increasing QDs PL and corresponding AF546 fluorescence decreasing. For gold nanoparticle based sensor this will cause decrease in the quenching effect. Both sensor are able to rapidly and effectively detect PRRSV in solution with a detection limit of 3 particles/μl [126]. Further for hepatitis B virus (HBV) sensor was reported consisting of MPA capped CdSe/ZnS QDs conjugated with amine-modified 15-meroligonucleotidesvia carbodiimde chemistry along with Cy5 dye used for labeling if the target DNAs. Bringing QDs-Cy5 FRET pair together by sandwiched hybridization fluorescence emission of the Cy5 was observed. Non-complementary and unbound DNAs did not produce any FRET signal because they could not hybridize with the QDs-DNA conjugate. Possibility of the nanosensor was also demonstrated in the detection of synthetic 30-mer oliginucleotide targets derived from the HBV with a sensitivity of 4.0nM by using a multilabel counter [127]. Relaying on the same procedure another HBV sensor was designed with the usage of 6-carboxy-X-rhodamine (ROX) fluorophore as energy acceptor [128]. FRET technique was applied forinfluenza A virus, subtype H5N1 detection as well. FRET system consisted CdTe QDs conjugated with ssDNA via EDC/NHS linkage as energy donor and as fluorescence quenchersoxidized carbon nanotubes (oxCNT) were used. Upon the recognition of the target efficient competitive binding toward QD-ssDNA occurred and resulted in the oxCNT removal from the system and PL recovery. Registered LOD was 9.39nM [129]. Moreover a nucleic acid sandwich hybridization assay based on QD-FRET was used for avian influenza virus, H5N1 detection where 16-mer oligonucleotide was attached to QD655 via sulfo-SMCC cross liker in the molar ratio of 10:1 (probe-to-QD) and 18-

meroligonucleotides was attached to Alexa Fluor 660 dye. Since these oligonucleotides recognize two separate but adjacent regions of the H5 sequences sandwich hybridization assay occurred. In presence of label-free hemagglutinin H5 sequences (60-mer DNA and 630-nt cDNA fragment) of avian influenza viruses Alexa Fluor 660 dye emission will increase as consequence of FRET [130].

Human Enterovirus 71 (EV71) and Coxsackievirus B3 (CVB3) immunoassays were proposed based on the energy transfer between QDs and GO. System uses an antibody-antigen specific reaction for probe constructing beside FRET. Streptavidin modified green CdSe/ZnS QDs were attached to biotinylated EV71 antibody (Ab1) and streptavidin modified red CdSe/ZnS QD were attached to biotinylated CVB3 antibody (Ab2) and in both cases graphene oxide was used as quenching acceptor. The QDs-Ab-GO complex was broken up in the presence of the targeted EV71 and CVB3 followed by PL recovery of QDs. Achieved LOD for EV71 and CVB3 were 0.42 and 0.39 ng/mL, respectively [131]. QDs-FRET based sensor are also applied in the detection of viruses like necrotic yellow vein virus (BNYVV) a plant virus which is responsible for most destructive disease in sugar beet called rhizomania transmitted by protozoan Polymyxa betae (Keskin). Nanosensor for BNYVV was proposed by Safarpouret et al. and as FRET occurred between TGA capped CdTe QDs conjugated with glutathione-S-transferase protein's (GST) corresponding antibody (anti-GST) via electrostatic interaction and fluorescent dye rhodamine attached to GST. QDs and rhodamine proximity was enabled through antigen-antibody interaction enabling FRET to occur [132].

4.8 Detection of others environment pollutant

Heavy metals are not the only pollutants that need to be detected and monitored. Substances that may cause pollution are numerous and some of them are directly connected to human activities, such as agriculture, mining industry and others. Few QD-FRET based nanosensor have been reported for some of the pollutants. Sensor for the detection of residues from organophosphorus pesticides was based on the simple ligand replacement on the QDs surface which resulted in turning off the FRET. CdTe QDs were quenched by bidentate ligand dithizone (DZ) attached on the surface due to FRET and presence of organophosphorothioate pesticides replaced DZ ligands on the QDs surface by the hydrolyzation of the organophosphorothioate and PL recovery occurred (Figure 6.). Model pesticide was chlorpyrifos and system achieved LOD of 0.1nM.

Organophosphorothioates were successfully detected in apples [133]. Glyphosate is a broad-spectrum herbicide brought up to the market in the 70's of the last century by Monsanto corporation. QD-FRET based glyphosate sensor was designed with the negatively charged TGA capped CdTe-QDs as energy donor and positively charged gold nanoparticles stabilized with cysteamine (CS-AuNPs) as energy acceptor. Electrostatic interaction approximated FRET pair resulting in the QDs fluorescence quenching. Glyphosate interaction with the FRET system induced aggregation of the CS-AuNPs due to electrostatic interaction and fluorescence recovery has been observed. The detection limit for glyphosate in the apples was 9.8ng/kg [134]. Octachlorostyrene (OCS) was never used as a commercial product but it can be produced during magnesium production, incineration, combustion processes involving chlorinated compounds and others. It is characterized as persistent, bioaccumulative and toxic compound, involved in the mutagenicity/genotoxicity and carcinogenicity in humans. OCS detection FRET system was built in a microtitration plate and contained several steps. Laboratory produced anti-OCS antibody were adsorbed on a microtiter plate and competitive immunoreaction occurred between rhodamine B-labeled OCS (RB-OCS) and OCS. Afterwards separated solution was mixed with TGA capped CdTe QDs and based on the electrostatic interaction between CdTe QDs donor and RB-OCS acceptor FRET occurred and increasing of the fluorescence emission of the rhodamine B was observed with corresponding decreasing of the QDs photoluminescence [135].

5 Summary

FRET has gained huge importance in the different researche fields and improved detection sensitivity in various analytical techniques since it first description. FRET has offered possibility of the studying and understanding of the biological pathways, valuable information of the protein conformation and protein-protein interaction. FRET in combination of the QDs with their superior properties, such as long fluorescence lifetime and resistance to photobleaching, has enabled designing of the new and improved sensors. In the designing QDs are very successfully applied as energy donors, nanoscaffolds which allow multiple assembly of the energy acceptors on the QDs surface greatly increasing FRET follow the detection sensitivity and possibility of multiple color QDs excitation with single light source was used for multiplexed detections. As it is presented in this review sensors applications are moving toward

various directions, from detection of biomolecules, environmental pollutants and many others. Despite that QD-FRET based sensor are dealing with several limitations and shortcomings which strongly limits their commercial and wider application. Relatively large size of QDs, stability of the surface modification chemistry, nonspecific interaction of the biomolecules as well as QDs core and ligand toxicity are some of them. Nevertheless, as it can be seen QD-FRET based sensor are giving a great contribution to the miniaturization of the sensors as well as through QDs immobilization to the inexpensive materials and employing phone cameras as detectors to the lowering of their costs which is a solid proof of their immense potential.

1. Rodriguez-Mozaz, S., et al., *Biosensors for environmental applications: Future development trends.* Pure and Applied Chemistry, 2004. **76**(4): p. 723-752.
2. Brewster, D., *XIX. On the Colours of Natural Bodies.* Earth and Environmental Science Transactions of the Royal Society of Edinburgh, 1834. **12**(02): p. 538-545.
3. Herschel, J.F.W., *On a Case of Superficial Colour Presented by a Homogeneous Liquid Internally Colourless.* Philosophical Transactions of the Royal Society of London, 1845. **135**: p. 143-145.
4. White, B.R. and J.A. Holcombe, *Short-chain peptide sensors utilizing fluorescence resonance energy transfer for the selective detection of heavy metals.* Abstracts of Papers of the American Chemical Society, 2007. **233**: p. 487-487.
5. Chan, N.Y., M. Chen, and D.E. Dunstan, *Elasticity of polymer solutions in Couette flow measured by fluorescence resonance energy transfer (FRET).* European Physical Journal E, 2009. **30**(1): p. 37-41.
6. Zhao, Y.S., H.Z. Zhong, and Q.B. Pei, *Fluorescence resonance energy transfer in conjugated polymer composites for radiation detection.* Physical Chemistry Chemical Physics, 2008. **10**(14): p. 1848-1851.
7. Carmona, F., et al., *Monitoring lactoferrin iron levels by fluorescence resonance energy transfer: a combined chemical and computational study.* Journal of Biological Inorganic Chemistry, 2014. **19**(3): p. 439-447.
8. Song, Y., et al., *Nicking enzyme-assisted biosensor for Salmonella enteritidis detection based on fluorescence resonance energy transfer.* Biosensors & Bioelectronics, 2014. **55**: p. 400-404.
9. Yu, J.Q., et al., *Study of endothelial cell apoptosis using fluorescence resonance energy transfer (FRET) biosensor cell line with hemodynamic microfluidic chip system.* Lab on a Chip, 2013. **13**(14): p. 2693-2700.
10. Tu, D.N., et al., *Investigation of A(2A)-adenosine receptor activation by fluorescence resonance energy transfer in living cells.* Purinergic Signalling, 2012. **8**(1): p. 119-120.

11. Lu, S.Y. and Y.X. Wang, *Fluorescence Resonance Energy Transfer Biosensors for Cancer Detection and Evaluation of Drug Efficacy.* Clinical Cancer Research, 2010. **16**(15): p. 3822-3824.
12. Dereli-Korkut, Z., et al., *Real-time detection of cellular death receptor-4 activation by fluorescence resonance energy transfer.* Biotechnology and Bioengineering, 2013. **110**(5): p. 1396-1404.
13. Solomon, M., et al., *Detection of enzyme activity in orthotopic murine breast cancer by fluorescence lifetime imaging using a fluorescence resonance energy transfer-based molecular probe.* Journal of Biomedical Optics, 2011. **16**(6): p. 6.
14. Bernardini, A., U. Brockmeier, and J. Fandrey, *Analysis of the erythropoietin receptor dimer in different cancer cell lines by means of Fluorescence Resonance Energy Transfer.* American Journal of Hematology, 2012. **87**(10): p. E104-E104.
15. Förster, T., *Zwischenmolekulare Energiewanderung und Fluoreszenz.* Annalen der Physik, 1948. **437**(1-2): p. 55-75.
16. Selvin, P.R., *The renaissance of fluorescence resonance energy transfer.* Nature Structural Biology, 2000. **7**(9): p. 730-734.
17. Uhl, J.R., Y.W. Tang, and E.R. Cockerill, *Fluorescence Resonance Energy Transfer*. Molecular Microbiology: Diagnostic Principles and Practice, Second Edition, ed. D.H. Persing, et al. 2011, Washington: Amer Soc Microbiology. 231-244.
18. Shanker, N. and S.L. Bane, *Basic aspects of absorption and fluorescence spectroscopy and resonance energy transfer methods*, in *Biophysical Tools for Biologists: Vol 1 in Vitro Techniques*, J.J. Correia and H.W. Detrich, Editors. 2008, Elsevier Academic Press Inc: San Diego. p. 213-242.
19. Elangovan, M., R.N. Day, and A. Periasamy, *Nanosecond fluorescence resonance energy transfer-fluorescence lifetime imaging microscopy to localize the protein interactions in a single living cell.* Journal of Microscopy-Oxford, 2002. **205**: p. 3-14.
20. Lakowicz, J., *Principles of Fluorescence Spectroscopy*. Principles of Fluorescence Spectroscopy. 1999, New York, Boston, Dordrecht, London, Moscow: Kluwer Academic/Plenum Publishers.
21. Leriche, G., et al., *A FRET-based probe with a chemically deactivatable quencher.* Chemical Communications, 2012. **48**(26): p. 3224-3226.
22. Zadran, S., et al., *Fluorescence resonance energy transfer (FRET)-based biosensors: visualizing cellular dynamics and bioenergetics.* Applied Microbiology and Biotechnology, 2012. **96**(4): p. 895-902.
23. Martinez-Zapata, O., et al., *Synthesis and characterization of amorphous aluminosilicates prepared by sol-gel to encapsulate organic dyes.* Journal of Non-Crystalline Solids, 2011. **357**(19-20): p. 3480-3485.
24. Arunkumar, E., C.C. Forbes, and B.D. Smith, *Improving the properties of organic dyes by molecular encapsulation.* European Journal of Organic Chemistry, 2005(19): p. 4051-4059.
25. Adams, F.C. and C. Barbante, *Nanoscience, nanotechnology and spectrometry.* Spectrochimica Acta Part B: Atomic Spectroscopy, 2013. **86**(0): p. 3-13.
26. Alivisatos, A.P., W.W. Gu, and C. Larabell, *Quantum dots as cellular probes*, in *Annual Review of Biomedical Engineering*. 2005, Annual Reviews: Palo Alto. p. 55-76.
27. Probst, C.E., et al., *Quantum dots as a platform for nanoparticle drug delivery vehicle design.* Advanced Drug Delivery Reviews, 2013. **65**(5): p. 703-718.

28. Larson, D.R., et al., *Water-soluble quantum dots for multiphoton fluorescence imaging in vivo.* Science, 2003. **300**(5624): p. 1434-1436.
29. Gao, X.H., et al., *In vivo molecular and cellular imaging with quantum dots.* Current Opinion in Biotechnology, 2005. **16**(1): p. 63-72.
30. Fu, A.H., et al., *Semiconductor nanocrystals for biological imaging.* Current Opinion in Neurobiology, 2005. **15**(5): p. 568-575.
31. Walling, M.A., J.A. Novak, and J.R.E. Shepard, *Quantum Dots for Live Cell and In Vivo Imaging.* International Journal of Molecular Sciences, 2009. **10**(2): p. 441-491.
32. Wolfgang, J.P., P. Teresa, and P. Christian, *Labelling of cells with quantum dots.* Nanotechnology, 2005. **16**(2): p. R9.
33. Zrazhevskiy, P., M. Sena, and X.H. Gao, *Designing multifunctional quantum dots for bioimaging, detection, and drug delivery.* Chemical Society Reviews, 2010. **39**(11): p. 4326-4354.
34. Li, L., et al., *Blinking, Flickering, and Correlation in Fluorescence of Single Colloidal CdSe Quantum Dots with Different Shells under Different Excitations.* Journal of Physical Chemistry C, 2013. **117**(9): p. 4844-4851.
35. Stopel, M.H.W., et al., *Blinking statistics of colloidal quantum dots at different excitation wavelengths.* Rsc Advances, 2013. **3**(38): p. 17440-17445.
36. Huang, P.C., et al., *Alkaline Post-Treatment of Cd(II)-Glutathione Coordination Polymers: Toward Green Synthesis of Water-Soluble and Cytocompatible CdS Quantum Dots with Tunable Optical Properties.* ACS Applied Materials & Interfaces, 2013. **5**(11): p. 5239-5246.
37. Beri, R.K. and P.K. Khanna, *"Green" Synthesis of Cadmium Selenide Nanocrystals: The Scope of 1,2,3-Selendiazoles in the Synthesis of Magic-Size Nanocrystals and Quantum Dots.* Journal of Nanoscience and Nanotechnology, 2011. **11**(6): p. 5137-5142.
38. Ahmed, M., et al., *Facile and Green Synthesis of CdSe Quantum Dots in Protein Matrix: Tuning of Morphology and Optical Properties.* Journal of Nanoscience and Nanotechnology, 2014. **14**(8): p. 5730-5742.
39. Bao, H.F., et al., *Biosynthesis of biocompatible cadmium telluride quantum dots using yeast cells.* Nano Research, 2010. **3**(7): p. 481-489.
40. Huang, H.Q., et al., *Biosynthesis of CdS Quantum Dots in Saccharomyces Cerevisiae and Spectroscopic Characterization.* Spectroscopy and Spectral Analysis, 2012. **32**(4): p. 1090-1093.
41. Sturzenbaum, S.R., et al., *Biosynthesis of luminescent quantum dots in an earthworm.* Nature Nanotechnology, 2013. **8**(1): p. 57-60.
42. Zhang, C.Y., et al., *Single-quantum-dot-based DNA nanosensor.* Nature Materials, 2005. **4**(11): p. 826-831.
43. Chen, H.H. and K.W. Leong, *Quantum-dots-FRET nanosensors for detecting unamplified nucleic acids by single molecule detection.* Nanomedicine, 2006. **1**(1): p. 119-122.
44. Zhang, C.Y. and L.W. Johnson, *Quantum dot-based fluorescence resonance energy transfer with improved FRET efficiency in capillary flows.* Analytical Chemistry, 2006. **78**(15): p. 5532-5537.
45. Zhou, D.J., et al., *A compact functional quantum dot-DNA conjugate: Preparation, hybridization, and specific label-free DNA detection.* Langmuir, 2008. **24**(5): p. 1659-1664.
46. Algar, W.R. and U.J. Krull, *Towards multi-colour strategies for the detection of oligonucleotide hybridization using quantum dots as energy donors in*

fluorescence resonance energy transfer (FRET). Analytica Chimica Acta, 2007. **581**(2): p. 193-201.
47. Peng, H., et al., *DNA hybridization detection with blue luminescent quantum dots and dye-labeled single-stranded DNA.* Journal of the American Chemical Society, 2007. **129**(11): p. 3048-+.
48. Lee, J., et al., *Positively Charged Compact Quantum Dot-DNA Complexes for Detection of Nucleic Acids.* ChemPhysChem, 2009. **10**(5): p. 806-811.
49. Mao, J., et al., *Interaction among cadmium sulfide nanoparticles, acridine orange, and deoxyribonucleic acid in fluorescence spectra and a method for deoxyribonucleic acid determination.* Journal of Fluorescence, 2008. **18**(3-4): p. 727-732.
50. Vannoy, C.H., et al., *A competitive displacement assay with quantum dots as fluorescence resonance energy transfer donors.* Analytica Chimica Acta, 2013. **759**: p. 92-99.
51. Michaelis, J., G.J.V. van Noort, and O. Seitz, *DNA-Triggered Dye Transfer on a Quantum Dot.* Bioconjugate Chemistry, 2014. **25**(1): p. 18-23.
52. Bakalova, R., et al., *Quantum dot-conjugated hybridization probes for preliminary screening of siRNA sequences.* Journal of the American Chemical Society, 2005. **127**(32): p. 11328-11335.
53. Lee, H., I.K. Kim, and T.G. Park, *Intracellular Trafficking and Unpacking of siRNA/Quantum Dot-PEI Complexes Modified with and without Cell Penetrating Peptide: Confocal and Flow Cytometric FRET Analysis.* Bioconjugate Chemistry, 2010. **21**(2): p. 289-295.
54. Zhang, Y. and C.Y. Zhang, *Sensitive Detection of microRNA with Isothermal Amplification and a Single-Quantum-Dot-Based Nanosensor.* Analytical Chemistry, 2012. **84**(1): p. 224-231.
55. Su, S., et al., *DNA-Conjugated Quantum Dot Nanoprobe for High-Sensitivity Fluorescent Detection of DNA and micro-RNA.* ACS Applied Materials & Interfaces, 2014. **6**(2): p. 1152-1157.
56. Kim, J.H., D. Morikis, and M. Ozkan, *Adaptation of inorganic quantum dots for stable molecular beacons.* Sensors and Actuators B-Chemical, 2004. **102**(2): p. 315-319.
57. Kim, J.H., S. Chaudhary, and M. Ozkan, *Multicolour hybrid nanoprobes of molecular beacon conjugated quantum dots: FRET and gel electrophoresis assisted target DNA detection.* Nanotechnology, 2007. **18**(19).
58. Cady, N.C., A.D. Strickland, and C.A. Batt, *Optimized linkage and quenching strategies for quantum dot molecular beacons.* Molecular and Cellular Probes, 2007. **21**(2): p. 116-124.
59. Medintz, I.L., et al., *A reactive peptidic linker for self-assembling hybrid quantum dot-DNA bioconjugates.* Nano Letters, 2007. **7**(6): p. 1741-1748.
60. Wu, C.S., et al., *Robust silica-coated quantum dot-molecular beacon for highly sensitive DNA detection.* Biosensors & Bioelectronics, 2011. **26**(9): p. 3870-3875.
61. Algar, W.R. and U.J. Krull, *Interfacial Transduction of Nucleic Acid Hybridization Using Immobilized Quantum Dots as Donors in Fluorescence Resonance Energy Transfer.* Langmuir, 2009. **25**(1): p. 633-638.
62. Algar, W.R. and U.J. Krull, *Toward A Multiplexed Solid-Phase Nucleic Acid Hybridization Assay Using Quantum Dots as Donors in Fluorescence Resonance Energy Transfer.* Analytical Chemistry, 2009. **81**(10): p. 4113-4120.

63. Algar, W.R. and U.J. Krull, *Developing Mixed Films of Immobilized Oligonucleotides and Quantum Dots for the Multiplexed Detection of Nucleic Acid Hybridization Using a Combination of Fluorescence Resonance Energy Transfer and Direct Excitation of Fluorescence.* Langmuir, 2010. **26**(8): p. 6041-6047.
64. Algar, W.R. and U.J. Krull, *Multiplexed Interfacial Transduction of Nucleic Acid Hybridization Using a Single Color of Immobilized Quantum Dot Donor and Two Acceptors in Fluorescence Resonance Energy Transfer.* Analytical Chemistry, 2010. **82**(1): p. 400-405.
65. Chen, L., et al., *Toward a solid-phase nucleic acid hybridization assay within microfluidic channels using immobilized quantum dots as donors in fluorescence resonance energy transfer.* Analytical and Bioanalytical Chemistry, 2011. **399**(1): p. 133-141.
66. Tavares, A.J., et al., *On-Chip Transduction of Nucleic Acid Hybridization Using Spatial Profiles of Immobilized Quantum Dots and Fluorescence Resonance Energy Transfer.* Analytical Chemistry, 2012. **84**(1): p. 312-319.
67. Noor, M.O., A.J. Tavares, and U.J. Krull, *On-chip multiplexed solid-phase nucleic acid hybridization assay using spatial profiles of immobilized quantum dots and fluorescence resonance energy transfer.* Analytica Chimica Acta, 2013. **788**: p. 148-157.
68. Noor, M.O., A. Shahmuradyan, and U.J. Krull, *Paper-Based Solid-Phase Nucleic Acid Hybridization Assay Using Immobilized Quantum Dots as Donors in Fluorescence Resonance Energy Transfer.* Analytical Chemistry, 2013. **85**(3): p. 1860-1867.
69. Noor, M.O. and U.J. Krull, *Paper-Based Solid-Phase Multiplexed Nucleic Acid Hybridization Assay with Tunable Dynamic Range Using Immobilized Quantum Dots As Donors in Fluorescence Resonance Energy Transfer.* Analytical Chemistry, 2013. **85**(15): p. 7502-7511.
70. Petryayeva, E., W.R. Algar, and U.J. Krull, *Adapting Fluorescence Resonance Energy Transfer with Quantum Dot Donors for Solid-Phase Hybridization Assays in Microtiter Plate Format.* Langmuir, 2013. **29**(3): p. 977-987.
71. Meeprasert, A., S. Hannongbua, and T. Rungrotmongkol, *Key Binding and Susceptibility of NS3/4A Serine Protease Inhibitors against Hepatitis C Virus.* Journal of Chemical Information and Modeling, 2014. **54**(4): p. 1208-1217.
72. Pokorna, J., et al., *Current and Novel Inhibitors of HIV Protease.* Viruses-Basel, 2009. **1**(3): p. 1209-1239.
73. Flores-Resendiz, D., E. Castellanos-Juarez, and L. Benitez-Bribiesca, *Proteases in cancer progression.* Gaceta Medica De Mexico, 2009. **145**(2): p. 131-142.
74. Chang, E., et al., *Protease-activated quantum dot probes.* Biochemical and Biophysical Research Communications, 2005. **334**(4): p. 1317-1321.
75. Shi, L.F., et al., *Synthesis and application of quantum dots FRET-based protease sensors.* Journal of the American Chemical Society, 2006. **128**(32): p. 10378-10379.
76. Shi, L.F., N. Rosenzweig, and Z. Rosenzweig, *Luminescent quantum dots fluorescence resonance energy transfer-based probes for enzymatic activity and enzyme inhibitors.* Analytical Chemistry, 2007. **79**(1): p. 208-214.
77. Li, X., et al., *Protease-activated quantum dot probes based on fluorescence resonance energy transfer.* Chinese Science Bulletin, 2013. **58**(21): p. 2657-2662.

78. Medintz, I.L., et al., *Proteolytic activity monitored by fluorescence resonance energy transfer through quantum-dot-peptide conjugates.* Nature Materials, 2006. **5**(7): p. 581-589.
79. Clapp, A.R., et al., *Monitoring of Enzymatic Proteolysis Using Self-Assembled Quantum Dot-Protein Substrate Sensors.* Journal of Sensors, 2008. **2008**.
80. Boeneman, K., et al., *Sensing Caspase 3 Activity with Quantum Dot-Fluorescent Protein Assemblies.* Journal of the American Chemical Society, 2009. **131**(11): p. 3828-+.
81. Prasuhn, D.E., et al., *Quantum Dot Peptide Biosensors for Monitoring Caspase 3 Proteolysis and Calcium Ions.* Acs Nano, 2010. **4**(9): p. 5487-5497.
82. Biswas, P., et al., *A quantum-dot based protein module for in vivo monitoring of protease activity through fluorescence resonance energy transfer.* Chemical Communications, 2011. **47**(18): p. 5259-5261.
83. Choi, Y., et al., *Fluorogenic assay and live cell imaging of HIV-1 protease activity using acid-stable quantum dot-peptide complex.* Chemical Communications, 2010. **46**(48): p. 9146-9148.
84. Cella, L.N., et al., *Quantitative Assessment of In Vivo HIV Protease Activity Using Genetically Engineered QD- Based FRET Probes.* Biotechnology and Bioengineering, 2014. **111**(6): p. 1082-1087.
85. Kim, Y.P., et al., *Chip-based protease assay using fluorescence resonance energy transfer between quantum dots and fluorophores.* Biochip Journal, 2007. **1**(4): p. 228-233.
86. Sapsford, K.E., et al., *Monitoring of enzymatic proteolysis on a electroluminescent-CCD microchip platform using quantum dot-peptide substrates.* Sensors and Actuators B-Chemical, 2009. **139**(1): p. 13-21.
87. Petryayeva, E. and W.R. Algar, *Proteolytic Assays on Quantum-Dot-Modified Paper Substrates Using Simple Optical Readout Platforms.* Analytical Chemistry, 2013. **85**(18): p. 8817-8825.
88. Petryayeva, E. and W.R. Algar, *Multiplexed Homogeneous Assays of Proteolytic Activity Using a Smartphone and Quantum Dots.* Analytical Chemistry, 2014. **86**(6): p. 3195-3202.
89. Kim, H., E. Petryayeva, and W.R. Algar, *Enhancement of Quantum Dot Forster Resonance Energy Transfer within Paper Matrices and Application to Proteolytic Assays.* Ieee Journal of Selected Topics in Quantum Electronics, 2014. **20**(3).
90. Goldman, E.R., et al., *A hybrid quantum dot-antibody fragment fluorescence resonance energy transfer-based TNT sensor.* Journal of the American Chemical Society, 2005. **127**(18): p. 6744-6751.
91. Xia, Y.S., L. Song, and C.Q. Zhu, *Turn-On and Near-Infrared Fluorescent Sensing for 2,4,6-Trinitrotoluene Based on Hybrid (Gold Nanorod)-(Quantum Dots) Assembly.* Analytical Chemistry, 2011. **83**(4): p. 1401-1407.
92. Medintz, I.L., et al., *Self-assembled nanoscale biosensors based on quantum dot FRET donors.* Nature Materials, 2003. **2**(9): p. 630-638.
93. Tang, B., et al., *A New Nanobiosensor for Glucose with High Sensitivity and Selectivity in Serum Based on Fluorescence Resonance Energy Transfer (FRET) between CdTe Quantum Dots and Au Nanoparticles.* Chemistry – A European Journal, 2008. **14**(12): p. 3637-3644.
94. Hu, B., et al., *The inhibition of fluorescence resonance energy transfer between quantum dots for glucose assay.* Biosensors & Bioelectronics, 2012. **32**(1): p. 82-88.

95. Wang, Y., et al., *A near infrared fluorescence resonance energy transfer based aptamer biosensor for insulin detection in human plasma.* Chemical Communications, 2014. **50**(7): p. 811-813.
96. Nikiforov, T.T. and J.M. Beechem, *Development of homogeneous binding assays based on fluorescence resonance energy transfer between quantum dots and Alexa Fluor fluorophores.* Analytical Biochemistry, 2006. **357**(1): p. 68-76.
97. Wei, O.D., et al., *Development of an open sandwich fluoroimmunoassay based on fluorescence resonance energy transfer.* Analytical Biochemistry, 2006. **358**(1): p. 31-37.
98. Long, F., H.C. Shi, and H.C. Wang, *Fluorescence resonance energy transfer based aptasensor for the sensitive and selective detection of 17 beta-estradiol using a quantum dot-bioconjugate as a nano-bioprobe.* RSC Advances, 2014. **4**(6): p. 2935-2941.
99. Li, J., et al., *Study on the fluorescence resonance energy transfer between CdTe QDs and butyl-rhodamine B in the presence of CTMAB and its application on the detection of Hg(II).* Spectrochimica Acta Part a-Molecular and Biomolecular Spectroscopy, 2008. **70**(4): p. 811-817.
100. Page, L.E., et al., *Detection of toxic mercury ions using a ratiometric CdSe/ZnS nanocrystal sensor.* Chemical Communications, 2011. **47**(27): p. 7773-7775.
101. Liu, B.Y., et al., *Nanoparticles as scaffolds for FRET-based ratiometric detection of mercury ions in water with QDs as donors.* Analyst, 2012. **137**(16): p. 3717-3724.
102. Hu, B., et al., *A FRET ratiometric fluorescence sensing system for mercury detection and intracellular colorimetric imaging in live Hela cells.* Biosensors & Bioelectronics, 2013. **49**: p. 499-505.
103. Tao, H.L., et al., *Determination of trace Hg2+ ions based on the fluorescence resonance energy transfer between fluorescent brightener and CdTe quantum dots.* Journal of Luminescence, 2014. **146**: p. 376-381.
104. Wang, X. and X.Q. Guo, *Ultrasensitive Pb(2+) detection based on fluorescence resonance energy transfer (FRET) between quantum dots and gold nanoparticles.* Analyst, 2009. **134**(7): p. 1348-1354.
105. Zhao, Q., et al., *Dithizone functionalized CdSe/CdS quantum dots as turn-on fluorescent probe for ultrasensitive detection of lead ion.* Journal of Hazardous Materials, 2013. **250**: p. 45-52.
106. Wu, C.S., M.K.K. Oo, and X.D. Fan, *Highly Sensitive Multiplexed Heavy Metal Detection Using Quantum-Dot-Labeled DNAzymes.* ACS Nano, 2010. **4**(10): p. 5897-5904.
107. Ganguly, R., S.H. Wang, and D.J. Huang, *Salen Derivatives Functionalized CdSe-ZnS Quantum Dots as Fluorescent Probes for Selective Cu(II) and Fe(II) Sensing.* Nanoscience and Nanotechnology Letters, 2010. **2**(3): p. 208-212.
108. Yang, P., et al., *Phenol Formaldehyde Resin Nanoparticles Loaded with CdTe Quantum Dots: A Fluorescence Resonance Energy Transfer Probe for Optical Visual Detection of Copper(II) Ions.* ACS Nano, 2011. **5**(3): p. 2147-2154.
109. Ruedas-Rama, M.J. and E.A.H. Hall, *Multiplexed energy transfer mechanisms in a dual-function quantum dot for zinc and manganese.* Analyst, 2009. **134**(1): p. 159-169.
110. Chen, C.Y., et al., *Potassium ion recognition by 15-crown-5 functionalized CdSe/ZnS quantum dots in H2O.* Chemical Communications, 2006(3): p. 263-265.

111. Xue, M., et al., *A new nanoprobe based on FRET between functional quantum dots and gold nanoparticles for fluoride anion and its applications for biological imaging.* Biosensors & Bioelectronics, 2012. **36**(1): p. 168-173.
112. Snee, P.T., et al., *A ratiometric CdSe/ZnS nanocrystal pH sensor.* Journal of the American Chemical Society, 2006. **128**(41): p. 13320-13321.
113. Suzuki, M., et al., *Quantum dot FRET Biosensors that respond to pH, to proteolytic or nucleolytic cleavage, to DNA synthesis, or to a multiplexing combination.* Journal of the American Chemical Society, 2008. **130**(17): p. 5720-5725.
114. Jin, T., et al., *A quantum dot-based ratiometric pH sensor.* Chemical Communications, 2010. **46**(14): p. 2408-2410.
115. Kurabayashi, T., et al., *CdSe/ZnS Quantum Dots Conjugated with a Fluorescein Derivative: a FRET-based pH Sensor for Physiological Alkaline Conditions.* Analytical Sciences, 2014. **30**(5): p. 545-550.
116. Dennis, A.M., et al., *Quantum Dot-Fluorescent Protein FRET Probes for Sensing Intracellular pH.* ACS Nano, 2012. **6**(4): p. 2917-2924.
117. Kattke, M.D., et al., *FRET-Based Quantum Dot Immunoassay for Rapid and Sensitive Detection of Aspergillus amstelodami.* Sensors, 2011. **11**(6): p. 6396-6410.
118. Wang, D., et al., *Detection of Staphylococcus aureus Carrying the Gene for Toxic Shock Syndrome Toxin 1 by Quantum-Dot-Probe Complexes.* Journal of Fluorescence, 2011. **21**(4): p. 1525-1530.
119. Liao, Y.H., X.M. Zhou, and D. Xing, *Quantum Dots and Graphene Oxide Fluorescent Switch Based Multivariate Testing Strategy for Reliable Detection of Listeria monocytogenes.* ACS Applied Materials & Interfaces, 2014. **6**(13): p. 9988-9996.
120. Burris, K.P., et al., *Mega-Nano Detection of Foodborne Pathogens and Transgenes Using Molecular Beacon and Semiconductor Quantum Dot Technologies.* IEEE Transactions on NanoBioscience, 2013. **12**(3): p. 233-238.
121. Shanehsaz, M., et al., *Detection of Helicobacter pylori with a nanobiosensor based on fluorescence resonance energy transfer using CdTe quantum dots.* Microchimica Acta, 2013. **180**(3-4): p. 195-202.
122. Sapsford, K.E., et al., *Monitoring Botulinum Neurotoxin A Activity with Peptide-Functionalized Quantum Dot Resonance Energy Transfer Sensors.* ACS Nano, 2011. **5**(4): p. 2687-2699.
123. Vinayaka, A.C. and M.S. Thakur, *Facile synthesis and photophysical characterization of luminescent CdTe quantum dots for Forster resonance energy transfer based immunosensing of staphylococcal enterotoxin B.* Luminescence, 2013. **28**(6): p. 827-835.
124. Zekavati, R., et al., *Highly sensitive FRET-based fluorescence immunoassay for aflatoxin B1 using cadmium telluride quantum dots.* Microchimica Acta, 2013. **180**(13-14): p. 1217-1223.
125. Xu, W., et al., *A homogeneous immunosensor for AFB(1) detection based on FRET between different-sized quantum dots.* Biosensors & Bioelectronics, 2014. **56**: p. 144-150.
126. Stringer, R.C., et al., *Development of an optical biosensor using gold nanoparticles and quantum dots for the detection of Porcine Reproductive and Respiratory Syndrome Virus.* Sensors and Actuators B-Chemical, 2008. **134**(2): p. 427-431.

127. Wang, X., et al., *QDs-DNA nanosensor for the detection of hepatitis B virus DNA and the single-base mutants.* Biosensors & Bioelectronics, 2010. **25**(8): p. 1934-1940.
128. Huang, S., et al., *A Simple QD-FRET Bioprobe for Sensitive and Specific Detection of Hepatitis B Virus DNA.* Journal of Fluorescence, 2013. **23**(5): p. 1089-1098.
129. Tian, J.P., et al., *Detection of influenza A virus based on fluorescence resonance energy transfer from quantum dots to carbon nanotubes.* Analytica Chimica Acta, 2012. **723**: p. 83-87.
130. Chou, C.C. and Y.H. Huang, *Nucleic Acid Sandwich Hybridization Assay with Quantum Dot-Induced Fluorescence Resonance Energy Transfer for Pathogen Detection.* Sensors, 2012. **12**(12): p. 16660-16672.
131. Chen, L., et al., *Simultaneous Determination of Human Enterovirus 71 and Coxsackievirus B3 by Dual-Color Quantum Dots and Homogeneous Immunoassay.* Analytical Chemistry, 2012. **84**(7): p. 3200-3207.
132. Safarpour, H., et al., *Development of a quantum dots FRET-based biosensor for efficient detection of Polymyxa betae.* Canadian Journal of Plant Pathology-Revue Canadienne De Phytopathologie, 2012. **34**(4): p. 507-515.
133. Zhang, K., et al., *Ligand Replacement-Induced Fluorescence Switch of Quantum Dots for Ultrasensitive Detection of Organophosphorothioate Pesticides.* Analytical Chemistry, 2010. **82**(22): p. 9579-9586.
134. Guo, J.J., et al., *Efficient fluorescence resonance energy transfer between oppositely charged CdTe quantum dots and gold nanoparticles for turn-on fluorescence detection of glyphosate.* Talanta, 2014. **125**: p. 385-392.
135. Wang, X., et al., *Fluorescence immunoassay of octachlorostyrene based on Forster resonance energy transfer between CdTe quantum dots and rhodamine B.* Biosensors & Bioelectronics, 2014. **60**: p. 52-56.

Property	Quantum dots	Fluorophores	Ref.
Absorption spectra	Broad spectra, possible excitation with UV light	in general narrow, but variable	[26-27]
Emission spectra	narrow, in band width 20-40nm	broad, asymmetric and tailed	[26-27]
Stokes shift	300-400 nm	less than 100nm	[30]
Quantum yield	40% to 90%,depending on buffer and surface modification	variable, depends on the chosen fluorophore	[32-33]
Fluorescence lifetime	20 -50 nanoseconds	few nanoseconds	[31]
Photostability	strong resistance to photobleaching	variable, depends on the chosenfluorophore	[32-33]
Molar extinction coefficient	< 200 000 M-1 cm -1	10-100 times less than QDs	[28-29]

Table 1.Short summary of charasteristics comparation between QDs and organic fluorophores

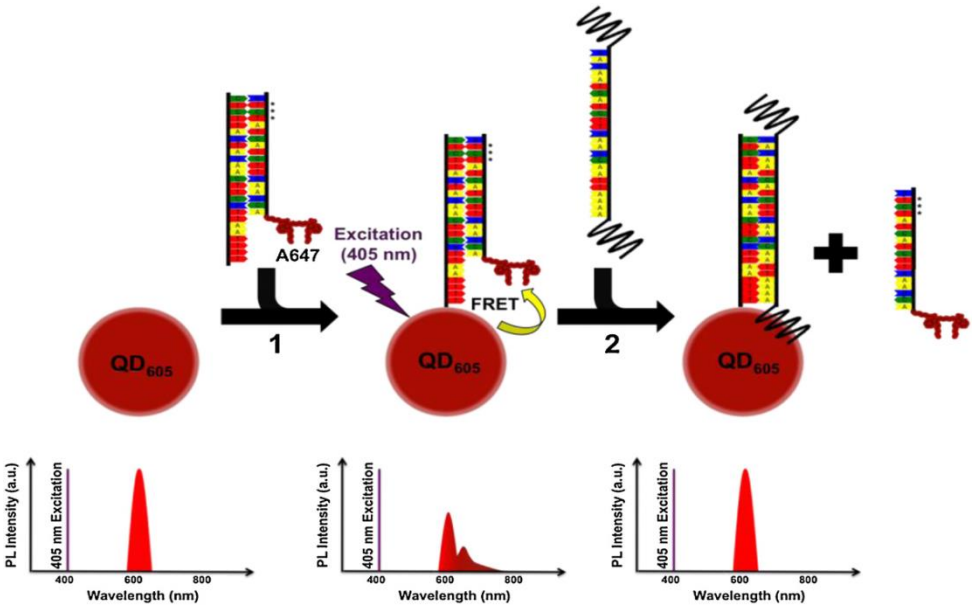

Figure 1. Competitive displacement-based QDs-FRET assay for intracellular detection of target DNA. System designed consisted of (1) CdSe/ZnSQD$_{605}$ and Alexa Fluor 647 (A647) labelled (dsDNA) containing mismatching bases (market with asterisks) as energy donor and acceptor with visible high PL of QDs, (2) streptavidin-biotin linkage between QDs and A647 labelled dsDNA followed, upon excitation with QDs PL quenching and (3) detachment of the single strand with designed mismatches of dsDNA in the presence of the fully complementary target ssDNA visible by QDs PL recovery. Reprinted from [50] with permission from Elsevier**.**

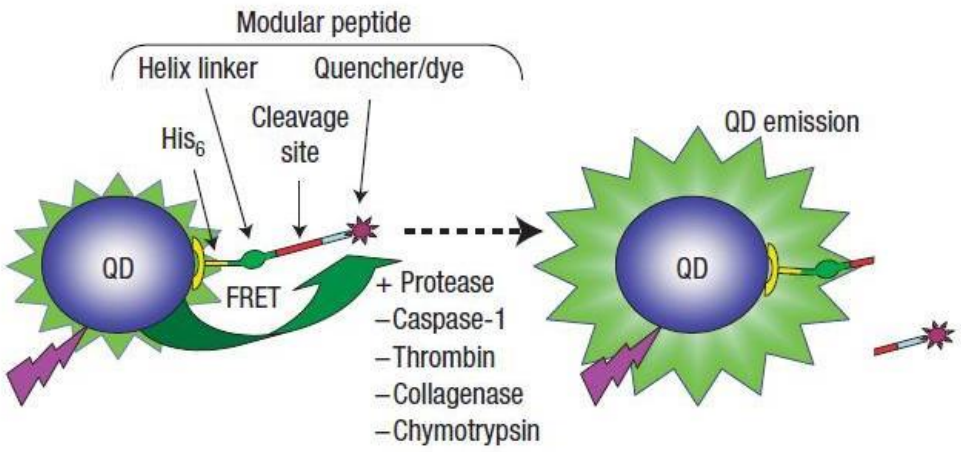

Figure 2. QD-FRET sensor for detection of the enzymes activity.

On the with N-terminal hexahistidine (His_6) sequence for easier attachement to the DHLA capped QDs as energy donors, while on C-terminal on the cysteine residues was used for dye attachment followed by helix linker for providing peptide rigidity, next part is cleavage site which was specific to the protease, capsase-1, thrombin, collagenase and chymotrypsin as enzyme of interest and on C-terminal site-specific location (cysteine thiol) for dye attachment. Cy3 and QXL™520 were used dyes in this sensor for QDs PL quenching and in the presence of the enzyme cleavage occurred drif away QDs and dyes as energy donor and acceptor preventing FRET causing QDs PL recovery. Adapted by permission from Macmillan Publishers Ltd: Nature Materials [78] copyright 2006.

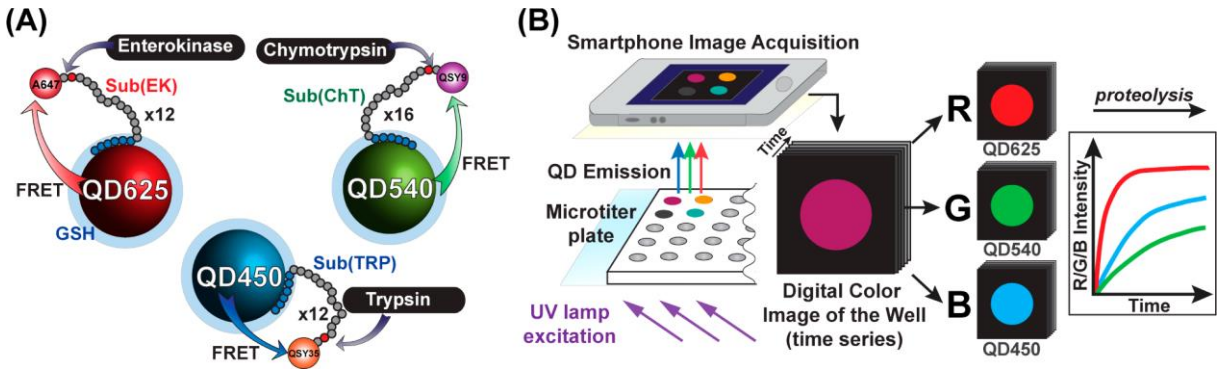

Figure 3. Multiplexed QD-FRET assays for the detection of proteolytic activity using a smartphone. (A) Design of the assay with three color different QDs as energy donors and as acceptors QSY35, QSY9 or A647 dyes were used for labeling peptide with enzyme-specific cleavage site. (B) Detection of the PL recovery as a result of proteolytic activity via smartphone camera and hand-held UV lamp as excitation source. Reprinted with permission from [88].Copyright 2014 American Chemical Society.

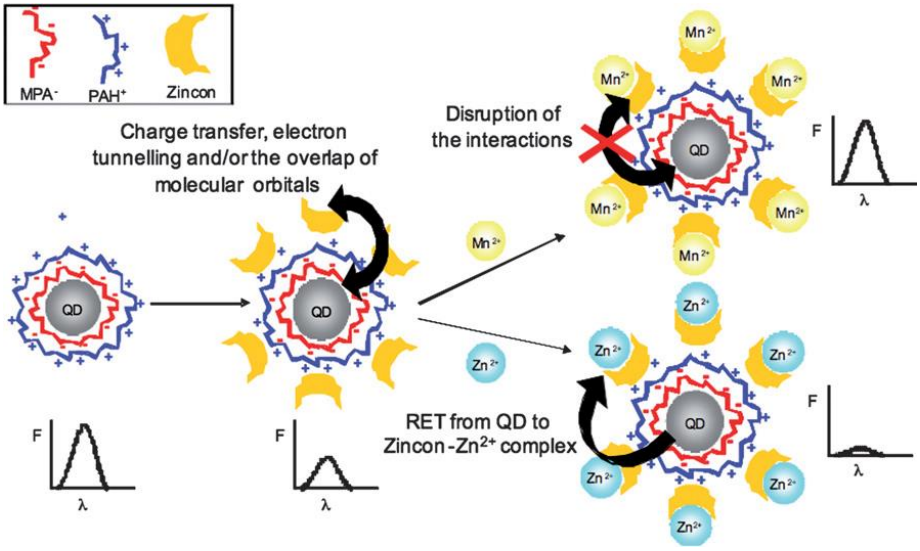

Figure 4. QD-FRET sensor for detection of Zn(II) and Mn(II) ions.

In designed system QDs capped with MPA were modified with poly(allylamine hydrochloride) (PAH^+) was chosen for achieving positive charge on the QDs surface used for electrostatic bindng of the zincon. System has exhibited QDs PL quenching due to metal-ion disruption of the QD-zincon system caused by formation of the zincon-metal complex and QDs PL enhancement due to RET and/or FRET in the detection of the Zn(II) and Mn(II) ions, respectively. Reproduced from [109] with permission of The Royal Society of Chemistry.

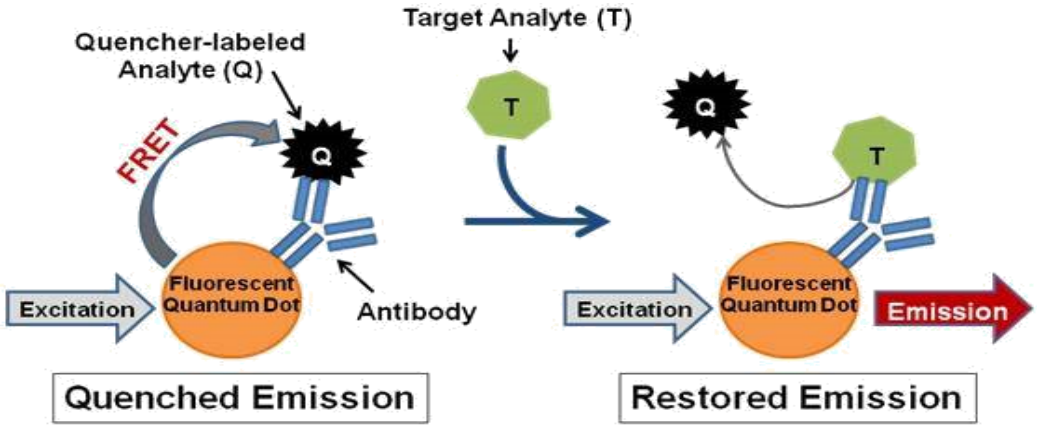

Figure 5. Schematic presentation of the QD-FRET based immunoassays for mold spores of the *Aspergillus amstelodami.* Amine-derivatized (PEG)-coated CdSe/ZnS QDs were linked to the ant-*Aspergilus* antibody via SMCC crosslinker which interacted with BHQ-3 labeled mold analytes with lower affinity than *A. Amstelodami* mold spores. As a result QDs PL was quenched but in the presence of the *A. Amstelodami* mold spores lower affinity mold analytes will be displaced recovering PL as detection signal. Reprinted with permission from [117].

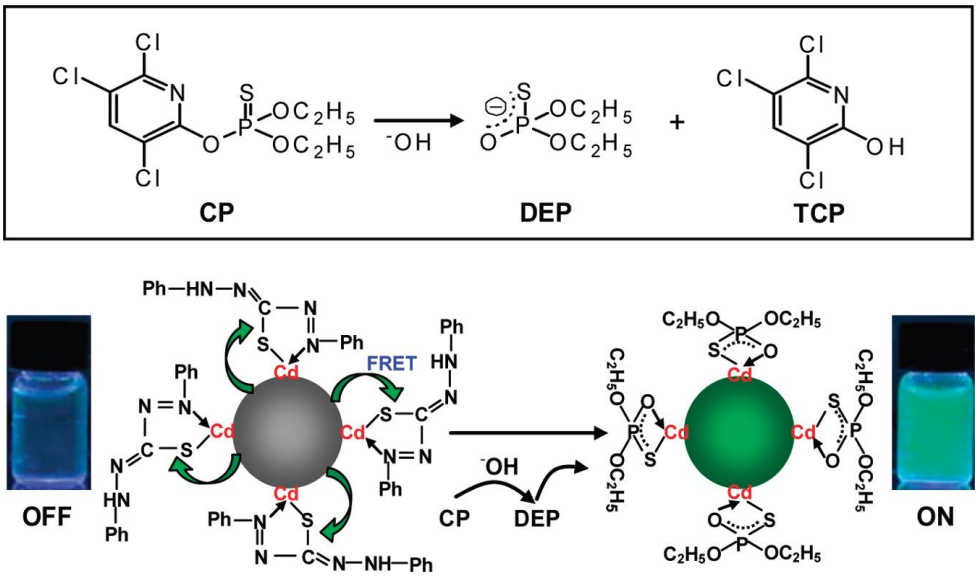

Figure 6. QD-FRET sensor for organophosphorus pesticides detection.

CdTe QDs were modified with dithizone (DZ) via surface coordinating reaction causing QDs PL quenching due to the spectral overlap between them. Organophosphorothioate pesticides chlorpyrifos in the basic condition of the sensor hydrolyzed to diethylphosphorothioate (DEP) and trichloro-2-pyridinol (TCP). DEP replaced DZ ligands on the QDs recovering its PL. Reprinted with the permission from [133].Copyright 2010 American Chemical Society.

4 Material and methods

4.1 Microwave synthesis of the CdTe QDs

All chemicals were purchased from Sigma Aldrich (St. Louis, MA, USA) in ACS purity unless stated otherwise. CdTe-MPA QDs were prepared by microwave synthesis (Anton Paar, Wien, Austria) according to the following procedure adapted from Duan et al. (Duan, Song et al. 2009): the solution of 4 mL of $CdCl_2$ (0.04 M) was mixed with 4 mL of Na_2TeO_3 (0.01 M), 100 mg of sodium citrate and 50 mg $NaBH_4$, 119 mg MPA and 42 mL of H_2O. The mixture was heated by microwave radiation for 10 min (300 W). For removing the excessive reagents CdTe-MPA QDs were precipitated in isopropanol by mixing 1 mL of CdTe-MPA QDs and 1 mL of isopropanol and centrifuged. After centrifugation supernatant has been removed and QDs were dissolved in 1 mL of water.

4.2 Spectroscopic analysis

Multifunctional microplate reader Tecan Infinite 200 PRO 132 (TECAN, Mannedorf, Switzerland) was used for obtaining fluorescence and absorbance spectra of QDs. Excitation wavelength was 350 nm and the fluorescence scan was measured within the range from 400 to 850 nm per 5 nm steps and each value is an average of 5 measurements pre vale. The absorbance was acquired within the range from 230 to 1000 nm per 5 nm step as an average of 5 measurements per vale as well. 50 μL of the sample was placed in transparent 96-well microplate with flat bottom by Nunc (ThermoScientific, Waltham, MA, USA).

4.3 Capillary electrophoresis with UV and LIF detection

Electrophoretic measurements were carried out using Beckman P/ACE MDQ capillary electrophoresis system equipped with absorbance detection at 214 nm or laser induced detector with excitation wavelength of 488 nm (argon ion laser)and emission wavelength was 510 nm. Separation was carried out in uncoated fused silica capillary with total length of 60 cm, effective length of 50 cm, internal diameter of 75 μm and outer diameter of 375 μm. 20 mM borate (pH 9.2) was used as background electrolyte. Separation was carried out at 20 kV in positive polarity and sample was injected hydrodynamically for 20s using 3.4 kPa.

4.4 SDS polyacrylamide electrophoresis (SDS-PAGE)

Electrophoresis was performed using a Mini Protean Tetra apparatus with gel dimensions of 8.3 × 7.3 × 0.1 cm (Bio-Rad, USA). First 7% w/v running, then 5% w/v stacking gel was poured. The gels were prepared from 30% w/v acrylamide stock solution with 1% w/v bisacrylamide. The polymerization of the running or stacking gels was carried out at room temperature for 45 min. Prior to analysis, the samples were mixed with reducing (3.3% mercaptoethanol, v/v) or non-reducing sample buffer in a 1:1 ratio. "Precision plus protein standards" protein ladder from Bio-Rad was used to determine molecular mass. The electrophoresis was run at 150 V for 45 min at laboratory temperature (Power Basic, Bio-Rad) in Tris-glycine buffer (0.025 M Trizma-base, 0.19 M glycine and 3.5 mM SDS, pH 8.3). After separation for protein staining Coomassie-blue was used.

4.5 Agarose gel electrophoresis

Agarose gel (2% v/v, highmelt, medium fragments, Chemos CZ, Prague, Czech Republic) was prepared with 1× TAE buffer (40 mMTris, 20 mM acetic acid, and 1 mM ethylenediaminetetraacetic acid. Five microliters of samples were prepared with 5% v/v bromphenol blue and 3% v/v glycerol and loaded into the gel. A 100 bp DNA ladder (New England Biolabs, Ipswich, MA, USA) was used to monitor the size of analyzed DNA. The electrophoresis was run at 60 V and 6°C for 160 min.100 mL of TAE buffer with 50 μL of ethidium bromide for 20 min was used for gel staining and visualized by UV transilluminator (312 nm). The intensity of fluorescence was quantified using Carestream molecular imaging software (Carestream, USA).

5 Results and discussion

5.1 Non-specific interaction with biomolecules

STANISAVLJEVIC, M.; CHOMOUCKA, J.; DOSTALOVA, S.; KRIZKOVA, S.; VACULOVICOVA, M.; ADAM, V.; KIZEK R. Interaction between CdTe quantum dots and DNA revealed by capillary electrophoresis with laser-induced fluorescence detection. Electrophoresis, 2014. 35(18): p. 2587-2592.
ISSN: 0173-0835
DOI: 10.1002/elps.201400204

Participation in the work of the author Stanisavljevic M.: experimental part 20% and manuscript preparation 50%.

DNA is one of the most important biomolecule due to its responsibility for development, growing and maintaining of the life. The discovery of the DNA secret has triggered a numerous development of illness treatments and labeling of DNA has been successfully applied in the diagnosis. Quantum dots are considered as a new generation of the labeling materials because of their optical and electronic characteristics aforementioned.

The aim of this work was aqueous synthesis of CdTe QDs capped with glutathione of the specific 2 nm size for labeling DNA based on QDs size fitting into the major groove of the DNA double helix.

Characterization of the nanoparticles was done by Zetasizer 3000 Has (Malvern Instruments, Worcestershire, UK) and has confirmed desired size of 2 nm. From fluorescent spectroscopy emission maximum at 525 nm and absorption maximum at 490 nm were obtained showing strong green light emission. The dependence of the fluorescence signal and QDs concentration solution has been observed by spectroscopy and with CE-LIF as well. Further, interaction between QDs and DNA have been studied, through time and different concentration interaction with double stranded genomic chicken DNA (dsDNA), ssDNA and PCR fragment.

Upon QDs and dsDNA mixing interaction was observed with CE-LIF and two peaks were detectable. The first one represents the complex of the labeled DNA with QDs and the second one is the excess of the QDs. It is clearly seen growth of complex peak

trough the interaction time, as well as with different DNA concentration QDs are creating peaks with different fluorescence intensity, the highest concentration creates the highest peak.

Further, comparison of the interaction between ssDNA and dsDNA have confirmed that dsDNA is needed for complex creation because peak complex was not observed in the case of ssDNA interaction with QDs. Interaction with 500bp long DNA fragment have shown the same tendency of creating complex as with genomic DNA. The presence of the QDs in the structure of QDs was observed with gel electrophoresis after ethidium bromide staining. With software analysis it is found that signal is decreasing due to inability of DNA and/or 500bp fragment to be stained by ethidium bromide due to QDs incorporation in the DNA structure.

This is a very simple way of nonspecific DNA labeling with QDs due to the matching sizes of the QDs and major groove of DNA.

Maja Stanisavljevic[1]
Jana Chomoucka[2]
Simona Dostalova[1]
Sona Krizkova[1,2]
Marketa Vaculovicova[1,2]
Vojtech Adam[1,2]
Rene Kizek[1,2]

[1]Department of Chemistry and Biochemistry, Faculty of Agronomy, Mendel University in Brno, Zemedelska, Czech Republic
[2]Central European Institute of Technology, Brno University of Technology, Technicka, Czech Republic

Received April 16, 2014
Revised June 12, 2014
Accepted June 18, 2014

Research Article

Interactions between CdTe quantum dots and DNA revealed by capillary electrophoresis with laser-induced fluorescence detection

Quantum dots (QDs) are one of the most promising nanomaterials, due to their size-dependent characteristics as well as easily controllable size during the synthesis process. They are promising label material and their interaction with biomolecules is of great interest for science. In this study, CdTe QDs were synthesized under optimal conditions for 2 nm size. Characterization and verification of QDs synthesis procedure were done by fluorimetric method and with CE. Afterwards, QDs interaction with chicken genomic DNA and 500 bpDNA fragment was observed employing CE-LIF and gel electrophoresis. Performed interaction relies on possible matching between size of QDs and major groove of the DNA, which is approximately 2.1 nm.

Keywords:
Bacteriophage / DNA / Interaction / Quantum dots
DOI 10.1002/elps.201400204

1 Introduction

Nanoscale materials with very good electronic, optical, magnetic, and catalytic properties have made nanotechnology one of the most perspective scientific fields today. Quantum dots (QDs) belong to a large family of nanoparticles attracting enormous attention especially due to the small size and size-dependent characteristics. With their size (1–20 nm) they do not obey rules of classical physics and they belong to unpredictable laws of quantum mechanics. Precisely, their optical and electronic properties are caused by phenomena called quantum confinement [1]. Wide absorbance band, narrow emission spectrum, and/or photostability are well-known properties of QDs, which made them the most promising substitute for organic dyes. Another advantage of these materials is their ability to be easily modified, which is primarily done to decrease potential danger of inorganic core toxicity, but these surface modification can be also done to target some biomolecules and, thus, to image biochemical pathways in vivo. Beside their successful application in in vivo imaging [2–5] and/or biology [6] in general, their applications into proteomics gain more and more attention [7–10]. Moreover, currently a great attention is paid to the targeted drug/gene delivery and the combination of therapeutic and diagnostic properties of various bioconjugates is explored, QDs are an excellent option for fluorescent labeling of numerous delivery systems. Not only a range of modern artificial nanomaterials but also traditionally utilized viral-based nanocarriers such as bacteriophages belong among such nanocarriers employed for targeted delivery [11]. In the case of nucleic acids delivery, revolutionary discovery of DNA structure done by Watson and Crick in 1953 [12] opened numerous challenges in this field of research. Rapid growth of nanomaterials such as QDs induced their inevitable encounter with DNA. Possible interaction between DNA and other molecules or species is provided by electrostatic binding in major groove of dsDNA and intercalation between base pairs [13]. Investigation of QDs and DNA have not been only directed to their interaction [14], but QDs have been successfully functionalized by DNA and used for fluorescence monitoring in vivo or in vitro [15, 16].

CE-LIF is a very powerful method for analysis of different nanoparticles in size, shape, or due to their charge [17–19]. QDs have been successfully characterized by CE-LIF [17, 20, 21], which have been also applied for separation and characterization of biomolecules labeled with QDs as a fluorescent marker [5, 22–25]. For biological application of QDs, their conjugation to biomolecules is an ongoing problematic and research challenge. The overview of advances can be found in various review articles [26–28].

Based on aforementioned knowledge, CE-LIF was chosen as a suitable method for monitoring of interaction between QDs and DNA depending on the concentration, time of interaction, length of the DNA strand, and/or its form (ssDNA

Correspondence: Dr. Rene Kizek, Department of Chemistry and Biochemistry, Mendel University in Brno, Zemedelska 1, CZ-613 00 Brno, Czech Republic
E-mail: kizek@sci.miuni.cz
Fax: +420-5-4521-2044

Abbreviations: **GSH**, glutathione; **QD**, quantum dot

Colour Online: See the article online to view Figs. 1–5 in colour.

vs. dsDNA). This method can be used for a very simple DNA labeling with QDs and/or observing possible toxic impact of QDs to DNA and its biological function.

2 Materials and methods

2.1 Chemicals

All chemicals were purchased from Sigma Aldrich (St. Louis, MA, USA) in ACS purity unless noted otherwise. Lyophilized highly polymerized DNA (Reanal, Hungary) was isolated from chicken erythrocytes (Mw = 400 000 g/mol). The stock solution of DNA (1 mg/mL) was prepared by dissolving in ACS water.

2.2 DNA amplification and isolation

Taq PCR kit and DNA isolated from bacteriophage λ (48 502 bp) were purchased from New England BioLabs (USA). Primers for PCR were synthesized by Sigma-Aldrich. The sequence of a forward primer was 5′-CCTGCTCTGCCG CTTCACGC-3′ and the sequence of a reverse primer was 5′-TCCGGATAAAAACGTCGATGACATTTGC-3′. Fifty microliters reaction mixture was composed of 5 μL 10× standard *Taq* reaction buffer, 1 μL of 10 μM dNTP solution mix, 1 μL of each primer (10 μM), 0.25 μL of 5 U/μL *Taq* DNA polymerase, 1 μL of 0.5 μg/μL λ DNA, and 40.75 μL H_2O (sterile). The PCR tubes with mixture were placed into the cycler (Eppendorf, Germany) and cycling conditions were as follows: initial denaturation at 95°C for 120 s; 25 cycles of denaturation at 95°C for 15 s, annealing at 64°C for 15 s, extension at 72°C for 45 s and a final extension at 72°C for 5 min. Hundred microliters of PCR product (500 bp) was purified by MinElute PCR Purification Kit (Qiagen, Germany) according to manufacturer's instruction and DNA was concentrated to 10 μL of water solution. DNA concentration was determined by spectrophotometric analysis at 260 nm using spectrophotometer Specord 210 (AnalytikJena, Germany).

2.3 CdTe quantum dots synthesis

The procedure for synthesis of these dots was adapted from the work of Duan et al. [29]. Briefly, the synthesis of CdTe QDs and their subsequent coating were as follows: 4 mL of the $CdCl_2$ solution (0.04 M) was diluted with 42 mL of water. During constant stirring, 100 mg of sodium citrate, 4 mL of Na_2TeO_3 solution (0.01 M), 300 mg of reduced glutathione (GSH), and 50 mg of $NaBH_4$ were added into water–cadmium(II) solution. The mixture was kept at 95°C under the reflux cooling for 4 h. As a result, yellow solution of the GSH-QDs was obtained.

2.4 Spectroscopic and size analysis

Fluorescence and absorbance spectra were measured by multifunctional microplate reader Tecan Infinite 200 PRO 132 (TECAN, Männedorf, Switzerland). Excitation wavelength was 230 nm and emission range was measured from 300 to 850 nm per 5 nm steps. The absorbance was acquired within the range from 230 to 800 nm with 5 nm steps as an average of five measurements per well. The detector gain was set to 80. The sample volume of 50 μL was placed in UV-transparent 96-well microplate with flat bottom by Costar (Corning, New York, USA). Zetasizer 3000 HSa (Malvern Instruments, Worcestershire, UK) was used for determination of size nanoparticles based on dynamic light scattering technique.

2.5 Capillary electrophoresis

Backman P/ACE™ MDQ electrophoresis system (Brea, CA, USA) with laser-induced detector was used for CE measurements. Excitation wavelength was 488 nm (argon ion laser) and emission wavelength was 520 nm. An uncoated fused silica capillary was used with total length of 60.5 cm, effective length of 50 cm, and internal diameter 75 μm. A 20 mM borate (pH 9.2) was used as BGE. Separation was carried out at 20 kV in positive polarity and sample was injected hydrodynamically for 20 s using 3.4 kPa.

2.6 Agarose gel electrophoresis

Agarose gel (2% v/v, high melt, medium fragments, Chemos CZ, Prague, Czech Republic) was prepared with 1× TAE buffer (40 mM Tris, 20 mM acetic acid, and 1 mM ethylenediaminetetraacetic acid). Five microliters of samples were prepared with 5% v/v bromphenol blue and 3% v/v glycerol and loaded into the gel. A 100 bp DNA ladder (New England Biolabs, Ipswich, MA, USA) was used to monitor the size of analyzed DNA. The electrophoresis was run at 60 V and 6°C for 160 min. The gel was stained in 100 mL of TAE buffer with 50 μL of ethidium bromide for 20 min and visualized by UV transilluminator (312 nm). The intensity of fluorescence was quantified using Carestream molecular imaging software (Carestream, USA)

3 Results and discussion

3.1 Quantum dots characterization

QDs are known as size-dependent nanomaterials. The size is controllable during the synthesis process, which can give us a desired absorbance and emission spectra important for their further application. In this study of DNA interaction with QDs, desired 2 nm sized QDs were synthesized according to the method described elsewhere [29]. The size of the QDs and

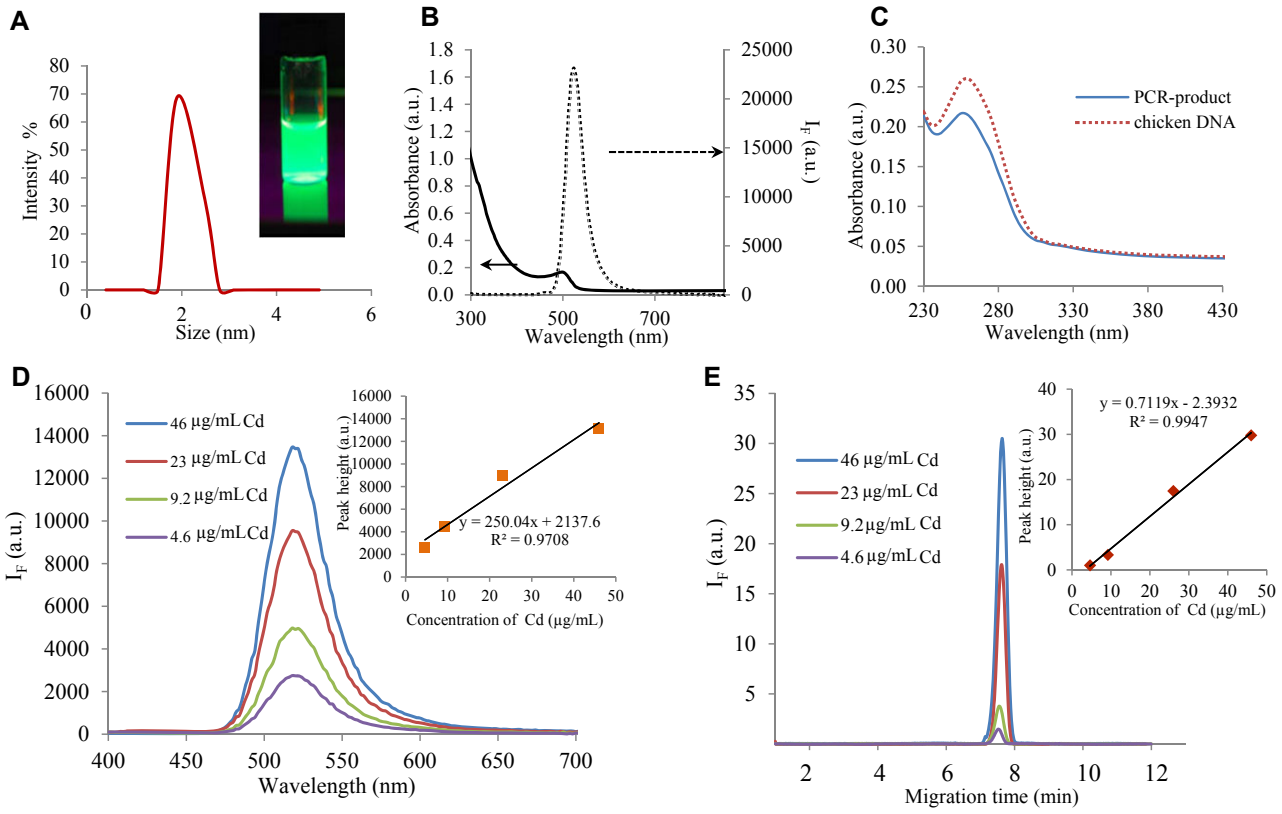

Figure 1. (A) Size determination of QDs by zeta-sizer, inset: photograph of QDs solution under UV light illumination. (B) Fluorescence and absorbance characterization of QDs. (C) Absorbance characterization of DNA and 500 bp fragment (200 μg/mL). (D) Fluorescence characterization of QDs diluted in water. All characterization was done by Tecan Infinite 200 PRO 132 under the following conditions: excitation wavelength was 230 nm and emission range was measured from 300 to 850 nm per 5 nm steps. The absorbance was acquired within the range from 230 to 1000 nm with 5 nm steps as an average of five measurements per well. Each intensity value is an average of five measurements. The detector gain was set to 80. The sample volume of 50 μL was placed in UV-transparent 96-well microplate with flat bottom by Costar. (E) CE characterization of QDs diluted in water. CE measurement is done by Beckman P/ACE™ MDQ electrophoresis system with LIF detector. Excitation wavelength was 488 nm and emission wavelength was 520 nm. An uncoated fused silica capillary was used with total length of 60.5 cm, effective length of 50 cm and internal diameter 75 μm. The 20 mM borate (pH 9.2) was used as BGE. Separation was carried out at 20 kV in positive polarity and sample was injected hydrodynamically for 20 s using 3.4 kPa. Concentration of QDs was recalculated to Cd concentration of 460 μg/mL according to [30].

their size-distribution is shown in Fig. 1A. The majority of the nanoparticles were 2 nm in diameter. The photograph of the solution of synthesized QDs under UV light illumination is shown in the inset in Fig. 1A exhibiting significant green light emission. Afterwards, their fluorescent properties were examined and their absorption maximum in visible range of spectra is 490 nm as indicated in Fig. 1B. The emission maximum after excitation by 490 nm light is at 525 nm. The absorption spectra of chicken genomic DNA and 498 bp fragment of bacteriophage λ used in the following experiments are shown in Fig. 1C.

To verify the linearity of the fluorescence signal depending on the concentration, the emission spectra of QDs were acquired (Fig. 1D). The concentration of QDs was expressed as the concentration of cadmium (inset in Fig. 1D). The Cd concentration in QDs was determined as described by Sobrova et al. [30]. The same characterization was performed by CE-LIF as shown in Fig. 1E. The peak of QDs with migration time of 7.5 min was observed and its height is linearly dependent on Cd concentration as shown in the inset in Fig. 1E.

3.2 CE-LIF analysis of interaction between DNA and quantum dots

After size and fluorescent characteristics of the QDs were verified, the interaction of these nanomaterials with DNA was studied. In the first experiment, the interaction between QDs and chicken genomic DNA was observed and results are shown in Fig. 2. The time dependence of complex formation can be seen in Fig. 2A. The peak 1 represents the DNA-QD complex and peak 2 represents the excess of the QDs. The increasing of the interaction time led to the increase of the peak 1 height. The dependence of the peak 1 height on time is shown in the inset in Fig. 2A. The same experiment measured by fluorescence spectroscopy exhibited only a very slight increase of the fluorescence intensity with the increasing time

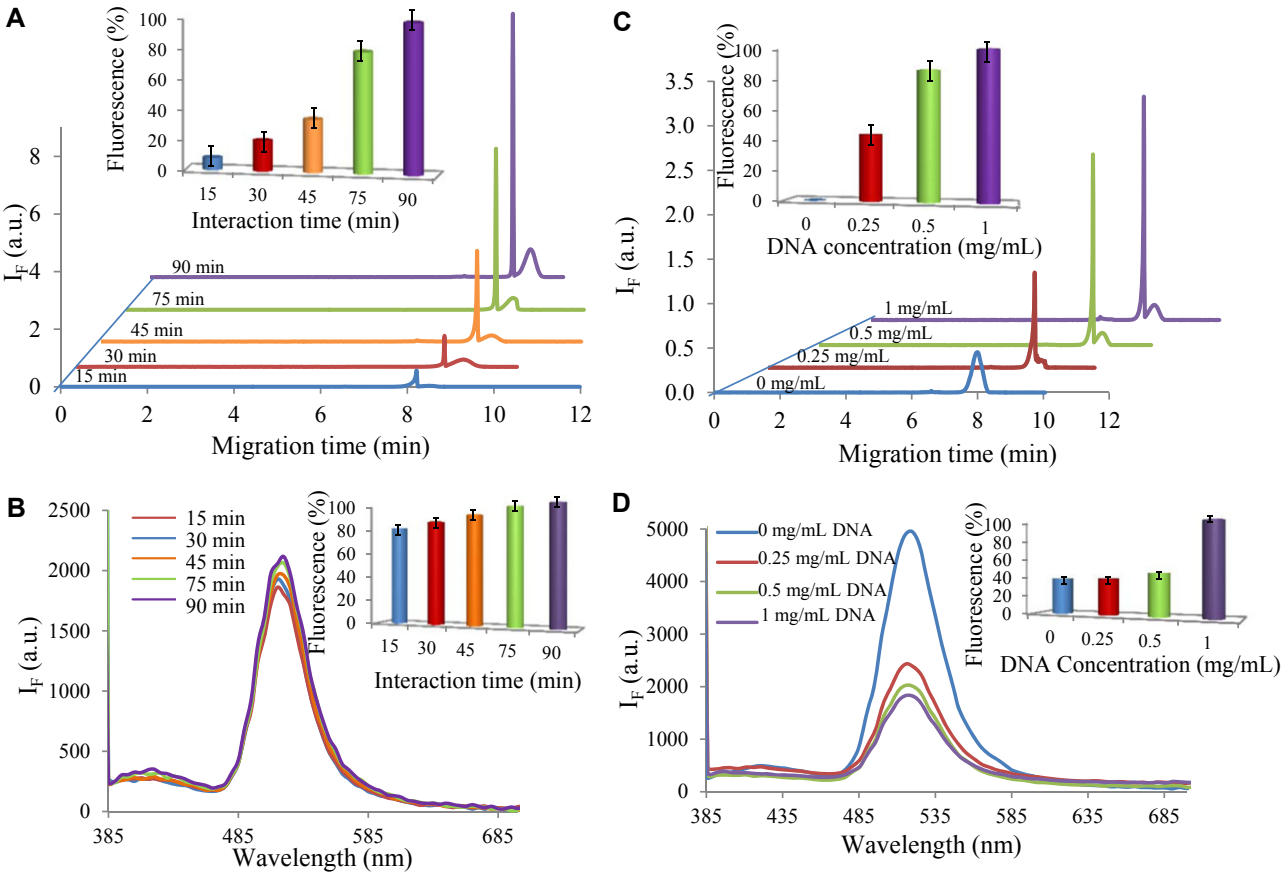

Figure 2. CE-LIF and fluorimetric characterization of QDs-DNA interaction. (A) QDs and DNA (500 μg/mL) time interaction (15, 30, 45, 75, and 90 min) monitored by CE-LIF, inset: the peak height dependence on time of interaction (peak 1 – QD-DNA complex, peak 2 – QDs). (B) QDs and DNA time interaction (15, 30, 45, 75, and 90 min) monitored by fluorescence spectrometry, inset: fluorescence intensity dependence on the interaction time. (C) QDs and DNA interaction with different concentrations of DNA (0, 0.25, 0.5, and 1 mg/mL) measured by CE-LIF, inset: dependence of created complex peak height on DNA concentration (peak 1 – QD-DNA complex, peak 2 – QDs). (D) QDs and DNA interaction with different concentrations of DNA (0, 0.25, 0.5, and 1 mg/mL) measured by fluorescence spectrometry, inset: fluorescence intensity dependence on the DNA concentration. CE and measurement with fluorimetric conditions are the same as in Fig. 1.

of interaction (Fig. 2B). The dependence of fluorescence intensities at 520 nm on the interaction time is shown in the inset in Fig. 2B. These results suggest that CE-LIF exhibits higher sensitivity for investigation of complex formation.

Subsequently, the dependence on DNA concentration was investigated. As it is shown in Fig. 2C, the increase in DNA concentration (from 0.25 to 1 mg/mL) led to the increase in peak height of the DNA-QD complex. Concentration dependence is shown in the inset in Fig. 2C. Using the fluorescence spectroscopy to verify the interaction, significant quenching effect of DNA on the QDs fluorescence was observed, however only a very small change of fluorescence was observed according to DNA concentration (Fig. 2D). In addition, the dependence of fluorescence intensities at 520 nm on the DNA concentration is shown in the inset in Fig. 2D.

The basic mechanism of interaction suggested in this study is based on the QDs incorporation into the major groove of DNA. The double-helical DNA structure creates major and minor grooves with dimensions of 2.1 nm and 0.6 nm, respectively. Due to the matching size of QD (2 nm) to the size of major groove (2.1 nm) it can be suggested that the QD is incorporated into the major groove of DNA. This conclusion corresponds to previous work done by [31]. The scheme is shown in the inset in Fig. 3. To confirm this hypothesis, the interaction between QDs and ssDNA or dsDNA was monitored (Fig. 3). Results showed that dsDNA is needed for the complex (peak 1) to be created, while the complex is not observed with ssDNA.

Further, the interaction of QDs with 500 bp-long DNA fragment and as well as the influence of the DNA length was investigated. The 500 bp-long fragment induced formation of the QD-DNA complex in the same way as long DNA (Fig. 4). The complex formation (peak 1) with the increasing tendency depending on the interaction time was observed. The dependence of the peak height on the interaction time is shown in the inset in Fig. 4A. However, compared to the genomic DNA, the interaction of the fragment with QDs monitored by

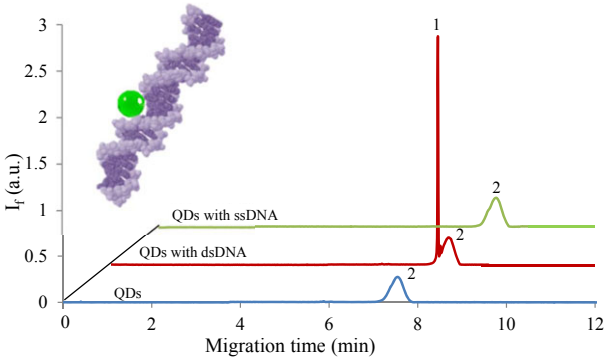

Figure 3. CE-LIF study of interaction between QDs (blue trace) and dsDNA (red trace, 500 μg/mL) or ssDNA (green trace, 500 μg/mL), (peak 1- QD-DNA complex, peak 2 – QDs), inset: the suggested scheme of the interaction between QD and major groove of dsDNA. Conditions of CE measurement are the same as in Fig. 1D.

fluorescence spectrometry did not exhibit the same increasing trend as observed by CE-LIF. Based on the comparison of the genomic DNA interaction to the DNA fragment interaction it can be assumed that the length of the DNA plays a key role especially due to the probability of the formation of numerous secondary structures. This has to be investigated in more details to reveal the impact of the DNA length on the interaction.

3.3 Gel electrophoresis

Gel electrophoresis was employed for DNA-QDs interaction verification. The gel after ethidium bromide staining is shown in Fig. 5A. The lines 1 and 13 were injected by the DNA ladder. The lines 2, 5, and 8 were injected with the QDs solution at concentration of 23, 46, and 460 μg/mL mixed 1:1 with

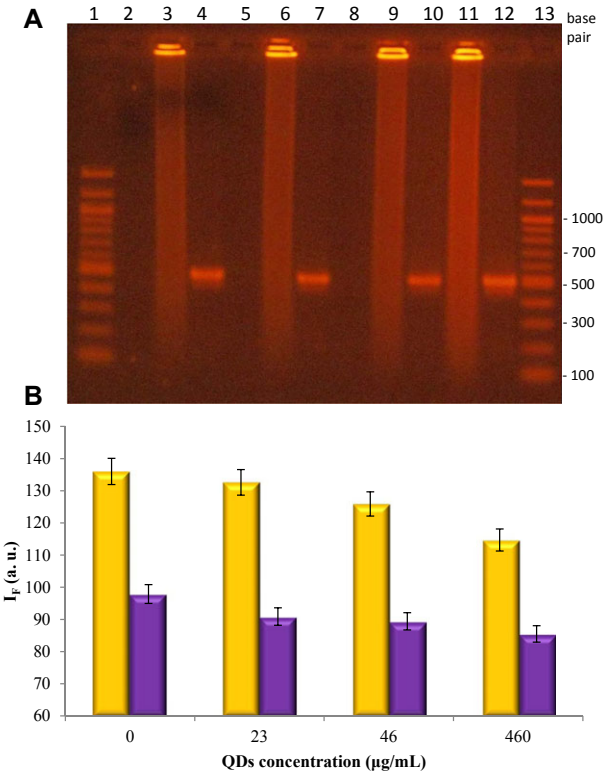

Figure 5. (A) Gel electrophoresis of the QD-DNA complex. (1) DNA Ladder, (2) QDs (230 μg/mL), (3) QDs 460 μg/mL + chicken DNA (400 μg/mL) (1:1 v/v), (4) QDs (460 μg/mL) + 500 bp (50 μg/mL) (1:1 v/v); (5) QDs (23 μg/mL), (6) QDs 46 μg/mL + DNA (400 μg/mL) (1:1 v/v), (7) QDs diluted 46 μg/mL + 500 bp (50 μg/mL) (1:1 v/v), (8) QDs 11.5 μg/mL, (9) QDs 23 μg/mL + DNA (400 μg/mL) (1:1 v/v), (10) QDs 23 μg/mL + 500 bp (50 μg/mL) (1:1 v/v), (11) DNA (200 μg/mL), (12) 500 bp (25 μg/mL), (13) DNA ladder. For measurements 2% agarose gel in TAE buffer was used and run for 160 min at 60 V. Total amount of the samples was 10 μL. (B) Quenching of the signal dependent on the amount of QDs (chicken DNA–yellow columns, 500 bp DNA fragment–purple columns).

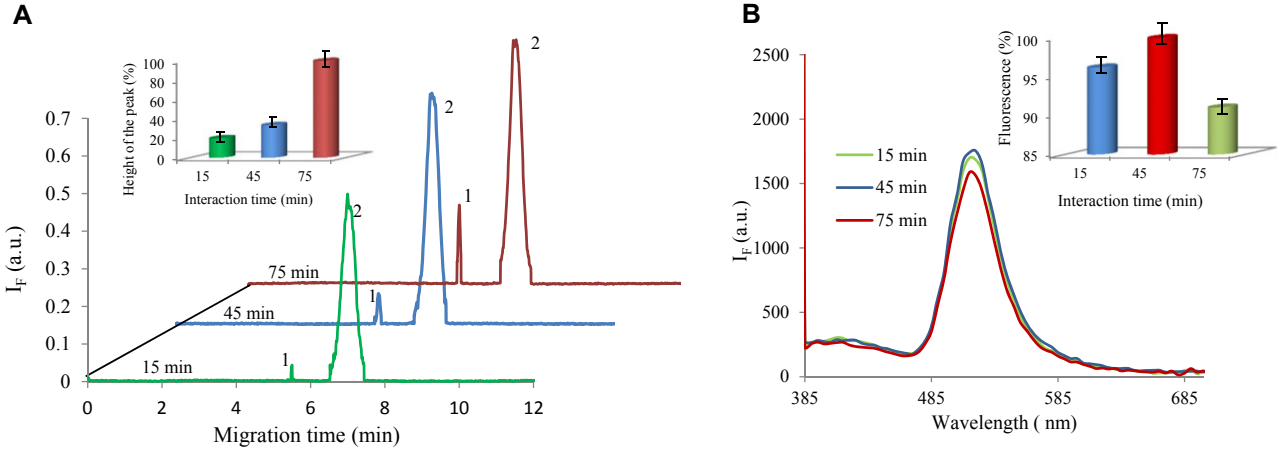

Figure 4. (A) CE-LIF and (B) fluorimetric characterization of the interaction between QDs (peak 2) and 500 bp long DNA fragment of bacteriophage λ (500 μg/mL). CE-LIF and fluorimetric measurement conditions are set as in the Fig. 1, inset: peak height dependence of QDs-DNA fragment complex on the reaction time.

water. In the lines 3, 6, and 9 there are the mixture samples of chicken DNA and 23, 46, and 460 μg/mL of QDs in ratio 1:1, respectively. The same samples prepared using 500 bp DNA fragment and QDs are shown in the lines 4, 7, and 10. In lines 11 and 12, DNA and 500 bp fragment signal is observed. After software analysis of the gel image, the quenching of the signal dependent on the amount of QDs was observed for both chicken DNA as well as 500 bp fragment (Fig. 5B). This is probably due to the fact that QDs are preventing the DNA to be stained by the ethidium bromide.

4 Concluding remarks

It clearly follows from the results obtained that the interaction between DNA and QDs occurs. Monitoring and verification was successfully done by combination of CE-LIF and gel electrophoresis, whereas CE is analytical method with excellent separation characteristics and in the combination with LIF detector it provides very high selectivity needed for monitoring of DNA-QDs interaction. The obtained data confirm the hypothesis that the interaction mechanism is based on the size of QDs, which matches the size of DNA major groove.

The author M.V. wishes to express her thanks to project CZ.1.07/2.3.00/30.0039 for financial support. The author J.C. thanks to project GP 13-20303P.

The authors have declared no conflict of interest.

5 References

[1] Adams, F. C., Barbante, C., *Spectroc. Acta Pt. B-Atom. Spectr.* 2013, *86*, 3–13.

[2] Mattoussi, H., Palui, G., Na, H. B., *Adv. Drug Deliv. Rev.* 2012, *64*, 138–166.

[3] Lacroix, L. M., Delpech, F., Nayral, C., Lachaize, S., Chaudret, B., *Interface Focus* 2013, *3*, 1–19.

[4] Acharya, A., *J. Nanosci. Nanotechnol.* 2013, *13*, 3753–3768.

[5] Wang, Y. C., Hu, R., Lin, G. M., Roy, I., Yong, K. T., *ACS Appl. Mater. Interfaces* 2013, *5*, 2786–2799.

[6] Byers, R. J., Hitchman, E. R., *Prog. Histochem. Cytochem.* 2011, *45*, 201–237.

[7] Wu, H. F., Gopal, J., Abdelhamid, H. N., Hasan, N., *Proteomics* 2012, *12*, 2949–2961.

[8] Fowler, B. A., Conner, E. A., Yamauchi, H., *Toxicol. Appl. Pharmacol.* 2008, *233*, 110–115.

[9] Marko, N. F., Weil, R. J., Toms, S. A., *Expert Rev. Proteomics* 2007, *4*, 617–626.

[10] Soman, C., Giorgio, T., *Nanomed.-Nanotechnol. Biol. Med.* 2009, *5*, 402–409.

[11] Henry, M., Debarbieux, L., *Virology* 2012, *434*, 151–161.

[12] Watson, J. D., Crick, F. H. C., *Cold Spring Harbor Symp. Quant. Biol.* 1953, *18*, 123–131.

[13] Pang, D. W., Zhao, Y. D., Fang, P. F., Cheng, J. K., Chen, Y. Y., Qi, Y. P., Abruna, W. D., *J. Electroanal. Chem.* 2004, *567*, 339–349.

[14] Mahtab, R., Sealey, S. M., Hunyadi, S. E., Kinard, B., Ray, T., Murphy, C. J., *J. Inorg. Biochem.* 2007, *101*, 559–564.

[15] Sun, D. Z., Gang, O., *Langmuir* 2013, *29*, 7038–7046.

[16] Zhang, C. L., Ji, X. H., Zhang, Y., Zhou, G. H., Ke, X. L., Wang, H. Z., Tinnefeld, P., He, Z. K., *Anal. Chem.* 2013, *85*, 5843–5849.

[17] Pereira, M., Lai, E. P. C., Hollebone, B., *Electrophoresis* 2007, *28*, 2874–2881.

[18] Clarot, I., Wolpert, C., Morosini, V., Schneider, R., Balan, L., Diez, L., Leroy, P., *Curr. Nanosci.* 2009, *5*, 154–159.

[19] Li, Y. Q., Wang, H. Q., Wang, J. H., Guan, L. Y., Liu, B. F., Zhao, Y. D., Chen, H., *Anal. Chim. Acta* 2009, *647*, 219–225.

[20] Song, X. T., Li, L., Chan, H. F., Fang, N. H., Ren, J. C., *Electrophoresis* 2006, *27*, 1341–1346.

[21] Stewart, D. T. R., Celiz, M. D., Vicente, G., Colon, L. A., Aga, D. S., *Trac-Trends Anal. Chem.* 2011, *30*, 113–122.

[22] Wang, J. H., Li, Y. Q., Zhang, H. L., Wang, H. Q., Lin, S., Chen, J., Zhao, Y. D., Luo, Q. M., *Colloid Surf. A-Physicochem. Eng. Asp.* 2010, *364*, 82–86.

[23] Akinfieva, O., Nabiev, I., Sukhanova, A., *Crit. Rev. Oncol./Hematol.* 2013, *86*, 1–14.

[24] Wang, F. B., Rong, Y., Fang, M., Yuan, J. P., Peng, C. W., Liu, S. P., Li, Y., *Biomaterials* 2013, *34*, 3816–3827.

[25] Stanisavljevic, M., Janu, L., Smerkova, K., Krizkova, S., Pizurova, N., Ryvolova, M., Adam, V., Hubalek, J., Kizek, R., *Chromatographia* 2013, *76*, 335–343.

[26] Frigerio, C., Ribeiro, D. S. M., Rodrigues, S. S. M., Abreu, V. L. R. G., Barbosa, J. A. C., Prior, J. A. V., Marques, K. L., Santos, J. L. M., *Analytica Chimica Acta* 2012, *735*, 9–22.

[27] Sang, F. M., Huang, X. Y., Ren, J. C., *Electrophoresis* 2014, *35*, 793–803.

[28] Kuang, H., Zhao, Y., Ma, W., Xu, L. G., Wang, L. B., Xu, C. L., *Trac-Trends Anal. Chem.* 2011, *30*, 1620–1636.

[29] Duan, J. L., Song, L. X., Zhan, J. H., *Nano Res.* 2009, *2*, 61–68.

[30] Sobrova, P., Ryvolova, M., Hubalek, J., Adam, V., Kizek, R., *Int. J. Mol. Sci.* 2013, *14*, 13497–13510.

[31] Xu, Q., Wang, J. H., Wang, Z., Yin, Z. H., Yang, Q., Zhao, Y. D., *Electrochem. Commun.* 2008, *10*, 1337–1339.

5.2 Streptavidin – biotin mediated interaction with biomolecules

The streptavidin–biotin interaction is considered as the strongest non covalent interaction with dissociation constant Kd = 4×10^{-14} M (Green 1990). Streptavidin-biotin complex is formed very fast and it is resistant to the extreme pH values, temperature and even to denaturing agent and it is employed in many detection methods. Due to strong and reliable affinity streptavidin-biotin interaction is often used in researches as well as in diagnostics application. In most of the assays when interaction is applied, streptavidin is coupled to solid phase, such as QDs, magnetic particles, microtiter plate and others while biotin is coupled to the molecule of the intrest (Holmberg, Blomstergren et al. 2005). In following work streptavidin-biotin interaction was successfully used for coupling biomolecules with QDs as well as with the magnetic nanoparticles which can be used for biomedical purposes after appropriate surface modification similarly like QDs.

5.2.1 Research article I

STANISAVLJEVIC, M.; JANU, L.; SMERKOVA, K.; KRIZKOVA, S.; PIZUROVA, N.; RYVOLOVA, M.; ADAM ,V.; HUBALEK, J.; KIZEK R. Study of streptavidin – modified quantum dots by capillary electrophoresis. Chromatographia, 2013. 76(7-8): p. 335-343. ISSN: 0009-5893
DOI: 10.1007/s10337-012-2372-8

Participation in the work of the author Stanisavljevic M.: experimental part 40% and manuscript preparation 20%.

As aforementioned streptavidin–biotin is one of the most commonly used biocojnugation methods and usually are applied in protein and/or nucleic acid detections. Possibility of QDs surface modification joined with unique streptavidin – biotin affinity might be good opportunity for improving detection methods.
In the article CdTe QDs capped with MPA were synthesized by microwave irradiation and modified with streptavidin for biotinylated oligonucleotides (ODN) labeling and

following their interaction in purposes of detection. Interaction was observed by capillary and gel electrophoresis.

Employing MPA as CdTe QDs capping agent provides presence of carboxylic groups on their surface enabling electrostatic interaction with streptavidin molecule by mixing. Characterization of the synthesized QDs was done by transmission electron microscopy for revealing less than 10 nm particles size and homogenous composition, while fluorescence spectroscopy revealed green emission of the QDs with emission maximum at 550 nm and absorbance maximum at 495 nm. Gel electrophoresis was used for confirmation of the streptavidin presence on the QDs surface as well as with CE-LIF.

Streptavidin modified QDs, further was used for labeling biotinylated ODN and monitored with capillary electrophoresis with UV and LIF detection. QDs were left to interact with two in length different ODN, biotinylated ODN cancer sequence of BCL-2 and sequence of virus hepatitis B. In both cases created complex was seen as sharp peak growing with the interaction time. CE-UV analysis of single components such as streptavidin and ODNs were used for final determination of the peak of the complex, as well as calculation of electrophoretic mobility of components.

MPA capped CdTe QDs successfully functionalized with streptavidin enable wide application of them as labeling material due to numerous molecules that can be easily biotinylated and overall it has potential to be included in sensor design for fast analysis based on hybridization processes in these particular cases.

Chromatographia (2013) 76:335–343
DOI 10.1007/s10337-012-2372-8

ORIGINAL

Study of Streptavidin-Modified Quantum Dots by Capillary Electrophoresis

Maja Stanisavljevic · Libor Janu · Kristyna Smerkova · Sona Krizkova · Nadezda Pizurova · Marketa Ryvolova · Vojtech Adam · Jaromir Hubalek · Rene Kizek

Received: 28 June 2012 / Revised: 31 October 2012 / Accepted: 30 November 2012 / Published online: 25 December 2012

Abstract Great boom of nanotechnologies impacts almost all areas of science and therefore detail understanding of the properties of nanomaterials as well as their interaction abilities is required. Surface modification and functionalization of nanoparticles is of a great interest due to the wide range of applications in the area of nanomedicine, nanobiology, and/or biochemistry. In this study, CdTe QDs were synthesized using microwave reactor and their surface was modified by streptavidin to ensure further suitability for bioconjugation with biotin-labelled oligonucleotides. For characterization of the synthesized QDs and for monitoring of the interaction with the oligonucleotide, capillary and gel electrophoresis was used. Moreover, complementary advantages of absorption (CE–UV) and laser-induced fluorescence detection (CE–LIF) were exploited. Comparison the electrophoretic mobilities obtained for streptavidin-modified QDs by CE–LIF (-9.87×10^{-9} m^2/V/s) and by CE–UV (-10.02×10^{-9} m^2/V/s) was in a good agreement enabling us to identify the peak of streptavidin-modified QDs in the CE–UV electropherogram containing also the peak of unreacted streptavidin. Subsequent conjugation of streptavidin-modified QDs with two model biotinylated oligonucleotides (BCL-2 and HBV) led to formation of the complex represented in the electropherograms as a very sharp peak. This peak height increased with time for 15.5 and 27 mAU using BCL-2 oligonucleotide and HBV oligonucleotide, respectively during 30 min interaction.

Keywords Capillary electrophoresis · Gel electrophoresis · Avidin–biotin technology · Oligonucleotide · Nanoparticle, quantum dots

Published in the special paper collection *Advances in Chromatography and Electrophoresis & Chiranal 2012* with guest editor Jan Petr.

M. Stanisavljevic · L. Janu · K. Smerkova · S. Krizkova · M. Ryvolova · V. Adam · J. Hubalek · R. Kizek (✉)
Department of Chemistry and Biochemistry, Faculty of Agronomy, Mendel University in Brno, Zemedelska 1, 613 00 Brno, Czech Republic
e-mail: kizek@sci.muni.cz

S. Krizkova · M. Ryvolova · V. Adam · J. Hubalek · R. Kizek
Central European Institute of Technology, Brno University of Technology, Technicka 3058/10, 616 00 Brno, Czech Republic

N. Pizurova
Institute of Physics of Materials, Academy of Sciences of the Czech Republic, Zizkova 22, 616 62 Brno, Czech Republic

Introduction

Streptavidin–biotin is one of the most commonly used bioconjugation approach due to the high affinity between biotin and streptavidin [1–3]. Therefore, it is not surprising that this technology is being also utilized in nanotechnology as one of the rapidly growing field of scientific interest [4, 5]. Nanotechnology is a multidisciplinary scientific field, which involves creation and utilization of nanoscale materials [6–10]. Quantum dots (QDs) are nanomaterials made of semiconductors, which have size-depending electronic and optical properties, which are between atoms and bulk materials [11, 12]. Due to convincing optical properties, QDs are new fluorescent materials, which are used instead of organic dyes for biological labelling. They have better photostability than organic dyes, narrow emission and continuous absorption spectra [13]. QDs applications are widespread such as for early detection of cancer, for drug delivery, in vivo imaging and targeting [9, 10, 14–18].

Due to the toxicity of their inorganic core, the surface of QDs has to be chemically modified. Thiol-group containing compounds such a mercaptopropionic acid [19], glutathione [20] and/or cysteine [21] are commonly used as capping agents. After modification, QDs are suitable for conjugation with biomolecules such as proteins, fragments of DNA and/or RNA, however, some covalent and non-covalent attachment methodologies must be applied. Common covalent conjugation is based on streptavidin–biotin linkage and non-covalent linkage is achieved through simple electrostatic linkage [22]. Such conjugated QDs with biomolecules have been successfully applied in biological and medical fields like immunoassay [23], DNA hybridization [24] and/or cell imaging [25].

To characterize nanoparticles, transmission electron microscopy (which is time consuming and very expensive) [26], size exclusion chromatography (very high surface activity may cause problem during measurement) [27], and dynamic light scattering (which is an expensive technique) [28] are usually used. Due to disadvantages, it is necessary to find a fast, effective and easy-to-use method for QDs size measurement and their separation according to size because of their rapidly increasing applications [29]. Capillary electrophoresis (CE) is a powerful separation technique for characterizing nanoparticles in size, shape or charge due to its simplicity, short analysis time, small sample and reagent requirements, high separation efficiency, and extremely high sensitivity. It has already been used to separate a numerous nanomaterials such as inorganic oxide [30], SiO_2 [31], gold and silver nanoparticles [32, 33] and carbon nanotubes [34]. In this study, capillary electrophoresis and gel electrophoresis are used as effective methods for quality control, functionality verification and interaction monitoring of streptavidin-modified CdTe QDs synthesized by rapid and efficient method using microwave reactor.

Experimental

Chemicals

All chemicals were purchased from Sigma Aldrich (St. Louis, MA, USA) in ACS purity. Solutions were made using MiliQ water (Milipore, Prague, Czech Republic). Oligonucleotide sequences were as follows: cancer sequence BCL-2: BIOTIN -5′-TCT CCC GGC TTG CGC CAT-3′ [35], viral VHB: BIOTIN-5′ CAT CCT GCT GCT ATG CCT CAT CT 3′ [36].

QDs Synthesis

CdTe QDs were prepared by microwave synthesis (Anton Paar, Wien, Austria) and capped by mercaptopropionic acid (MPA) according to the following procedure: the solution of $CdCl_2$ (4 mL, 0.04 M) was mixed with Na_2TeO_3 (4 mL, 0.01 M), 100 mg of sodium citrate and 50 mg $NaBH_4$, 119 mg MPA and 42 mL of H_2O. The mixture was heated by microwave radiation for 10 min (300 W). The product was precipitated by isopropanol to remove the excessive reagents according to the following: 1 mL of CdTe QDs solution was mixed with 1 mL of isopropanol and centrifuged. The supernatant was removed and precipitated CdTe QDs were dissolved in 1 mL of ACS water [37].

TEM Characterization

Morphology studies were carried out with the transmission electron microscope (TEM) Philips CM 12 (tungsten cathode, using a 120 kV electron beam). Samples for TEM measurements were prepared by placing drops of the solution (sample and water) on coated Cu grids (holey carbon and holey SiO_2/SiO) and subsequently drying in air.

Streptavidin Modification

100 μL of MPA capped CdTe QDs (MPA-QDs) were diluted to 1 mL and the pH was adjusted to 7 by MPA solution. Streptavidin (9.6 μL, 5 mg/mL) was added and the solution was intensively agitated for 60 min. Subsequently, the solution was centrifuged for 80 min. The supernatant was disposed and the precipitated CdTe QDs-MPA-strep were dissolved in 100 μL of water [38].

Spectroscopic Analysis

Fluorescence and absorbance spectra were acquired by multifunctional microplate reader Tecan Infinite 200 PRO (TECAN, Männedorf, Switzerland). 350 nm was used as an excitation wavelength and the fluorescence scan was measured within the range from 400 to 850 nm per 5 nm steps. Each intensity value is an average of 5 measurements. The detector gain was set to 100. The absorbance was acquired within the range from 230 to 1,000 nm with 5 nm steps as an average of 5 measurements per well. The sample (50 μL) was placed in transparent 96-well microplate with flat bottom by Nunc (ThermoScientific, Waltham, MA, USA).

Electrophoretic Analysis

DNA Electrophoresis

Non-denaturing electrophoresis of DNA was performed in 15 % polyacrylamide gels in TAE buffer (40 mM Tris, 20 mM acetic acid, 1 mM EDTA, pH = 8.0, Bio-Rad, USA) in a Mini Protean Tetra apparatus (Bio-Rad, Hercules, CA, USA) at 120 V for 45 min. After the

electrophoresis was completed, the gels were photographed in In vivo imaging system Xtreme (Carestream Health, Rochester, NY, USA) at excitation wavelength of 510 nm and emission wavelength of 600 nm to visualize the QDs. In order to visualize the ssDNA and dsDNA, the gels were stained with GelRed™ Nucleic Acid Gel Stain (Biotium, Hayward, CA, USA) in dilution 1:5000 in water for 30 min and consequently photographed on a transluminator at 324 nm. To visualize the proteins, the gels were stained with Coomassie blue according to Wong et al. [39].

Sodium Dodecyl Sulphate Polyacrylamide Gel Electrophoresis (SDS-PAGE)

The electrophoresis was performed using a Mini Protean Tetra apparatus with gel dimension of 8.3 × 7.3 cm (Bio-Rad, USA). First 10 % (m/V) running, and then 5 % (m/V) stacking gels were poured. The gels were prepared from 30 % (m/V) acrylamide stock solution with 1 % (m/V) bisacrylamide. The polymerization of the running or stacking gels was carried out at room temperature for 45 min or 30 min, respectively. Prior to analysis the samples were mixed either with reducing (5 % β-mercaptoethanol) or non-reducing sample buffer (50 mM Tris/HCl, 2 % SDS, 20 % glycerol, 0.1 % bromophenol blue, pH = 8.8) in a 1:1 ratio. The samples were incubated at 93 °C for 3 min, and the sample was loaded onto a gel. For determination of the molecular mass, the protein ladder "Precision plus protein standards" from Biorad was used. The electrophoresis was run at 150 V for 1 h at laboratory temperature (23 °C) (Power Basic, Biorad, Hercules, CA, USA) in tris–glycine buffer (0.025 M Trizma-base, 0.19 M glycine and 3.5 mM SDS, pH = 8.3). After the electrophoresis was completed, the gels were photographed in In vivo imaging system Xtreme (Carestream Health, Rochester, NY USA) at excitation wavelength of 470 nm and emission of 535 nm to visualize the QDs. Then, the gels were stained with silver according to Krizkova et al. [40] to visualize proteins.

Capillary Electrophoresis

Capillary electrophoresis with UV absorbance detection (CE–UV) measurement was performed using capillary electrophoresis system (Beckman P/ACE 5500, Brea, CA, USA) at 214 nm and with laser-induced fluorescence detection (CE–LIF) at $\lambda_{ex} = 488$ and $\lambda_{em} = 520$ nm. An uncoated fused silica capillary with total capillary length of 47 cm, effective length of 40 cm and internal diameter of 75 μm was used. 0.02 M sodium borate (pH 9.2) was used as background electrolyte. Separation was carried out at 20 kV and the sample was injected hydrodynamically for 20 s using 3.4 kPa. Coumarin 334 and coumarin were used as electroosmotic flow (EOF) markers for CE–LIF and CE–UV, respectively.

Results and Discussion

Synthesis of CdTe QDs

MPA-capped CdTe QDs were synthesized by rapid microwave synthesis enabling formation of required QDs within 10 min. QDs as modern fluorescent labels require being surface modified to provide both biocompatibility as well as functionality. One of the most important biochemical interactions, biotin–avidin (streptavidin) interaction, plays a key role in QDs functionalization process. Both biotin-modified and streptavidin-modified QDs were utilized for these purposes [41]. In this study, the bioconjugation of CdTe QDs capped with MPA via electrostatic interaction with streptavidin was done. The scheme of formation of bioconjugate QD-streptavidin and biotin-modified oligonucleotide is shown in Fig. 1. Primarily, the metal CdTe nanocrystal is formed and capped by MPA to form a stable and optically active colloidal solution. After isopropanol precipitation the surface was modified by streptavidin to provide required functionality.

Prepared MPA capped CdTe QDs were characterized by TEM and by fluorescent spectroscopy. The characterization of both properties is needed due to their further applications as fluorescent nanoparticles. TEM analysis can reveal dimensions of the particles as well as to confirm the elemental composition. TEM micrograph of CdTe QDs is shown in Fig. 2a. The TEM examination of the QDs sample indicates the morphology and phase composition were clearly homogeneous. The TEM pictures (at higher magnifications) show that dried droplets consisted of a fine grain powder of a typical size of particles below 10 nm.

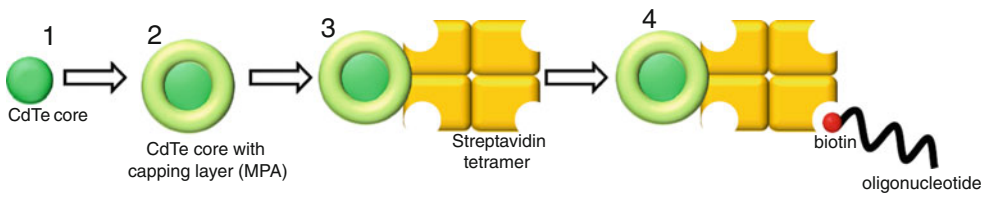

Fig. 1 Scheme of the formation of the streptavidin-modified CdTe QDs. *1* metallic core of the CdTe QD; *2* capping with mercaptopropionic acid (MPA); *3* coupling with streptavidin; *4* interaction of streptavidin-modified QDs with biotinylated oligonucleotide

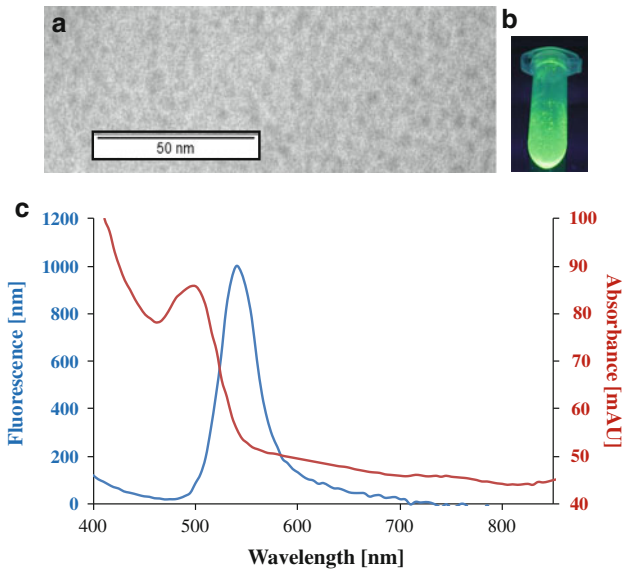

Fig. 2 Characterization CdTe QDs. **a** TEM micrograph of the MPA capped CdTe QDs. **b** *Photograph* of the streptavidin-modified CdTe QDs under UV light illumination (260 nm). **c** Absorption and emission spectrum (λ_{ex} = 350 nm)

After that we found that we synthesized nanoparticles of assumed composition, we aimed our attention at their fluorescent properties. The solution of CdTe QDs under UV light illumination (260 nm) is shown in Fig. 2b and the fluorescence and absorbance spectra of the prepared QDs are shown in Fig. 2c. It clearly follows from these results that the emission maximum of the streptavidin-modified CdTe QDs (QDs-MPA-strep) is at 550 nm and therefore strong green emission is observed. In the absorption spectrum, except strong absorption in UV region, maximum at 495 nm was observed.

Electrophoretic Characterization of CdTe QDs

Streptavidin is a 60 kDa protein purified from the bacterium *Streptomyces avidinii* composed of four identical streptavidin monomer units with extraordinarily high affinity for biotin [42]. The analysis of streptavidin by SDS-PAGE confirmed that QDs-MPA-strep contained streptavidin in form of monomer, dimer and tetramer (Fig. 3a). To compare electrophoretic behavior, the streptavidin standard and QDs-MPA-strep conjugate were observed both under reducing (lanes 2 and 4) and non-reducing conditions (lane 3 and 5). Under non-reducing conditions main band corresponding to streptavidin tetramer (60 kDa) was observed both in streptavidin standard and QDs-MPA-strep. Except these two, bands corresponding monomeric (15 kDa) and dimeric form (25 kDa) were observed. Although same protein amount was loaded, the band at QDs-MPA-strep appears less intensive and higher portion of streptavidin monomer is present. Under reducing conditions at streptavidin standard two bands corresponding to monomeric and dimeric form were observed, but at QDs-MPA-strep only one band corresponding to monomer was present. The increase of monomeric form of streptavidin at QDs-MPA-strep conjugate observed both under reducing and non-reducing conditions might cause decomposition of tetrameric form of streptavidin as a consequence of QDs binding.

Gel electrophoresis is however unable to distinguish between streptavidin and QDs-MPA-strep probably due to the low separation power and expected small difference in

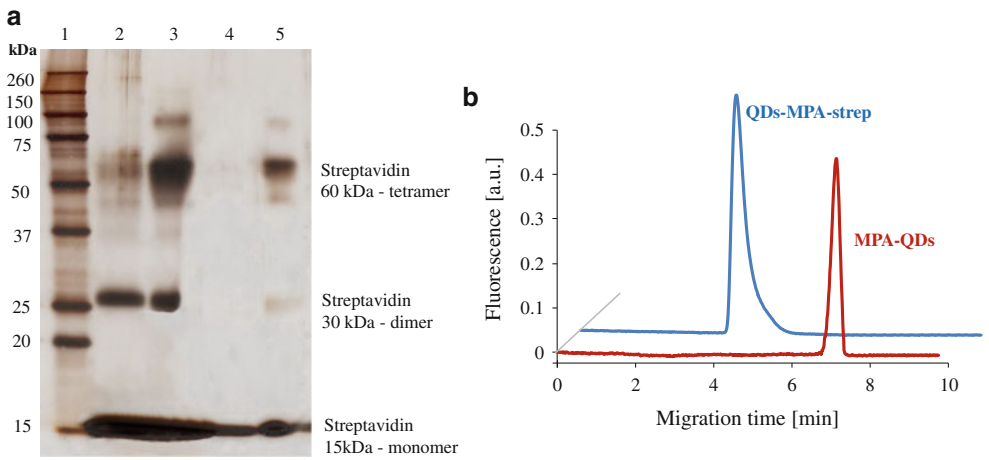

Fig. 3 Electrophoretic characterization of the QDs solution. **a** SDS-PAGE of streptavidin and QDs-MPA-strep under reducing and non-reducing conditions, (acrylamide gel: 10 % (m/V) separation gel, 5 % (m/V) stacking gel, separation voltage: 150 V for 1 h at 23 °C, electrolyte: 0.025 M Trizma-base, 0.19 M glycine and 3.5 mM SDS, pH = 8.3). Silver staining according to Krizkova et al. [40], 1 Molecular weight standard, 2 Streptavidin Reducing, 3 Streptavidin Non-reducing, 4 QDs-MPA-strep Reducing, 5 QDs-MPA-strep Non-reducing; **b** CE–LIF analysis of QDs-MPA-strep and MPA-QDs (electrolyte: 0.02 M sodium borate, voltage: 20 kV, capillary: 47/40 cm, 75 μm ID, injection : 20 s, 3.4 kPa)

molecular mass of streptavidin itself and QDs-MPA-strep. The migration behaviour of QDs-MPA in SDS-PAGE may be different from the proteins such as the molecular weight standards and streptavidin, therefore, it might be difficult to estimate the molecular mass of QDs-MPA by the SDS-PAGE. Moreover, CE–LIF was used to prove the bioconjugation of CdTe QDs. As shown above, the absorption maximum at 495 nm enabled the Ar^+ laser with emission wavelength of 488 nm to be used as an excitation light source. Electropherograms showed in Fig. 3b indicates that the migration time of MPA-QDs is 7.1 min; however, the peak of QDs-MPA-strep has the migration time of 4.2 min. The electrophoretic mobilities calculated for MPA-QDs and QDs-MPA-strep were -27.82×10^{-9} $m^2/V/s$ and -9.87×10^{-9} $m^2/V/s$, respectively (calculated according to the Eq. 1).

$$\mu = \frac{L \times l}{V} \times \left(\frac{1}{t} - \frac{1}{t_0}\right) \quad (1)$$

where μ is electrophoretic mobility, L is total capillary length, l is effective capillary length, V is applied voltage, t_0 is migration time of EOF marker and t is analyte migration time.

Due to the selectivity of laser-induced fluorescence detection, which is enabling only fluorescent molecules to be detected and significant differences of electrophoretic mobilities of MPA-QDs and QDs-MPA-strep, it can be concluded that bioconjugation was successful.

CE–LIF of CdTe QDs Oligonucleotides

Even though the LIF detection provides excellent selectivity, the UV absorbance detection was used for further CE analyses offering the versatility needed for monitoring of the interactions in the solutions. This powerful combination of detection modalities enabled detail monitoring of complex formation and identification of reaction components. After verification of successful surface modification of CdTe QDs by streptavidin, the functionality was confirmed by interaction with biotinylated oligonucleotide. The first model oligonucleotide was the fragment of BCL-2 gene. CE–UV electropherograms of individual components

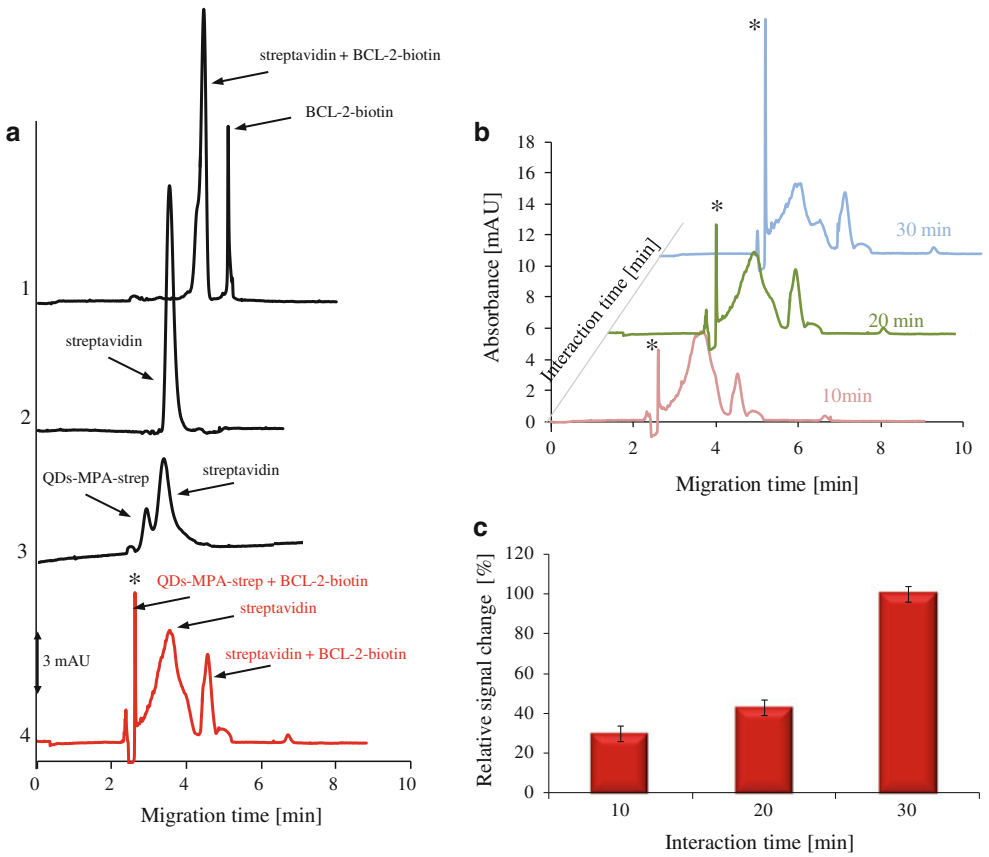

Fig. 4 Monitoring of interaction of QDs-MPA-strep with biotinylated BCL-2 oligonucleotide. **a** CE–UV identification of mixture components, 1 mixture of streptavidin with biotinylated BCL-2 oligonucleotide, 2 streptavidin, 3 QDs-MPA-strep solution, mixture of QDs-MPA-strep solution with biotinylated BCL-2 oligonucleotide, (*asterisk*) complex of QDs-MPA-strep and BCL-2-biotin (electrolyte: 0.02 M sodium borate, voltage: 20 kV, capillary: 47/40 cm, 75 µm ID, injection : 20 s, 3.4 kPa). **b** Time dependence of the formation of QDs-MPQ-strep-BCL-2-biotin complex. **c** Time dependent increase of the complex signal

of the reaction mixture are shown in Fig. 4a. It follows from the results that BCL-2 oligonucleotide gave a sharp peak with migration time of 5.19 min and electrophoretic mobility of -35.09×10^{-9} m^2/V/s. During the interaction with streptavidin, a peak of the complex with the migration time of 4.52 min and electrophoretic mobility of -30.70×10^{-9} m^2/V/s was formed. Streptavidin peak had the migration time of 3.42 min and electrophoretic mobility of -19.47×10^{-9} m^2/V/s. The electropherogram of QDs-MPA-strep gave two peaks corresponding to the streptavidin excess (electrophoretic mobility -19.47×10^{-9} m^2/V/s) and QDs-MPA-strep with electrophoretic mobility of -10.02×10^{-9} m^2/V/s. Comparing the electrophoretic mobilities obtained for QDs-MPA-strep by CE–LIF and CE–UV, we found that they are in a good agreement enabling us to identify the peak of QDs-MPA-strep in the CE–UV electropherogram. Finally, the electropherogram of the mixture of biotinylated BCL-2 oligonucleotide and QDs-MPA-strep (red line) is shown in Fig. 4a (sample of oligonucleotide was mixed with quantum dots in 1:1 ratio (*v*/*v*) and the final concentration of oligonucleotide was 5 μM). A number of signals occurred in this electropherogram with migration times corresponding to streptavidin, streptavidin-BCL-2-biotin complex and a very sharp peak (marked with a star). This peak probably belongs to the complex of QDs-MPA-strep and oligonucleotide BCL-2-biotin. As shown in Fig. 4b and c, the signal intensity of this peak increased with time of interaction between the QDs-MPA-strep and BCL-2-biotin solution.

The interaction of QDs-MPA-strep was verified also by second oligonucleotide fragment, specific for hepatitis B virus labelled with biotin (HBV-biotin). There was no aim to separate BCL-2 from HBV. The electropherogram of the mixture of QDs-MPA-strep and HBV-biotin oligonucleotide contained a peak of unreacted HBV-biotin oligonucleotide at migration time of 4.92 min, unreacted streptavidin at migration time of 3.49 min and a peak of the complex QDs-MPA-strep + HBV-biotin at migration time of 2.8 min (Fig. 5a). The signal intensity of this peak increased with time (Fig. 5b, c). During 30 min of interaction the intensity of this peak increased to 27 mAU in comparison to BCL-2-biotin oligonucleotide, where the increase in the signal was 15.5 mAU only.

Gel Electrophoresis of CdTe QDs Oligonucleotides

After that we characterized the complex by CE, agarose gel electrophoretic was used to detect DNA (Fig. 6a). In the lane 2, MPA-QDs were injected exhibiting no signal, but in the lane 3 streptavidin-modified CdTe QDs coupled to biotinylated HBV oligonucleotide were injected showing a weak signal (marked by arrow) confirming the presence of oligonucleotide. In the lane 4, QDs-MPA-strep were injected and as expected no DNA-specific signal was observed. Lane 5 was filled by streptavidin and there was a

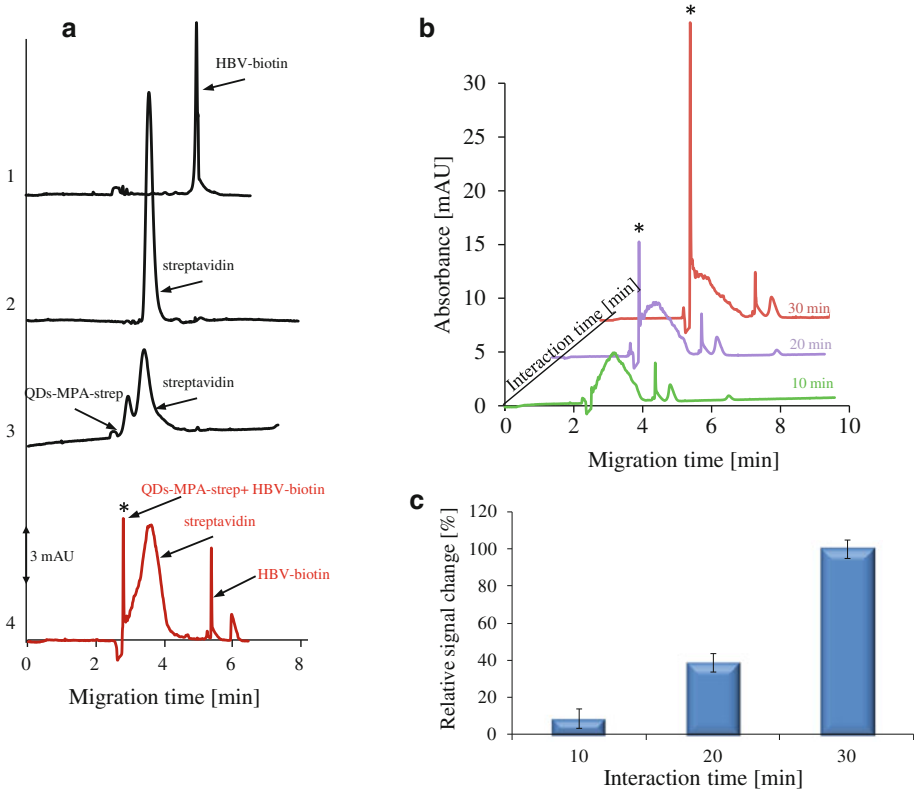

Fig. 5 Monitoring of the interaction of QDs-MPA-strep with biotinylated HBV oligonucleotide. **a** CE–UV identification of mixture components *1* biotinylated HBV oligonucleotide, *2* streptavidin, *3* QDs-MPA-strep solution, mixture of QDs-MPA-strep solution with biotinylated HBV oligonucleotide, (*asterisk*)complex of QDs-MPA-strep and HBV-biotin (for other experimental conditions see caption for Fig. 4). **b** Time dependence of the formation of QDs-MPQ-strep-HBV-biotin complex. **c** Time dependent increase of the complex signal

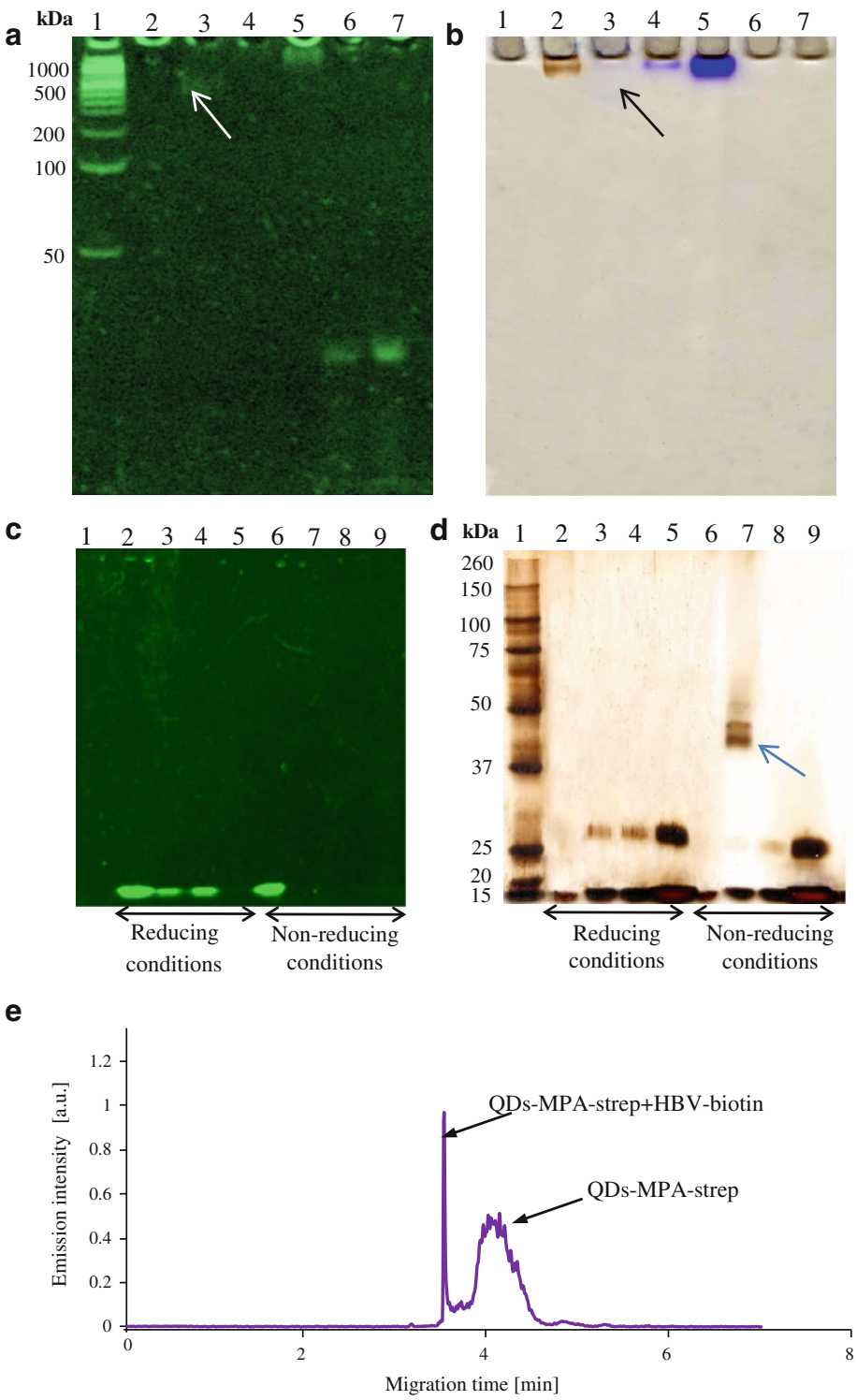

Fig. 6 **a** Agarose gel electrophoresis labelled by DNA-specific staining (GelRed^{TM}) visualized by fluorescence under 510 nm illumination and emission at 600 nm, *1* Ladder, *2* MPA-QDs, *3* QD-MPA-strep-VHB-biotin, *4* QDs-MPA-strep, *5* Streptavidin, *6* BCL-2-biotin, *7* VHB-biotin. **b** Agarose gel electrophoresis labelled by protein-specific staining—*Coomassie blue*, lane captions same as in (**b**). **c** SDS-PAGE non-labelled, visualized by fluorescence under 470 nm illumination and emission at 535 nm, *1* Ladder, 2 MPA-QDs, 3 QD-MPA-strep-VHB-biotin, 4 QDs-MPA-strep, 5 Streptavidin, 6 MPA-QDs, 7 QD-MPA-strep-VHB-biotin, 8 QDs-MPA-strep, 9 Streptavidin (*2–5* reducing conditions, *6–9* non-reducing conditions). **d** SDS-PAGE labelled by silver, lane captions same as in (**c**). **e** CE–LIF identification of complex of QDs-MPA-strep + biotinylated HBV oligonucleotide (electrolyte: 0.02 M sodium borate, voltage: 20 kV, capillary: 47/40 cm, 75 µm ID, injection : 20 s, 3.4 kPa)

remarkable signal visible, however we believe that it is an undesirable artefact, because DNA-specific staining should not be able to label this protein. In lanes 6 and 7, oligonucleotides BCL-2 and HBV were injected, respectively and bands can be seen in the low-molecular mass region.

In Fig. 6b, the same gel as in Fig. 6a was used; however, protein-specific staining by Coomassie blue was used. In lanes 1, 6 and 7, no signal were observed due to the presence of DNA only. In the lane 2, a brown band was visible corresponding probably to the MPA-QDs damaged by precipitation in the staining solutions. In the lane 3, a very weak signal occurred under careful observation (marked by arrow). Based on the comparison to the signal in the Fig. 6a (in the same position), it can be concluded

that both DNA and proteins are present, however, in very low concentrations. This leads us to the opinion that this band corresponds to the complex of MPA-QD-strep with biotinylated HBV oligonucleotide. Lane 4 contained MPA-QD-strep, which was confirmed by band of streptavidin at the beginning of the lane. Similarly, in the lane 5, the intensive signal of streptavidin standard was detected. It should be noted that agarose gel electrophoresis is optimized for DNA separation and therefore, poor migration of analytes not containing DNA is observed. On the other hand, it clearly follows from the results obtained that the migration of the complex of MPA-QD-strep with biotinylated oligonucleotide was significantly improved due to the presence of DNA fragment.

To support our hypothesis, SDS-PAGE analysis was carried out under both reducing and non-reducing conditions. At first, the separated analytes were analysed with fluorescent visualization under illumination by light with 480-nm wavelength. Several intensive signals are present due to the intrinsic fluorescence of QDs (Fig. 6c). In lane 1, only the protein ladder was injected and therefore no fluorescence is observed, however in lanes 2, 3, and 4 samples containing MPA-QDs, QD-MPA-strep-VHB-biotin and QDs-MPA-strep were injected, respectively. Interestingly, all these samples maintained their fluorescent properties even though they did not differ in migration through the gel. In lane 5, streptavidin standard was injected and therefore no fluorescence was observed. Lanes 6–9 were analysed under non-reducing conditions, and fluorescent signal was observed only in the lane 6 injected with MPA-QDs. In lanes 7 and 8, the fluorescence of QDs was quenched by the conditions.

Subsequently, the gel was stained with silver to visualize the proteins (Fig. 6d). In lane 2, signal at molecular mass of 15 kDa was detected, however due to the absence of proteins it can be concluded that the signal belongs to the MPA-QDs. In lanes 3 and 4, two bands at molecular masses of 15 and 30 kDa occurred. The band at 15 kDa belongs to the MPA-QD-strep and the band at 30 kPa belongs to the streptavidin dimer due to the excess of the streptavidin in the solution. The signals in lanes 3 and 4 are very similar because the presence of the biotinylated oligonucleotide did not influence the migration under protein-specific conditions. Finally, streptavidin standard was injected in lane 5 confirming that monomer and dimer forms of this protein were in the solution used for modification of MPA-QDs. Under non-reducing conditions, significant changes are present. In lane 6, only a band of MPA-QDs with molecular mass of approx. 15 kDa was observed, however in lane 7, number of bands at molecular masses of 40–50 kDa were visible. As known from the literature [43], under non-reducing conditions the biotin bound to the streptavidin causes the streptavidin units not to be divided. This leads us to the conclusion that the complex of MPA-QD-strep-HBV-biotin is formed and these bands belong to this complex. In contrary in lane 8, in which sample of MPA-QD-strep is injected only; no such shift was observed. Finally, the streptavidin standard injected in lane 9 provided signals of monomeric and dimeric forms only.

For final verification of MPA-QD-strep-HBV-biotin complex formation, CE–LIF was used taking advantage of the selectivity of fluorimetric detection neglecting non fluorescent components of the solution such as unreacted oligonucleotide as well as unreacted streptavidin. Two distinguished signals are present in the electropherogram, shown in Fig. 6e. The broad peak with migration time of approx. 4 min belongs to the QDs-MPA-strep and the sharp peak with migration time of 3.5 min belongs to the complex of MPA-QD-strep-HBV-biotin.

Conclusion

It clearly follows from the obtained results that successful synthesis of MPA capped CdTe QDs was performed followed by functionalization by streptavidin enabling the bioconjugation with biotinylated analytes such as oligonucleotides. The quality of prepared MPA-QDs-strep as well as their interaction with selected oligonucleotides was verified by CE–UV and CE–LIF methods. By combination of gel electrophoresis and CE, the efficiency of functionalization process as well as monitoring of the interactions was verified. Importance of streptavidin–biotin linkage relies on numerous of biomolecules, which can be easily biotinylated and through it rather than linked with streptavidin. In this paper, this linkage was used as streptavidin-modified QDs to label and detect biotinylated oligonucleotide cancer sequence of BCL-2 and sequence of virus hepatitis B (VHB). This detection might help to have fast and precise diagnosis of these diseases in the future.

Acknowledgments Financial support from the following projects NanoBioTECell GA CR P102/11/1068, IGA IP10/2012 and CEITEC CZ.1.05/1.1.00/02.0068 is highly acknowledged.

References

1. Perez-Ruiz T, Martinez-Lozano C, Sanz A, Bravo E (2003) Chromatographia 58:757–762
2. Tanaka Y, Terabe S (1999) Chromatographia 49:489–495
3. Green NM (1990) Method Enzymol 184:51–67
4. Sakahara H, Saga T (1999) Adv Drug Deliv Rev 37:89–101
5. Caswell KK, Wilson JN, Bunz UHF, Murphy CJ (2003) J Am Chem Soc 125:13914–13915
6. Roco MC, Mirkin CA, Hersam MC (2011) J Nanopart Res 13:897–919
7. Chomoucka J, Drbohlavova J, Huska D, Adam V, Kizek R, Hubalek J (2010) Pharmacol Res 62:144–149

8. Prasek J, Drbohlavova J, Chomoucka J, Hubalek J, Jasek O, Adam V, Kizek R (2011) J Mater Chem 21:15872–15884
9. Drbohlavova J, Chomoucka J, Adam V, Ryvolova M, Eckschlager T, Hubalek J, Kizek R (2012) Curr Drug Metab (in press)
10. Chomoucka J, Drbohlavova J, Masarik M, Ryvolova M, Huska D, Prasek J, Horna A, Trnkova L, Provaznik I, Adam V, Hubalek J, Kizek R (2012) Int J Nanotechnol 9:746–783
11. Sahoo SK, Parveen S, Panda JJ (2007) Nanomed Nanotechnol Biol Med 3:20–31
12. Rao CNR, Kulkarni GU, Thomas PJ, Edwards PP (2002) J Chem Eur 8:29–35
13. Yu WW, Chang E, Drezek R, Colvin VL (2006) Biochem Biophys Res Commun 348:781–786
14. Bharali DJ, Mousa SA (2010) Pharmacol Ther 128:324–335
15. Mudshinge SR, Deore AB, Patil S, Bhalgat CM (2011) Saudi Pharm J 19:129–141
16. Walling MA, Novak JA, Shepard JRE (2009) Int J Mol Sci 10:441–491
17. Ryvolova M, Chomoucka J, Janu L, Drbohlavova J, Adam V, Hubalek J, Kizek R (2011) Electrophoresis 32:1619–1622
18. Trojan V, Chomoucka J, Krystofova O, Hubalek J, Babula P, Kizek R, Havel L (2010) J Biotechnol 150:S479–S479
19. Wang C, Gao X, Ma Q, Su XG (2009) J Mater Chem 19:7016–7022
20. Zheng YG, Gao SJ, Ying JY (2007) Adv Mater 19:376–380
21. Liu WH, Choi HS, Zimmer JP, Tanaka E, Frangioni JV, Bawendi M (2007) J Am Chem Soc 129:14530–14531
22. Huang XY, Weng JF, Sang FM, Song XT, Cao CX, Ren JC (2006) J Chromatogr A 1113:251–254
23. Aoyagi S, Kudo M (2005) Biosens Bioelectron 20:1680–1684
24. Xiao Y, Barker PE (2004) Nucleic Acids Res 32:e28
25. Smith AM, Duan HW, Mohs AM, Nie SM (2008) Adv Drug Deliv Rev 60:1226–1240
26. Wilcoxon JP, Martin JE, Provencio PP (2000) Langmuir 16:9912–9920
27. Kirkland JJ (1979) J Chromatogr 185:273–288
28. Kazakov S, Kaholek M, Kudasheva D, Teraoka I, Cowman MK, Levon K (2003) Langmuir 19:8086–8093
29. Li YQ, Wang HQ, Wang JH, Guan LY, Liu BF, Zhao YD, Chen H (2009) Anal Chim Acta 647:219–225
30. Vanifatova NG, Spivakov BY, Mattusch J, Franck U, Wennrich R (2005) Talanta 66:605–610
31. Alonso MCB, Prego R (2000) Anal Chim Acta 416:21–27
32. Liu FK, Tsai MH, Hsu YC, Chu TC (2006) J Chromatogr A 1133:340–346
33. Schnabel U, Fischer CH, Kenndler E (1997) J Microcolumn Sep 9:529–534
34. Krupke R, Hennrich F, von Lohneysen H, Kappes MM (2003) Science 301:344–347
35. Olivas WM, Maher LJ (1996) Nucleic Acids Res 24:1758–1764
36. Kondili L, Argentini C, La Sorsa V, Chionne P, Costantino A, Mele A, Brunetto MR, Rapicetta M (2002) J Hepatol 36:224–225
37. Duan JL, Song LX, Zhan JH (2009) Nano Res 2:61–68
38. Baumle M, Stamou D, Segura JM, Hovius R, Vogel H (2004) Langmuir 20:3828–3831
39. Wong C, Sridhara S, Bardwell JCA, Jakob U (2000) Biotechniques 28:426–428
40. Krizkova S, Adam V, Eckschlager T, Kizek R (2009) Electrophoresis 30:3726–3735
41. Algar WR, Tavares AJ, Krull UJ (2010) Anal Chim Acta 673:1–25
42. Petrlova J, Masarik M, Potesil D, Adam V, Trnkova L, Kizek R (2007) Electroanalysis 19:1177–1182
43. O'Sullivan VJ, Barrette-Ng I, Hommema E, Hermanson GT, Schofield M, Wu S-C, Honetschlaeger C, Ng KKS, Wong S-L (2012) PLoS ONE 7:e35203

5.2.2 Research article II

BLAZKOVA, I.; NGUYEN, V.H.; DOSTALOVA, S.; KOPEL, P.; **STANISAVLJEVIC, M.**; VACULOVICOVA, M.; STIBOROVA, M.; ECKSCHLAGER, T.; KIZEK, R.; ADAM, V. Apoferritin modified magnetic nanoparticles as doxorubicin carriers for anticancer drug delivery. Int.J.Mol.Sci. 2013. 14(7): p. 13391-13402. ISSN: 1422-0067
DOI: 10.3390/ijms140713391

Participation in the work of the author Stanisavljevic M.: Experimental work 30% and manuscript preparation 20%.

Apoferritin is protein consisted out of 24 polypeptide subunits which form a cavity with the internal diameter of 8 nm. Naturally, in this cavity iron oxide has been storaged and released in controlled fashion. Containing iron this protein is called ferritin and it is produced in all living organisms. However, created cavity after removing of the iron can be employed for carring any molecule of intrest such as doxorubicin. Doxorubicin (DOX) is an anthracycline antibiotic used for cancer treatment known for sever cardiotoxicity as well as for it natural fluorescent properties.
In this work apoferritin was used for encapsulation of the doxorubicin (APODOX) in purposes of the toxicity elimination and due to his fluorescent nature CE-LIF was used as appropriate technique for the monitoring of the process. Also, it is known that almost every molecule could be biotinylated and follow coupled with streptavidin, which was used in this work for coupling apoferritin with magnetic nanoparticles for targeted therapy as current direction in which anticancer treatment is going.
Biotinylated APODOX was prepared by mixing APODOX and biotinamidohexanoyl-6-aminohexanoic acid, further sample was dialyzed for removal of the DOX excess.
For coupling with the streptavidin modified magnetic nanoparticles (Dynabeads M-270 Streptavidin, Life Technologies, Invitrogen, Prague, Czech Republic) an external magnetic field was applied for immobilization of the particles in the vial followed by adding solution of biotinylated APODOX. After incubation, supernatant containing unreacted APODOX has been removed. Prepared samples were first observed with fluorescent microscope (Mircoscope Olympus ix 71, Olympus Czech Group Ltd.,

Prague, Czech Republic) and under the 480 nm weak signal of particles modified by biotinylated APODOX was observed. CE-LIF was used for characterisation of APODOX and APODOX conjugated with magnetic nanoparticles as well as their pH trigerred DOX release. In first analysis of the solely APODOX two peaks are visible with migration time of 2.9 min and 3.3 min. Peak at 2.9 min was identified as as free DOX which has been adsorbed on the surface of the apoferritin cage and due to applied field used in CE analysis DOX was desorbed and can be detected in the electropherograms. Reasonably, follows that peak at 3.3 min belongs to the APODOX.
pH triggered release of the DOX from magnetic nanoparticles conjugated to APODOX in CE-LIF analysis have shown only presence of free DOX as it was expected.

Int. J. Mol. Sci. **2013**, *14*, 13391-13402; doi:10.3390/ijms140713391

OPEN ACCESS
International Journal of
Molecular Sciences
ISSN 1422-0067
www.mdpi.com/journal/ijms

Article

Apoferritin Modified Magnetic Particles as Doxorubicin Carriers for Anticancer Drug Delivery

Iva Blazkova [1], Hoai Viet Nguyen [1], Simona Dostalova [1], Pavel Kopel [1,2], Maja Stanisavljevic [1], Marketa Vaculovicova [1,2], Marie Stiborova [3], Tomas Eckschlager [4], Rene Kizek [1,2] and Vojtech Adam [1,2,*]

[1] Department of Chemistry and Biochemistry, Faculty of Agronomy, Mendel University in Brno, Zemedelska 1, Brno CZ-613 00, Czech Republic; E-Mails: iva.blazkova@seznam.cz (I.B.); nguyenviethoai@hus.edu.vn (H.V.N.); esedinka@seznam.cz (S.D.); paulko@centrum.cz (P.K.); maja.stani85@gmail.com (M.S.); marketa.ryvolova@seznam.cz (M.V.); kizek@sci.muni.cz (R.K.)

[2] Central European Institute of Technology, Brno University of Technology, Technicka 3058/10, Brno CZ-616 00, Czech Republic

[3] Department of Biochemistry, Faculty of Science, Charles University, Albertov 2030, Prague 2 CZ-128 40, Czech Republic; E-Mail: stiborov@yahoo.com

[4] Department of Paediatric Haematology and Oncology, 2nd Faculty of Medicine and University Hospital Motol, Charles University, V Uvalu 84, Prague 5 CZ-150 06, Czech Republic; E-Mail: tomas.eckschlager@fnmotol.cz

* Author to whom correspondence should be addressed; E-Mail: vojtech.adam@mendelu.cz; Tel.: +420-545-133-350; Fax: +420-5-4521-2044.

Received: 19 April 2013; in revised form: 18 May 2013 / Accepted: 23 May 2013 / Published: 27 June 2013

Abstract: Magnetic particle mediated transport in combination with nanomaterial based drug carrier has a great potential for targeted cancer therapy. In this study, doxorubicin encapsulation into the apoferritin and its conjugation with magnetic particles was investigated by capillary electrophoresis with laser-induced fluorescence detection (CE-LIF). The quantification of encapsulated doxorubicin was performed by fluorescence spectroscopy and compared to CE-LIF. Moreover, the significant enhancement of the doxorubicin signal was observed by addition of methanol into the sample solution.

Keywords: cancer; nanomedicine; magnetic particles; doxorubicin; nanoparticles

1. Introduction

Magnetic particles can be the size of several nanometers to several micrometers and consist mainly of iron, nickel, cobalt and gadolinium [1–6]. Magnetic nanoparticles with appropriate surface coatings can be used for various biomedical purposes, such as drug delivery, hyperthermia, tissue repairing, cell and tissue targeting, transfection and magnetic resonance imaging [2,7–9].

Surface functionalization allows us to use nanoparticles as probes for molecular imaging [10]. The material employed for surface coating of the magnetic particles must be nontoxic and biocompatible and has to enable us a targeted delivery with localization in a required area [2,11]. Nanoparticles have a large surface area and provide a large number of functional groups for cross-linking to tumor-targeting ligands such as monoclonal antibodies, peptides, or small molecules for diagnostic imaging or delivery of therapeutic agents [12,13]. The linkage of the drug with magnetic nanoparticle has to be stable to prevent drug release during its transport [14]. Varied surface modifications can be used for the biomedical applications [11,15–17]. Polymers, poly(ethylene glycol) (PEG), *N*-(2-hydroxypropyl)methacrylamide (HPMA), and poly(lactide-*co*-glycolide) (PLGA) copolymers have been successfully utilized in clinical research [14]. Surface modifications can be also carried out using tetraethoxysilane (TEOS), triethoxysilane (TES) and 3-aminopropyltrimethoxysilane (APTMS) [6]. The transport to the vessel wall is essential for localizing therapy [18].

Superparamagnetic iron oxide could be used as an emerging therapeutic delivery system [19]. Anticancer drugs reversibly bound to magnetic fluids (ferrofluids) could be concentrated in tumors by magnetic fields that are arranged at the tumor surface outside of the organism [20]. Moreover, delivery by magnetic particles can be coupled to specialized nanocarriers such as lipid- [21] and/or protein-based carriers [22,23] enabling selective release of the drug in the site of the action. Such release may be performed by various mechanisms including photo- [24] or thermoiniciated [25] or pH triggered release [23,26]. In this study, magnetic particle-based targeted, apoferritin mediated and pH triggered transport of doxorubicin (DOX) was studied using capillary electrophoresis with laser-induced fluorescence detection.

2. Results and Discussion

Apoferritin is a protein composed of 24 polypeptide subunits, structurally arranged to create an internal cavity with size of 8 nm in diameter [27]. This cavity is naturally used for storage of iron ions; however, artificially it can be employed for carrying of any molecule of interest. Doxorubicin (DOX), an anthracycline antibiotic, which is due to its structure (Figure 1A) exhibiting an intrinsic fluorescence, belongs to such molecules. The encapsulation of DOX into the apoferritin cavity (formation of APODOX) is reflected in the fact that non-fluorescent apoferritin becomes fluorescent. Photograph of solution of DOX and APODOX in the ambient light is shown in Figure 1B and fluorescence photograph of solution of DOX and APODOX is shown in Figure 1C. The disassembling and reassembling mechanism based on pH of the environment is schematically illustrated in Figure 1D. The apoferritin structure is assembled at physiological conditions and by decreasing the pH to highly acidic region (pH 2) the protein is disassembled to its subunits. The mixture of apoferritin subunits and DOX molecules creates the basic solution for the encapsulation process. By increasing

the pH of this solution the apoferritin structure is reassembled and DOX molecules are encapsulated in the cavity. This feature allows the application of apoferritin as a drug nanocarrier with specific low pH initiated release. For microencapsulation using the so-called "double emulsion" method, proteins in solution state may easily leak to the outer aqueous continuous phase, resulting in unacceptable low encapsulation efficiency [28–30]. Replacing the inner protein solution with solidified protein particles may substantially improve encapsulation efficiency, but protein particles still have the chance to contact with the outer aqueous continuous phase, leading to considerable loss of proteins. In general, higher encapsulation efficiency may be obtained by atomizing a protein-in-polymer suspension through a drying (or solidification) atmosphere prior to entering a collecting buffer [31].

Figure 1. (**A**) Chemical structure of doxorubicin (DOX); (**B**) Photograph of solution of DOX (left) and apoferritin encapsulated doxorubicin (APODOX) (right) in the ambient light; (**C**) Fluorescence photograph of solution of DOX (left) and APODOX (right)—λ_{ex} = 480 nm, λ_{em} = 600 nm, exposition time 6 s, f_{Stop} 1.1, FOV 7.2; (**D**) Scheme of pH dependent disassembling and reassembling of apoferritin and encapsulation of DOX (1—schematic structure of assembled apoferritin at physiological conditions, 2—mixture of disassembled apoferritin units and DOX molecules at pH 2, 3) encapsulation of DOX molecules into the apoferritin cavity at increased pH and formation of APODOX).

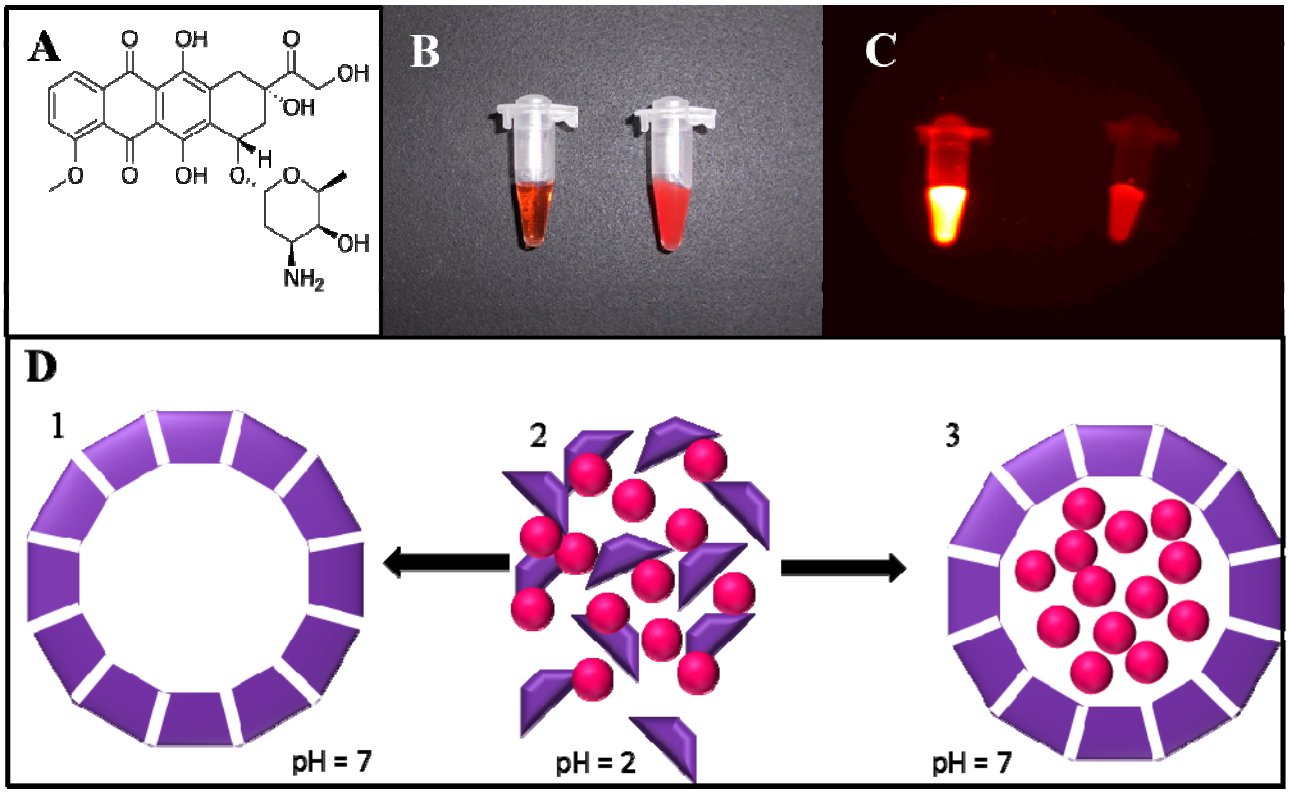

2.1. Fluorimetric Characterization

DOX exhibits the fluorescence with excitation maximum of 480 nm and emission maximum at 600 nm. Its encapsulation into the apoferritin cage does not influence the emission maximum and no shift is observed and the fluorescence intensity increased with the increasing concentration of free

DOX used for encapsulation reaction (Figure 2A). However, the significant decrease in the intensity compared to the free DOX at the same concentration was detected. This decrease is caused by the incomplete encapsulation and by the removal of the free DOX using dialysis. According to the calibration curve of DOX with regression equation y = 1131.2ln(x) + 6870.8 the amount of encapsulated DOX was determined. It was observed that the encapsulation yield increased with the increased applied DOX concentration (Figure 2B).

Figure 2. Fluorimetric characterization of APODOX. (**A**) Emission spectra (λ_{ex} = 480 nm) of APODOX prepared using various concentrations of DOX (0, 6.25, 12.5, 25, 50 μg/mL) and 1 mg/mL of apoferritin (Inset: Dependence of fluorescence intensities in the maximum (600 nm) on applied DOX concentration); (**B**) Dependence of total DOX concentration (free and encapsulated form) in the solution on concentration of applied DOX.

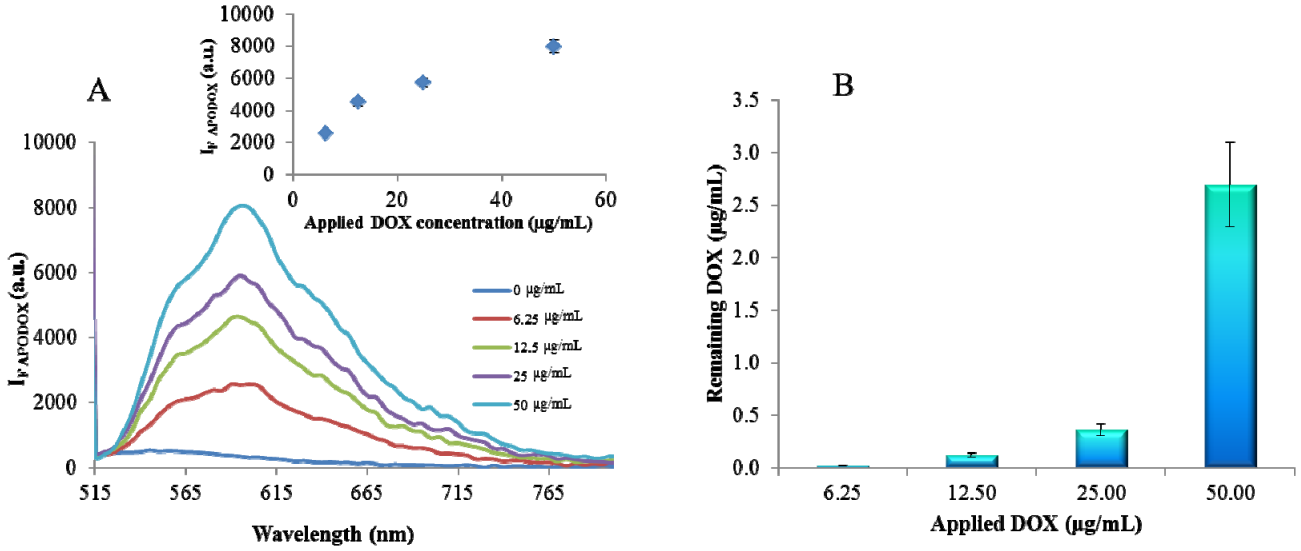

2.2. CE Characterization

Capillary electrophoresis offers several benefits compared to stationary fluorimetric analysis. The most important of these is the ability to distinguish different forms of doxorubicin. As it is shown in Figure 3A, certain portion of free DOX was still remaining in the solution of the sample of APODOX even after the purification by dialysis. Therefore two peaks can be found in the electropherogram. The one with migration time of 2.9 min was identified as free DOX and the peak with migration time of 3.3 min belonged to the APODOX. At first, the hypothesis of inefficient dialysis purification was adopted. For this reason 3 times repeated 24 h long dialysis was performed and the fluorescence was acquired after each step. The fluorescence intensities of all three measurements were equal. Based on these results we came to the conclusion that some molecules of DOX were adsorbed on the surface of APODOX and therefore the dialysis purification was not capable of removing them. However, we assume that these molecules were desorbed from the APODOX surface in the CE probably due to the presence of the electric field and therefore a peak of free DOX can be detected in the electropherograms. The intensity of both peaks (DOX and APODOX) increased linearly with the increased concentration of applied DOX (Figure 3B). The lower slope of the DOX curve can be explained by gradual saturation of the APODOX surface by DOX molecules, which are subsequently desorbed.

Figure 3. CE characterization of APODOX. (**A**) Typical electropherograms of APODOX solutions prepared by different concentrations (0, 6.25, 12.5, 25 and 50 μg/mL) of applied DOX; (**B**) Dependence of peak heights of DOX and APODOX peaks on the concentrations of applied DOX (0, 6.25, 12.5, 25, 50 μg/mL); (**C**) Dependence of the concentration of free DOX in the solution on the applied DOX concentration (0, 6.25, 12.5, 25 and 50 μg/mL); (**D**) Dependence of encapsulated DOX concentration on the applied DOX concentration (0, 6.25, 12.5, 25 and 50 μg/mL).

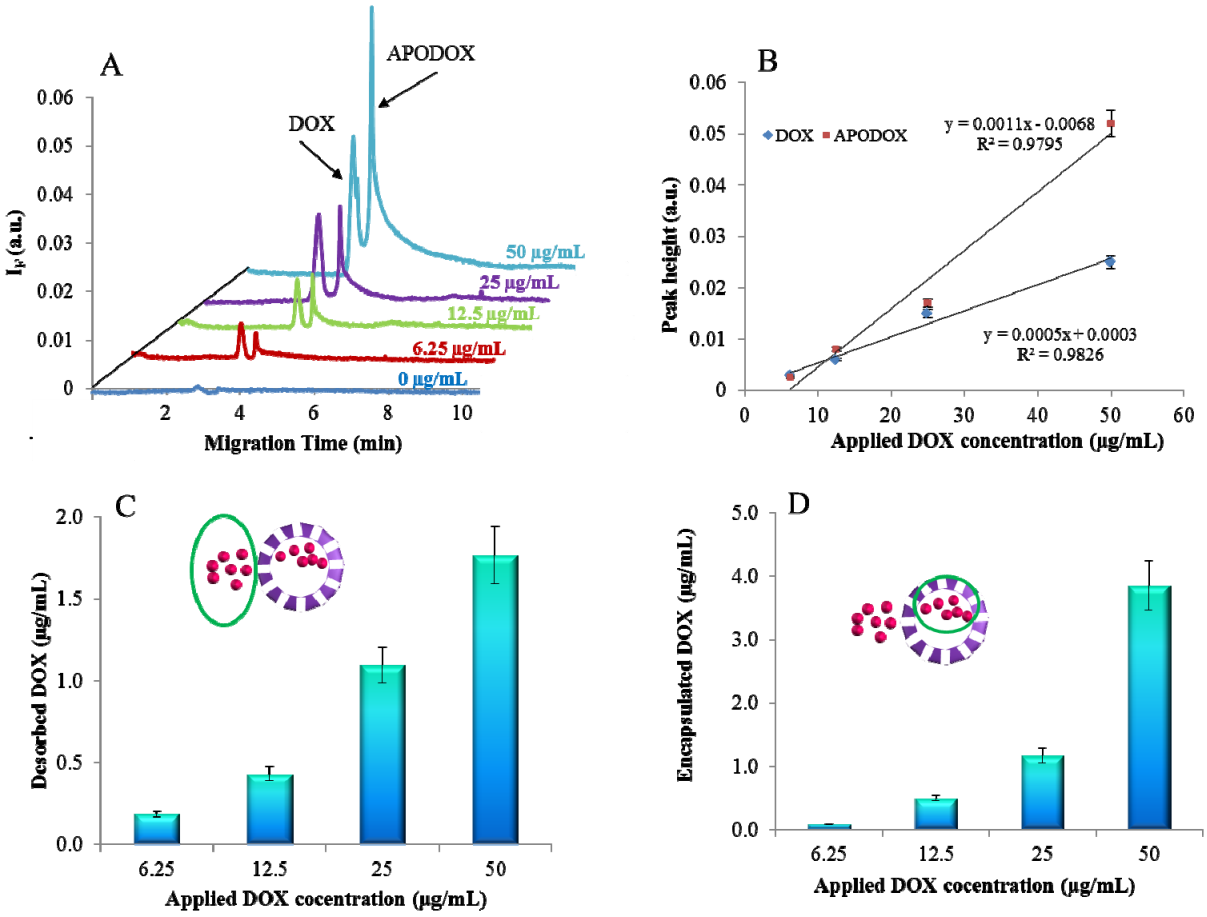

Based on calibration curve for DOX with the regression equation y = 1.34x + 0.0013 the amount of DOX in both forms was quantified. The dependence of the amount of free DOX on the DOX amount applied to the encapsulation process is shown in Figure 3C. It follows from the results that the increasing applied amount led to the increased amount of desorbed DOX, however at the same time the amount of the encapsulated DOX (Figure 3D) increased nearly twice as much.

2.3. pH Triggered DOX Release

It has been established that employment of separation technique such as CE-LIF is beneficial for APODOX investigation due to the ability to distinguish between encapsulated and desorbed DOX occurring in the solution. This can be utilized for monitoring of selective release of the drug. As noticed above lowering of pH to the highly acidic range leads to the release of the content of the apoferritin cavity. In the case of APODOX this was observed by the increasing of the intensity of the DOX peak in the APODOX electropherogram. The dependence of the peak intensity on pH is shown

in Figure 4. This dependence is linear with regression equation y = 0.012x + 0.0146 and the coefficient of determination R^2 = 0.9782. The results show that lowering the pH from 6.2 to 2.4 led to the increase of the desorbed DOX signal to the 272.9% of the original intensity. A schematic DOX release is illustrated by the schemes in the insets in Figure 4.

Figure 4. Dependence of fluorescence intensity of DOX peaks (obtained by CE-LIF, λ_{ex} = 480 nm, λ_{em} = 600 nm) released from APODOX by pH change. Insets: the scheme of DOX released from APODOX by decrease of pH.

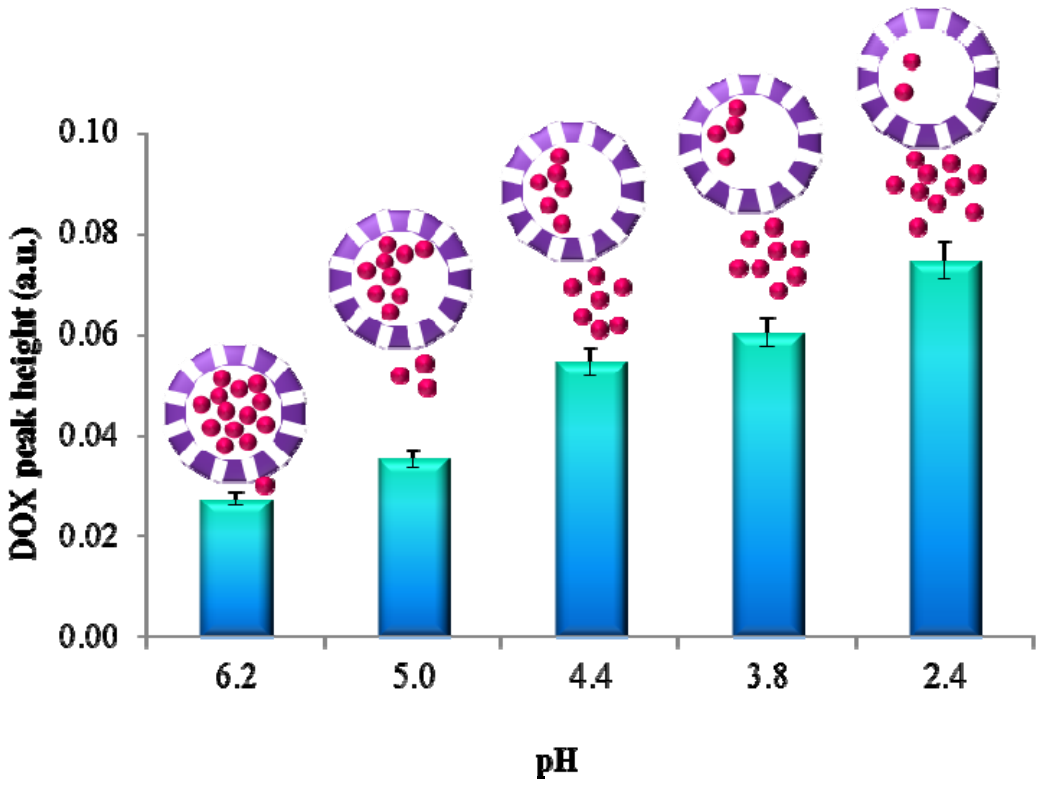

2.4. Influence of MeOH

It was observed that the presence of MeOH in the sample improves the LIF detection during the CE analysis. It is shown in Figure 5A that, as expected, the dilution of APODOX by 1:1 by water led to the decrease in the fluorescence signal by 50%; however, dilution by MeOH caused an increase in the signal of desorbed DOX peak by 18-fold. Figure 5B shows the dependence of the height of DOX peak on the MeOH content in the analyte solution. It clearly follows from the results obtained that while the free (desorbed) DOX peak intensity increased linearly (R^2 = 0.9778), the signal of APODOX peak remained unchanged.

Figure 5. Methanol influence on fluorescent analysis of APODOX. (**A**) CE-LIF of APODOX (25 μg/mL) nondiluted (blue trace), diluted 1:1 by H_2O (red trace) and diluted 1:1 by MeOH (green trace), for conditions see Figure 2; (**B**) Dependence of peak heights on MeOH percentage in the injected sample.

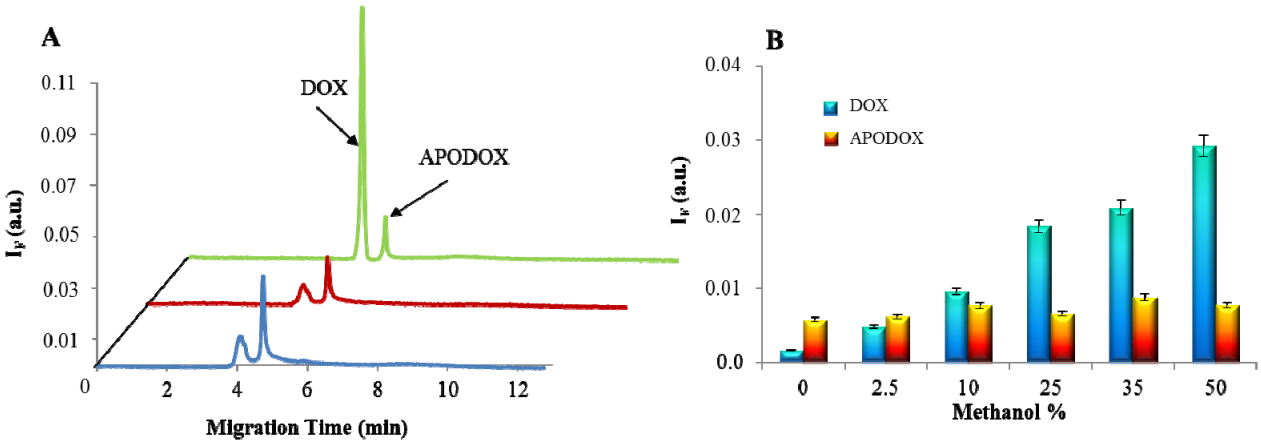

Figure 6. MPs-based transport of APODOX. (**A**) Micrographs of magnetic parties (1–unmodified MPs, 2–MPs modified by biotinylated apoferritin, 3–MPs modified by APODOX); (**B**) Scheme of the process–APODOX sample (No. 1) mixed with MPs, immobilized by magnetic field, unbound APODOX removed (No. 2), DOX released by pH decrease (No. 3), release of DOX from APODOX immobilized on MPs surface (No. 4); (**C**) Intensities of peaks (CE-LIF) in particular solution obtained during the procedure shown in panel (B); (**D**) Intensities of peaks (CE-LIF) in particular solution obtained during the procedure shown in panel (B) in 50% MeOH, for CE conditions see Figure 2.

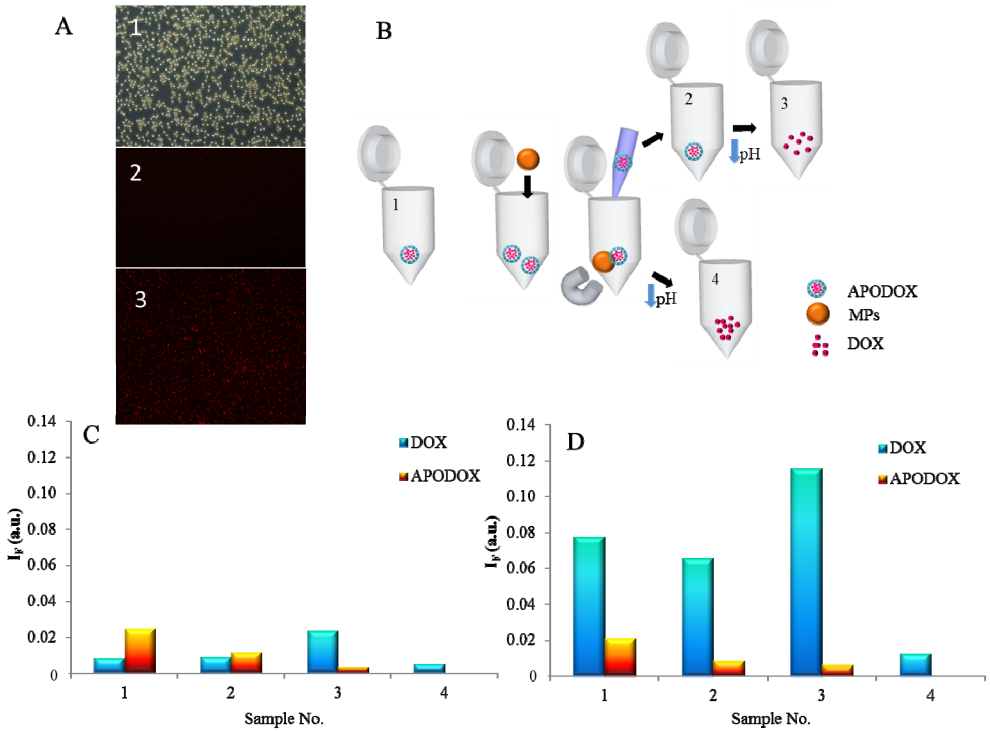

2.5. Magnetic Particle Mediated APODOX Transport

First, magnetic particles and their conjugates with biotinylated APODOX were observed by fluorescence microscopy. The micrographs of the particles are shown in Figure 6A. The micrograph No. 1 shows unmodified particles under ambient light and the micrograph No. 2 shows the magnetic particles modified by the biotinylated apoferritin under illumination by the light with wavelength of 480 nm. As expected no fluorescence is observed, however the micrograph No. 3 shows a weak signal of particles modified by biotinylated APODOX.

The scheme of the procedure is shown in Figure 6B. Biotinylated APODOX (sample No. 1) was coupled to the streptavidin-functionalized magnetic particles and after application of an external magnetic field the unreacted solution was removed and analyzed by CE-LIF (Sample No. 2). Subsequently, the pH was decreased to release the DOX and the solution (Sample No. 3) was analyzed (CE-LIF). Finally, the magnetic particles with conjugated APODOX were resuspended in water and pH was decreased to release the DOX from the particles (Sample No.4). The peak intensities of all four solutions are summarized in Figure 6C.

3. Experimental Section

3.1. Apoferritin Encapsulated Doxorubicin (APODOX) Synthesis

Apoferritin solution 20 μL (50 mg/mL, equine spleen, Sigma-Aldrich) was diluted with 200 μL of ACS water. Doxorubicin (100 μL) was added and mixture was shaken. 1 M HCl (0.5 μL) was added and turbidity was observed. 15 min later 1M NaOH (0.5 μL) was added and turbidity disappeared. Solution was subsequently 2 h shaken on Vortex Genie2 (Scientific Industries Inc, Bohemia, NY, USA). Dialyses for 24 h were realized on membrane filter (0.025 μm VSWP, Millipore) against 2 L of water. Thus obtained solution was diluted with ACS water to final volume of 1 mL.

3.2. Magnetic Particle Mediated APODOX Transport

3.2.1. Preparation of Biotinylated Apoferritin Filled with Doxorubicin

Biotinamidohexanoyl-6-aminohexanoic acid 100 μL (1 mg/mL) was added to the solution of APODOX prepared in Section 2.2. The mixture was shaken for 2 h on Vortex Genie2 and dialysis was accomplished as described in previous part.

3.2.2. Modification of Streptavidin-Functionalized Particles with Biotinylated APODOX

Exactly 100 μL of streptavidin coated magnetic particles (Dynabeads M-270 Streptavidin, Life Technologies, Invitrogen, Prague, Czech Republic) in a clean vial were placed on a magnetic stand (Dynal MPC™-S, Life Technologies, Invitrogen, Prague, Czech Republic) and after the beads were immobilized on the vial by the magnetic field the storage solution was carefully removed by a pipette. The particles were subsequently washed (3×) by 100 μL of PBS buffer pH 7.4. After the last washing step was completed, 100 μL of biotinylated APODOX was added and the suspension was incubated for 30 min at 20 °C using Multi RS-60 Programmable rotator-mixer (Biosan, Riga, Latvia) (60 rpm,

90 °C). Subsequently the supernatant was removed using magnetic stand and the particles were washed 3× with PBS buffer pH 7.4. Finally, the washed particles were resuspended in the final volume (100 μL) of PBS buffer (pH 7.4).

3.3. Fluorescent Microscopy

Fluorescent microscopy was carried out using Mircoscope Olympus ix 71 (Olympus Czech Group Ltd., Pregue, Czech Republic) emploing an excitation wavelength of 480 nm and emission wavelength of 580 nm. The magnification was 200-times and the exposure time was 121 s.

3.4. Fluorimetric Analysis

Fluorescence spectra were acquired by multifunctional microplate reader Tecan Infinite 200 PRO (TECAN Group Ltd., Mannedorf, Switzerland). 480 nm was used as an excitation wavelength and the fluorescence scan in the range from 510 to 850 nm was measured every 5 nm. Each intensity value is an average of 5 measurements. The detector gain was set to 100. The sample (50 μL) was placed in transparent 96 well microplate with flat bottom by Nunc.

3.5. Capillary Electrophoresis with Laser-Induced Fluorescence Detection

Electrophoretic measurements were carried out using capillary electrophoresis system Beckman PACE/5000 with laser-induced fluorescence detection with excitation at 488 nm (CE-LIF). Uncoated fused silica capillary was used with total length of 47 cm and effective length of 40 cm. The internal diameter of the capillary was 75 μm. Tris-HCl buffer (50 mM, pH 8.2) was used as a background electrolyte and the separation was carried out using 20 kV with hydrodynamic injection for 20 s at 3.4 kPa.

4. Conclusions

The targeted therapy is a direction of current anticancer treatment and therefore numerous transporters are searched. Apoferritin enabling pH triggered content release in combination with magnetic particles is one of the systems providing required properties and behavior for this purpose. As shown in this work, doxorubicin can be effectively encapsulated into the apoferritin cavity and transported by magnetic field to the site of action.

Even though magnetic particles have been nowadays widely employed for target transport of a variety of cargos within the living organisms, their toxicity causing problems in terms of inflammation, formation of apoptotic bodies, generation of reactive oxygen species, and chromosome condensation has to be addressed. As shown in a number of studies, the toxicity can be influenced by a range of factors such as size, surface coating and/or surface charge. It is obvious that certain toxicity risks do exist and when magnetic particles are employed and a number of tests are required. However, we believe that the benefits of targeted delivery of extremely toxic cytostatic drugs by magnetic particles prevail over the disadvantages which are being moreover continuously eliminated by extensive research.

Similarly, the way of the most effective administration is widely investigated and so far the intravenous, subcutaneous and/or intratumoral fashion is generally accepted and performed even though each of these modes has both advantages and disadvantages.

Acknowledgments

Financial support from CYTORES GA CR P301/10/0356 (EA 14), CEITEC CZ.1.05/1.1.00/02.0068, IGA IP22/2013, MH CZ – DRO, University Hospital Motol, Prague, Czech Republic 00064203 and LPR 2013 and by is highly acknowledged.

Conflict of Interest

The authors declare no conflict of interest.

References

1. El-Okr, M.M.; Salem, M.A.; Salim, M.S.; El-Okr, R.M.; Ashoush, M.; Talaat, H.M. Synthesis of cobalt ferrite nano-particles and their magnetic characterization. *J. Magn. Magn. Mater.* **2011**, *323*, 920–926.
2. Gupta, A.K.; Naregalkar, R.R.; Vaidya, V.D.; Gupta, M. Recent advances on surface engineering of magnetic iron oxide nanoparticles and their biomedical applications. *Nanomedicine* **2007**, *2*, 23–39.
3. Nakamura, K.; Ueda, K.; Tomitaka, A.; Yamada, T.; Takemura, Y. Self-heating temperature and AC hysteresis of magnetic iron oxide nanoparticles and their dependence on sary particle size. *IEEE Trans. Magn.* **2013**, *49*, 240–243.
4. Nejati, K.; Zabihi, R. Preparation and magnetic properties of nano size nickel ferrite particles using hydrothermal method. *Chem. Cent. J.* **2012**, *6*, 1–6.
5. Thorek, D.L.J.; Tsourkas, A. Size, charge and concentration dependent uptake of iron oxide particles by non-phagocytic cells. *Biomaterials* **2008**, *29*, 3583–3590.
6. Tran, N.; Webster, T.J. Magnetic nanoparticles: Biomedical applications and challenges. *J. Mater. Chem.* **2010**, *20*, 8760–8767.
7. Nandori, I.; Racz, J. Magnetic particle hyperthermia: Power losses under circularly polarized field in anisotropic nanoparticles. *Phys. Rev. E* **2012**, *86*, 1–8.
8. Wu, A.G.; Ou, P.; Zeng, L.Y. Biomedical applications of magnetic nanoparticles. *Nano* **2010**, *5*, 245–270.
9. Schlorf, T.; Meincke, M.; Kossel, E.; Gluer, C.C.; Jansen, O.; Mentlein, R. Biological properties of iron oxide nanoparticles for cellular and molecular magnetic resonance imaging. *Int. J. Mol. Sci.* **2011**, *12*, 12–23.
10. Nune, S.K.; Gunda, P.; Thallapally, P.K.; Lin, Y.Y.; Forrest, M.L.; Berkland, C.J. Nanoparticles for biomedical imaging. *Expert Opin. Drug Deliv.* **2009**, *6*, 1175–1194.
11. Mahmoudi, M.; Simchi, A.; Imani, M. Recent advances in surface engineering of superparamagnetic iron oxide nanoparticles for biomedical applications. *J. Iran Chem. Soc.* **2010**, *7*, S1–S27.

12. Peng, X.H.; Qian, X.M.; Mao, H.; Wang, A.Y.; Chen, Z.; Nie, S.M.; Shin, D.M. Targeted magnetic iron oxide nanoparticles for tumor imaging and therapy. *Int. J. Nanomed.* **2008**, *3*, 311–321.
13. Liu, D.; Zhu, G.L.; Tang, W.Q.; Yang, J.Q.; Guo, H.Y. PCR and magnetic bead-mediated target capture for the isolation of short interspersed nucleotide elements in fishes. *Int. J. Mol. Sci.* **2012**, *13*, 2048–2062.
14. Khandare, J.; Minko, T. Polymer-drug conjugates: Progress in polymeric prodrugs. *Prog. Polym. Sci.* **2006**, *31*, 359–397.
15. Braconnot, S.; Eissa, M.M.; Elaissari, A. Morphology control of magnetic latex particles prepared from oil in water ferrofluid emulsion. *Colloid Polym. Sci.* **2013**, *291*, 193–203.
16. Ding, G.B.; Guo, Y.; Lv, Y.Y.; Liu, X.F.; Xu, L.; Zhang, X.Z. A double-targeted magnetic nanocarrier with potential application in hydrophobic drug delivery. *Colloid Surf. B* **2012**, *91*, 68–76.
17. Eberbeck, D.; Dennis, C.L.; Huls, N.F.; Krycka, K.L.; Gruttner, C.; Westphal, F. Multicore magnetic nanoparticles for magnetic particle imaging. *IEEE Trans. Magn.* **2013**, *49*, 269–274.
18. Freund, J.B.; Shapiro, B. Transport of particles by magnetic forces and cellular blood flow in a model microvessel. *Phys. Fluids* **2012**, *24*, 1–12.
19. Mok, H.; Zhang, M.Q. Superparamagnetic iron oxide nanoparticle-based delivery systems for biotherapeutics. *Expert Opin. Drug Deliv.* **2013**, *10*, 73–87.
20. Lubbe, A.S.; Bergemann, C.; Riess, H.; Schriever, F.; Reichardt, P.; Possinger, K.; Matthias, M.; Dorken, B.; Herrmann, F.; Gurtler, R.; *et al.* Clinical experiences with magnetic drag targeting: A phase I study with 4'-epidoxorubicin in 14 patients with advanced solid tumors. *Cancer Res.* **1996**, *56*, 4686–4693.
21. Silva, A.C.; Santos, D.; Ferreira, D.; Lopes, C.M. Lipid-based nanocarriers as an alternative for oral delivery of poorly water-soluble drugs: Peroral and mucosal routes. *Curr. Med. Chem.* **2012**, *19*, 4495–4510.
22. Elzoghby, A.O.; Samy, W.M.; Elgindy, N.A. Protein-based nanocarriers as promising drug and gene delivery systems. *J. Control. Release* **2012**, *161*, 38–49.
23. Kilic, M.A.; Ozlu, E.; Calis, S. A novel protein-based anticancer drug encapsulating nanosphere: Apoferritin-doxorubicin complex. *J. Biomed.Nanotechnol.* **2012**, *8*, 508–514.
24. Banerjee, S.S.; Chen, D.H. A multifunctional magnetic nanocarrier bearing fluorescent dye for targeted drug delivery by enhanced two-photon triggered release. *Nanotechnology* **2009**, *20*, 1–10.
25. Li, L.; ten Hagen, T.L.M.; Schipper, D.; Wijnberg, T.M.; van Rhoon, G.C.; Eggermont, A.M.M.; Lindner, L.H.; Koning, G.A. Triggered content release from optimized stealth thermosensitive liposomes using mild hyperthermia. *J. Control. Release* **2010**, *143*, 274–279.
26. Xu, X.W.; Flores, J.D.; McCormick, C.L. Reversible imine shell cross-linked micelles from aqueous raft-synthesized thermoresponsive triblock copolymers as potential nanocarriers for "pH-Triggered" drug release. *Macromolecules* **2011**, *44*, 1327–1334.
27. Suzumoto, Y.; Okuda, M.; Yamashita, I. Fabrication of zinc oxide semiconductor nanoparticles in the apoferritin cavity. *Cryst. Growth Des.* **2012**, *12*, 4130–4134.
28. Wu, F.; Jin, T. Polymer-based sustained-release dosage forms for protein drugs, challenges, and recent advances. *AAPS PharmSciTech* **2008**, *9*, 1218–1229.

29. Li, X.H.; Zhang, Y.H.; Yan, R.H.; Jia, W.X.; Yuan, M.L.; Deng, X.M.; Huang, Z.T. Influence of process parameters on the protein stability encapsulated in poly-DL-lactide-poly(ethylene glycol) microspheres. *J. Control Release* **2000**, *68*, 41–52.
30. Sanchez, A.; Villamayor, B.; Guo, Y.Y.; McIver, J.; Alonso, M.J. Formulation strategies for the stabilization of tetanus toroid in poly(lactide-co-glycolide) microspheres. *Int. J. Pharm.* **1999**, *185*, 255–266.
31. Gander, B.; Johansen, P.; NamTran, H.; Merkle, H.P. Thermodynamic approach to protein microencapsulation into poly(D,L-lactide) by spray drying. *Int. J. Pharm.* **1996**, *129*, 51–61.

6 Conclusion

QDs and their interaction with biomolecules as one of the most important application of the QDs imply usage of different conjugation methods between these two components. Conjugations methods should provide efficient and stable connection and not alter the function of biomolecule or QD. In this work for, as a first step, QDs interaction with nucleic acid without any specific linker was investigated. Subsequently, surface was modified with streptavidin for non-covalent interaction and finally, specially designed synthetic peptide for highly specific interaction.

Streptavidin-modified QDs were used for coupling with biotinylated oligonucleotide cancer sequence of BCL-2 and sequence of virus hepatitis B enabling their detection with fluorescence detection methods. The bioconjugation with proteins was realized using synthetic peptide assembled on the QDs via cysteine residues and employed to label antibody. Advantage of designed peptide relies on its interaction with Fc region of antibody leaving Fab region active and in that way conserves biological function of the antibody intact which is not always the case with other conjugation methods.

However, choice of the conjugation methods is strongly dependent on the targeted biomolecule. Biomolecules used as biomarkers for example is very fast growing research field and because of it constant development and improvement of conjugation methods with QDs is required.

In spite of all their imperfections QDs have future in biological and/or clinical applications and milestone have been laid out and demonstrated but a lot of challenges are still ahead.

7 Literature

Ahmed, M., A. Guleria, et al. (2014). "Facile and Green Synthesis of CdSe Quantum Dots in Protein Matrix: Tuning of Morphology and Optical Properties." Journal of Nanoscience and Nanotechnology **14**(8): 5730-5742.

Algar, W. R. and U. J. Krull (2009). "Interfacial Transduction of Nucleic Acid Hybridization Using Immobilized Quantum Dots as Donors in Fluorescence Resonance Energy Transfer." Langmuir **25**(1): 633-638.

Algar, W. R. and U. J. Krull (2009). "Toward A Multiplexed Solid-Phase Nucleic Acid Hybridization Assay Using Quantum Dots as Donors in Fluorescence Resonance Energy Transfer." Analytical Chemistry **81**(10): 4113-4120.

Algar, W. R., D. E. Prasuhn, et al. (2011). "The Controlled Display of Biomolecules on Nanoparticles: A Challenge Suited to Bioorthogonal Chemistry." Bioconjugate Chemistry **22**(5): 825-858.

Ali, E. M., Y. G. Zheng, et al. (2007). "Ultrasensitive Pb2+ detection by glutathione-capped quantum dots." Analytical Chemistry **79**(24): 9452-9458.

Asokan, S., K. M. Krueger, et al. (2005). "The use of heat transfer fluids in the synthesis of high-quality CdSe quantum dots, core/shell quantum dots, and quantum rods." Nanotechnology **16**(10): 2000-2011.

Ayele, D. W., H. M. Chen, et al. (2011). "Controlled Synthesis of CdSe Quantum Dots by a Microwave-Enhanced Process: A Green Approach for Mass Production." Chemistry-a European Journal **17**(20): 5737-5744.

Ballou, B., L. A. Ernst, et al. (2007). "Sentinel Lymph Node Imaging Using Quantum Dots in Mouse Tumor Models." Bioconjugate Chemistry **18**(2): 389-396.

Bao, H., N. Hao, et al. (2010). "Biosynthesis of biocompatible cadmium telluride quantum dots using yeast cells." Nano Research **3**(7): 481-489.

Biswas, P., L. N. Cella, et al. (2011). "A quantum-dot based protein module for in vivo monitoring of protease activity through fluorescence resonance energy transfer." Chemical Communications **47**(18): 5259-5261.

Blanco-Canosa, J. B., M. Wu, et al. (2014). "Recent progress in the bioconjugation of quantum dots." Coordination Chemistry Reviews **263**: 101-137.

Boeneman, K., B. C. Mei, et al. (2009). "Sensing Caspase 3 Activity with Quantum Dot-Fluorescent Protein Assemblies." Journal of the American Chemical Society **131**(11): 3828-+.

Bruchez, M., M. Moronne, et al. (1998). "Semiconductor nanocrystals as fluorescent biological labels." Science **281**(5385): 2013-2016.

Byers, R. J. and E. R. Hitchman (2011). "Quantum Dots Brighten Biological Imaging." Progress in Histochemistry and Cytochemistry **45**(4): 201-237.

Cai, W., D.-W. Shin, et al. (2006). "Peptide-Labeled Near-Infrared Quantum Dots for Imaging Tumor Vasculature in Living Subjects." Nano Letters **6**(4): 669-676.

Cao, Y. C. and J. H. Wang (2004). "One-pot synthesis of high-quality zinc-blende CdS nanocrystals." Journal of the American Chemical Society **126**(44): 14336-14337.

Cella, L. N., P. Biswas, et al. (2014). "Quantitative Assessment of In Vivo HIV Protease Activity Using Genetically Engineered QD- Based FRET Probes." Biotechnology and Bioengineering **111**(6): 1082-1087.

Dahl, J. A., B. L. S. Maddux, et al. (2007). "Toward greener nanosynthesis." Chemical Reviews **107**(6): 2228-2269.

Dennis, A. M., W. J. Rhee, et al. (2012). "Quantum Dot-Fluorescent Protein FRET Probes for Sensing Intracellular pH." ACS Nano **6**(4): 2917-2924.

Duan, J. L., L. X. Song, et al. (2009). "One-Pot Synthesis of Highly Luminescent CdTe Quantum Dots by Microwave Irradiation Reduction and Their Hg2+-Sensitive Properties." Nano Research **2**(1): 61-68.

Efros, A. L. (1982). "INTERBAND ABSORPTION OF LIGHT IN A SEMICONDUCTOR SPHERE." Soviet Physics Semiconductors-Ussr **16**(7): 772-775.

Ekimov, A. I. and A. A. Onushchenko (1981). "QUANTUM SIZE EFFECT IN 3-DIMENSIONAL MICROSCOPIC SEMICONDUCTOR CRYSTALS." Jetp Letters **34**(6): 345-349.

Farkhani, S. M. and A. Valizadeh (2014). "Review: three synthesis methods of CdX (X = Se, S or Te) quantum dots." Iet Nanobiotechnology **8**(2): 59-76.

Feynman, R. P. (1960). "There's Plenty of Room at the Bottom." Engineering and Science **23**: 22-36.

Gaponik, N., D. V. Talapin, et al. (2002). "Thiol-capping of CdTe nanocrystals: An alternative to organometallic synthetic routes." Journal of Physical Chemistry B **106**(29): 7177-7185.

Gattas-Asfura, K. A. and R. M. Leblanc (2003). "Peptide-coated CdS quantum dots for the optical detection of copper(II) and silver(I)." Chemical Communications(21): 2684-2685.

Goldman, E. R., I. L. Medintz, et al. (2005). "A hybrid quantum dot-antibody fragment fluorescence resonance energy transfer-based TNT sensor." Journal of the American Chemical Society **127**(18): 6744-6751.

Guyot-Sionnest, P. (2008). "Colloidal quantum dots." Comptes Rendus Physique **9**(8): 777-787.

Hahn, M. A., P. C. Keng, et al. (2008). "Flow Cytometric Analysis To Detect Pathogens in Bacterial Cell Mixtures Using Semiconductor Quantum Dots." Analytical Chemistry **80**(3): 864-872.

Holmberg, A., A. Blomstergren, et al. (2005). "The biotin-streptavidin interaction can be reversibly broken using water at elevated temperatures." Electrophoresis **26**(3): 501-510.

Hoshino, A., K. Fujioka, et al. (2004). "Quantum dots targeted to the assigned organelle in living cells." Microbiology and Immunology **48**(12): 985-994.

Hu, B., L. L. Hu, et al. (2013). "A FRET ratiometric fluorescence sensing system for mercury detection and intracellular colorimetric imaging in live Hela cells." Biosensors & Bioelectronics **49**: 499-505.

Huang, L. and H. Y. Han (2010). "One-step synthesis of water-soluble ZnSe quantum dots via microwave irradiation." Materials Letters **64**(9): 1099-1101.

Chan, W. C. W. and S. M. Nie (1998). "Quantum dot bioconjugates for ultrasensitive nonisotopic detection." Science **281**(5385): 2016-2018.

Chen, L., J. H. Zhang, et al. (2004). "Effect of Zn2+ and Mn2+ introduction on the luminescent properties of colloidal ZnS : Mn2+ nanoparticles." Applied Physics Letters **84**(1): 112-114.

Chen, M., X. X. He, et al. (2014). "Inorganic fluorescent nanoprobes for cellular and subcellular imaging." Trac-Trends in Analytical Chemistry **58**: 120-129.

Chen, Y. F. and Z. Rosenzweig (2002). "Luminescent CdS quantum dots as selective ion probes." Analytical Chemistry **74**(19): 5132-5138.

Chou, C. C. and Y. H. Huang (2012). "Nucleic Acid Sandwich Hybridization Assay with Quantum Dot-Induced Fluorescence Resonance Energy Transfer for Pathogen Detection." Sensors **12**(12): 16660-16672.

Jin, S., Y. Hu, et al. (2011). "Application of Quantum Dots in Biological Imaging." Journal of Nanomaterials.

Kattke, M. D., E. J. Gao, et al. (2011). "FRET-Based Quantum Dot Immunoassay for Rapid and Sensitive Detection of Aspergillus amstelodami." Sensors **11**(6): 6396-6410.

Kaul, Z., T. Yaguchi, et al. (2003). "Mortalin imaging in normal and cancer cells with quantum dot immuno-conjugates." Cell Research **13**(6): 503-507.

Ke, J., X. Y. Li, et al. (2012). "A facile and highly sensitive probe for Hg(II) based on metal-induced aggregation of ZnSe/ZnS quantum dots." Nanoscale **4**(16): 4996-5001.

Kobayashi, H., Y. Hama, et al. (2007). "Simultaneous multicolor imaging of five different lymphatic basins using quantum dots." Nano Letters **7**(6): 1711-1716.

Kosaka, N., M. Ogawa, et al. (2009). "In Vivo Real-Time, Multicolor, Quantum Dot Lymphatic Imaging." Journal of Investigative Dermatology **129**(12): 2818-2822.

Lakowicz, J. (1999). Principles of Fluorescence Spectroscopy. New York, Boston, Dordrecht, London, Moscow, Kluwer Academic/Plenum Publishers.

Lee, J., Y. Choi, et al. (2009). "Positively Charged Compact Quantum Dot-DNA Complexes for Detection of Nucleic Acids." ChemPhysChem **10**(5): 806-811.

Li, X., B. Xue, et al. (2013). "Protease-activated quantum dot probes based on fluorescence resonance energy transfer." Chinese Science Bulletin **58**(21): 2657-2662.

Mattoussi, H., J. M. Mauro, et al. (2000). "Self-assembly of CdSe-ZnS quantum dot bioconjugates using an engineered recombinant protein." Journal of the American Chemical Society **122**(49): 12142-12150.

Medintz, I. L., A. R. Clapp, et al. (2006). "Proteolytic activity monitored by fluorescence resonance energy transfer through quantum-dot-peptide conjugates." Nature Materials **5**(7): 581-589.

Medintz, I. L., A. R. Clapp, et al. (2003). "Self-assembled nanoscale biosensors based on quantum dot FRET donors." Nature Materials **2**(9): 630-638.

Mi, C., Y. Wang, et al. (2011). "Biosynthesis and characterization of CdS quantum dots in genetically engineered Escherichia coli." Journal of Biotechnology **153**(3–4): 125-132.

Murray, C. B., D. J. Norris, et al. (1993). "SYNTHESIS AND CHARACTERIZATION OF NEARLY MONODISPERSE CDE (E = S, SE, TE) SEMICONDUCTOR NANOCRYSTALLITES." Journal of the American Chemical Society **115**(19): 8706-8715.

Narayanan, K. B. and N. Sakthivel (2010). "Biological synthesis of metal nanoparticles by microbes." Advances in Colloid and Interface Science **156**(1-2): 1-13.

Noor, M. O., A. Shahmuradyan, et al. (2013). "Paper-Based Solid-Phase Nucleic Acid Hybridization Assay Using Immobilized Quantum Dots as Donors in Fluorescence Resonance Energy Transfer." Analytical Chemistry **85**(3): 1860-1867.

Peng, H., L. Zhang, et al. (2007). "DNA hybridization detection with blue luminescent quantum dots and dye-labeled single-stranded DNA." Journal of the American Chemical Society **129**(11): 3048-+.

Petryayeva, E. and W. R. Algar (2013). "Proteolytic Assays on Quantum-Dot-Modified Paper Substrates Using Simple Optical Readout Platforms." Analytical Chemistry **85**(18): 8817-8825.

Pic, E., T. Pons, et al. (2010). "Fluorescence Imaging and Whole-Body Biodistribution of Near-Infrared-Emitting Quantum Dots after Subcutaneous Injection for Regional Lymph Node Mapping in Mice." Molecular Imaging and Biology **12**(4): 394-405.

Prasuhn, D. E., J. B. Blanco-Canosa, et al. (2010). "Combining Chemoselective Ligation with Polyhistidine-Driven Self-Assembly for the Modular Display of Biomolecules on Quantum Dots." Acs Nano **4**(1): 267-278.

Qian, H. F., L. Li, et al. (2005). "One-step and rapid synthesis of high quality alloyed quantum dots (CdSe-CdS) in aqueous phase by microwave irradiation with controllable temperature." Materials Research Bulletin **40**(10): 1726-1736.

Qu, L. H., Z. A. Peng, et al. (2001). "Alternative routes toward high quality CdSe nanocrystals." Nano Letters **1**(6): 333-337.

Rosenthal, S. J., J. C. Chang, et al. (2011). "Biocompatible Quantum Dots for Biological Applications." Chemistry & Biology **18**(1): 10-24.

Ruedas-Rama, M. J. and E. A. H. Hall (2009). "Multiplexed energy transfer mechanisms in a dual-function quantum dot for zinc and manganese." Analyst **134**(1): 159-169.

Sapsford, K. E., W. R. Algar, et al. (2013). "Functionalizing Nanoparticles with Biological Molecules: Developing Chemistries that Facilitate Nanotechnology." Chemical Reviews **113**(3): 1904-2074.

Sapsford, K. E., T. Pons, et al. (2006). "Biosensing with luminescent semiconductor quantum dots." Sensors **6**(8): 925-953.

Shanehsaz, M., A. Mohsenifar, et al. (2013). "Detection of Helicobacter pylori with a nanobiosensor based on fluorescence resonance energy transfer using CdTe quantum dots." Microchimica Acta **180**(3-4): 195-202.

Shi, L. F., N. Rosenzweig, et al. (2007). "Luminescent quantum dots fluorescence resonance energy transfer-based probes for enzymatic activity and enzyme inhibitors." Analytical Chemistry **79**(1): 208-214.

Schumacher, W., A. Nagy, et al. (2009). "Direct Synthesis of Aqueous CdSe/ZnS-Based Quantum Dots Using Microwave Irradiation." Journal of Physical Chemistry C **113**(28): 12132-12139.

Smith, A. M. and S. Nie (2010). "Semiconductor Nanocrystals: Structure, Properties, and Band Gap Engineering." Accounts of Chemical Research **43**(2): 190-200.

Snee, P. T., R. C. Somers, et al. (2006). "A ratiometric CdSe/ZnS nanocrystal pH sensor." Journal of the American Chemical Society **128**(41): 13320-13321.

So, M. K., C. J. Xu, et al. (2006). "Self-illuminating quantum dot conjugates for in vivo imaging." Nature Biotechnology **24**(3): 339-343.

Stuerzenbaum, S. R., M. Hoeckner, et al. (2013). "Biosynthesis of luminescent quantum dots in an earthworm." Nature Nanotechnology **8**(1): 57-60.

Sukhanova, A., M. Devy, et al. (2004). "Biocompatible fluorescent nanocrystals for immunolabeling of membrane proteins and cells." Analytical Biochemistry **324**(1): 60-67.

Walling, M. A., J. A. Novak, et al. (2009). "Quantum Dots for Live Cell and In Vivo Imaging." International Journal of Molecular Sciences **10**(2): 441-491.

Wei, O. D., M. Lee, et al. (2006). "Development of an open sandwich fluoroimmunoassay based on fluorescence resonance energy transfer." Analytical Biochemistry **358**(1): 31-37.

Wu, P., T. Zhao, et al. (2014). "Semicondutor quantum dots-based metal ion probes." Nanoscale **6**(1): 43-64.

Yezhelyev, M. V., A. Al-Hajj, et al. (2007). "In situ molecular profiling of breast cancer biomarkers with multicolor quantum dots." Advanced Materials **19**(20): 3146-+.

Zekavati, R., S. Safi, et al. (2013). "Highly sensitive FRET-based fluorescence immunoassay for aflatoxin B1 using cadmium telluride quantum dots." Microchimica Acta **180**(13-14): 1217-1223.

Zhang, C. Y., H. C. Yeh, et al. (2005). "Single-quantum-dot-based DNA nanosensor." Nature Materials **4**(11): 826-831.

Zhang, K., Q. S. Mei, et al. (2010). "Ligand Replacement-Induced Fluorescence Switch of Quantum Dots for Ultrasensitive Detection of Organophosphorothioate Pesticides." Analytical Chemistry **82**(22): 9579-9586.

Zhang, Y. and A. Clapp (2011). "Overview of Stabilizing Ligands for Biocompatible Quantum Dot Nanocrystals." Sensors **11**(12): 11036-11055.

Zhao, Q., X. L. Rong, et al. (2013). "Dithizone functionalized CdSe/CdS quantum dots as turn-on fluorescent probe for ultrasensitive detection of lead ion." Journal of Hazardous Materials **250**: 45-52.

Zhou, D. J., L. M. Ying, et al. (2008). "A compact functional quantum dot-DNA conjugate: Preparation, hybridization, and specific label-free DNA detection." Langmuir **24**(5): 1659-1664.

Zimmer, J. P., S. W. Kim, et al. (2006). "Size series of small indium arsenide-zinc selenide core-shell nanocrystals and their application to in vivo imaging." Journal of the American Chemical Society **128**(8): 2526-2527.

8 Abbreviations

Cys	Cysteine
DNA	Deoxyribonucleic acid
dsDNA	Double stranded deoxyribonucleic acid
DHLA	Dihydrolipoic acid
EDC	N-(3-dimethylaminopropyl)-N'-ethylcarbodiimide
EG_3OH	11-mercaptoundecyl tri(ethylene glycol) alcohol
EG_3COOH	11-mercaptoundecyl tri(ethylene glycol) acetic acid
FRET	Fluorescence resonance energy transfer
Fc	Fragment crystallizable region
Fab	Antigen-binding fragment
Gly	Glycine
GSH	Glutathione
His	Histidine
His_n	Polyhistidine
IgG	Immunoglobuline
LIF	Laser-induced fluorescence
LeuLeucine	
MBP	Maltose binding protein
MPA	Mercaptopropionic acid
NIR	Near-infra red
ODN	Oligonucleotides
PCR	Polymerase chain reaction
PL	Photoluminescence
PEG	Polyethyleneglycol
QDs	Quantum dots
SDS-PAGE	Sodium dodecyl sulfate
ssDNA	Single stranded deoxyribonucleic acid
sulfo-NHS	N-hydroxysulfosuccinimide
sulfo-SMCC	Sulfosuccinimidyl 4-(N-maleimidomethyl)cyclohexane-1-carboxylate
TGA	Thioglycolic acid

TOP	Trioctylphosphine
TOPO	Trioctylphosphine oxide
TOPTe	Trioctylphosphine telluride
TNT	Trinitrotoluene
UV	Ultraviolet